CENTRE FOR ORE DEPOSIT AND EXPLORATION STUDIES

STRUCTURE AND MINERALISATION OF WESTERN TASMANIA

AMIRA PROJECT P.291
Report No.3

University of Tasmania

CONTENTS

Structure of the Rosebery Deposit

R.F. Berry
Centre for Ore Deposit and Exploration Studies

ABSTRACT

The detailed assessment of drill sections and level plans from 14 to 19 level support the existence of an imbricate array of high angle reverse faults in the mine from 0–500 m N. These faults have a combined displacement of 250 m. Restoration of the mine lenses in this area shows G lens was originally stacked on top of E lens. H lens is completely separate but may have formed along the same Cambrian growth fault. The metal zonation and host sequence distribution support a complex seafloor topography and syn-depositional fault pattern which influence the ore deposition geometry. The present level of understanding allows the rationalisation of the presently known pattern but has little predictive capability. It strongly supports the existing exploration search for down dip extensions. A more accurate definition of the footwall boundary is the most obvious target for improving this situation.

INTRODUCTION

This structural study of Rosebery aims to apply the structural ideas arising out of the AMIRA project to a detailed assessment of the structural control on the geometry of the Rosebery ore lenses. The study builds on a small amount of underground observations by the author which are relevant to the structural style of the deposit. This has been followed by detailed assessment of drill sections and finally a major effort has been put into making the data on mine level plans more accessible for structural purposes. Since the last report a structure contour map of footwall and hanging wall boundaries has been compiled and integrated with the level plans from 14 to 19 level in the south of the mine and from 13 to 17 level in the north. These level plans are being digitised and some of them will be available at the meeting.

The major results are

1. There are many small reverse faults in the deposit and these are especially common in the complex area from 0 to 500 m N. The sum of displacements on the faults can be estimated from a number of constraints as 130–500 m with the preferred estimate of 250 m.
2. The displacement of the faults simplifies the picture slightly since G lens can now be seen as a stacked lens over D/E lens. H lens is still quite distinct.
3. The level plans can be used to show the pattern of metal distribution with a great deal more resolution than possible from drill hole data and they show a number of discrete centres for mineralisation.

A major problem with detailed analysis is the ambiguity in recognising footwall boundaries for the mine. While the overwhelming weight of evidence supports the footwall distribution in this report the detail is subject to revision. A possible mechanism for improving this relationship is to use a geochemical signature such as Ti/Zr ratio to distinguish footwall from host rocks.

Within the context of the AMIRA project, two months was available to work on this problem. This has not allowed a complete analysis of all the possible lines of evidence available. Much more work could be done.

METHODS

The basic test of viability applied here was to extend the structural model suggested by Berry (1989) and provide detailed assessment of its viability. The basic constraints on any structural model are that it:

- predicts a conformable origin for the ore lenses before the faulting and cleavage development,
- explains the repetition of lenses within the centre of the mine and in general the overlap of minor lenses,
- does not require major fold repetitions, at least in the host sequence, and
- is compatible with the general style of brittle-ductile deformation widespread throughout the mine.

The aim of this project was to progress the reverse fault model to the point where individual faults can be identified in the underground development or in core and followed through the level plans leading to the production of accurate restorable sections.

The first approach was to consider faults of other easily recognisable boundaries. A major offset of the upper contact of the host sequence has been recognised in the central part of the mine for a long time (e.g. Brathwaite 1974). While this offset has been explained by a number of mechanisms, reverse faulting appears to be the major model applied.

Further work using the modern 1:1000 drill sections led to a structure contour map of the footwall and hanging wall boundaries in the mine (Fig. 1). These boundaries confirm the offsets reported in early work but also indicate footwall offsets are compatible with a fault model for the mine and the multiple positions of the footwall requires a number of faults. These complexities have not been interpreted as faults previously but have been used to support fold models in some cases. The distribution of the footwall based on drill hole data alone is ambiguous, but with the addition of level plan data the fault model is clearly superior (see below). In addition many other smaller complexities in the footwall and hanging wall boundary remain to be explained. for example at the 2800 m RL structure contour of the footwall at 200 m N is discontinuous and indicates a number of footwall positions.

The level plans at Rosebery remain as a largely untapped data base in the assessment of the structure of the ore, at least since the work of Brathwaite (1974). His work was largely in the upper levels of the mine (down to 16 level). Progress of the mine has now produced a detailed database down to 19 level. The detailed 1:240 and 1:250 level plans have a resolution which cannot be equalled from the drill sections. Especially major faults are shown and the continuity of structures is much better constrained. A week was spent getting all the plans from 14 level to 19 level onto a common scale of 1:500. This intermediate scale allowed an overview of the mine while retaining most of the structural detail in the original plans. The structure contour information on hanging wall and footwall boundaries, from the drill sections, was added to these level plans and the resulting database was used to test the fault model for the Rosebery deposit.

Plans for the main levels in the mine are enclosed.

RESULTS

Major faults are recognisable on many levels and some of these can be carried through from level to level. The major fault reported in Berry (1990) is only one of a dozen such faults of which there appears to be three major ones in the area from 0 m N to 500 m N.

The major reverse fault (Fault A) can be recognised from 18/1 level through to 16/2 level as it lifts G lens about 130 m with respect to D/E lens. The fault style varies dramatically in different rock types. The fault is a discrete brittle structure in the host sequence at 400 m N where it cuts a drive on 16 level. At 16 level it also cuts through the major G lens/E lens contact as a wide zone of imbricate faulting (Fig. 2). At 17 level the fault lies within a narrow mineralised zone and the drive along the fault shows the complex lens structure which I expect within the intensely sheared ore near the fault (Fig. 2). In part this fault splits into a pair of parallel structures (e.g. 16 level) but the present mapping is not detailed enough to determine the relative importance of the two faults.

A second major reverse fault (B) cuts across and terminates the E lens extension of the host sequence in the deeper levels (e.g. 18/1 level). The fault has only been mapped where it emerges from the ore zone at 16, 17/1 and 17/2 levels.

A third structure is required to explain the relationship between F and H lens at the 17/2 level. This structure is poorly constrained by the present data. In addition, a large number of other faults are shown on the level plans. Minor crossfaults are especially common in the F lens at 250 m S on 16 level and in the north of the mine.

Thus the general view of a large number of reverse faults suggested from limited underground observations is supported by the existing level plans. The effect of these faults on the geometry can now be tested. Cross sections have been drawn for the 14 to 19 level for the area where the major faults are offsetting both footwall and hanging wall (Figs 3, 4, 5, 6). The faults can be traced over a large number of levels through these plans. They often appear to diverge into imbricate structures near the ore lenses but the overall position is fixed by the existing data base. These sections show that a substantial proportion of the thickening of the host sequence in this region

is due to faulting. Berry (1990) estimated the offset from the displacement of the hanging wall as about 130 m. The footwall offsets in these sections can be explained by 250 m of displacement. In order to simplify the ore body to 1 lens a displacement over 500 m is required (Berry 1988) and these detailed sections do not support this amount of total movement. The host sequence is two to three times normal thickness over a vertical distance of 250 m suggesting a total offset of 250–500 m in line with the estimates above. The sections have been reconstructed here to bring the footwall boundary into one line.

The essential features of the restored sections (Fig. 7) are:

(i) G lens now sits exactly on top of E lens in a stacked geometry. The base of G and E lens now coincide.

(ii) The strong thickening of the host sequence at the bottom of E lens is still visible in the 100 m N section but decreases to the north. Either a larger displacement is required in the southern sections or the thickening is a primary feature. (The latter model is preferred here — see below.)

(iii) H lens still remains as a completely separate lens and has a different geometry.

Alternative models for the geometry of Rosebery need to explain the complex distribution of footwall rocks in the lower levels of the mine. The level plans indicate a large mass of footwall compositions structurally above E lens in the mine below 17 level with E lens diverging dramatically from the hanging wall towards 19 level. The geometry of the ore lenses does not support a fold. The alignment with offsets of the black slate fit a fault model. No stratigraphic model exists to explain the complex footwall geometry. One weak link here is the difficulty in identification of footwall but the large area of footwall implied from both drillhole and level plan data is difficult to disregard.

Pyrrhotite-rich ore is common in the south end of the mine. These have been studied in detail and are the result of reaction of granitic fluids with pre-existing massive sulphide (Solomon et al., 1987; Zaw, 1991). The distribution is linked to the southern margin of F lens but also has a strong spatial association with reverse faults (16 level) suggesting that these structures have acted as conduits for the granitic fluids.

Berry (1990) noted that the general shape of the ore lenses as a group in the area of E, F, G and H lens is reproduced on a smaller scale in level plans in North Rosebery. In this area, the structure appears very simple. The change in thickness and increase in number of lenses from 1050 m N to 1100 m N cannot be explained by a duplex structure. The change occurs across an east–west sub-vertical fault very obvious on 13 and 15 level but very variable in its shape between levels. At 50 m N, even after the restoration of the reverse fault movements, an offset and thickening of the host sequence is still required. Structures of this type are show in Fig. 8. The northern growth fault dies out both up and down the mine. There are 2 similar structures in F lens. A basin like structure with double lenses of ore is visible on 17 level and appears to continue down to 18/2 sublevel. A possible upward continuation is visible at 260 m S on 15 level. Lastly, the largest, and most important in terms of mineralisation, forms the southern edges of G and E lenses (Figs 8, 9), and based on the reconstruction in Fig. 7, probably turns just below 19 level to close off these lenses. The genetic relationship controlling the pattern of these faults is not clear.

The level plans show the ore divided into a number of types which, within the VHMS model, are related to temperature. The Cu rich zones reflecting the highest temperature and therefore near source conditions. Each lens has been divided into zones dominated by one of four types. In many cases the lens may have a different type at the top to the bottom but a general pattern based on dominant type has been produced for 14 to 19 level (Figs 8, 9, 10). Because of the structural interpretation of offsets between E, G and H lens they have been treated separately. F lens is tied to G lens in 15 level plans and the structural information suggests these are moving a similar amount so they are grouped together in this exercise.

The G/F long section shows a number of centres. A major high Cu-pyrite zone occurs at 50 to 150 m N apparently related to the growth fault shown in Fig. 8. In contrast there is a large Cu–pyrite centre 18/1 sublevel in F lens and a less pyritic Cu zone at 15–16 level. Neither appear to be linked to the possible growth fault zone further south. Barite is concentrated to the north of the lens although there is a great deal of barite throughout G lens. In plan the Cu-pyrite centre at 18/2 sublevel 125 m S has many of the classic features of an exhalative VHMS. There is an extensive pyrite altered footwall enriched in Cu, a high pyrite zone over the proposed vent centre and a wide stratabound Pb/Zn ore lens.

There is much less detail for the northern part of the mine. The Cu-rich zone on 15/1 sublevel does appear to be linked to the normal fault recognised at 1100 m N and occurs at the maximum displacement of this interpreted growth fault. In contrast the pyritic ore lies largely on the upthrown block and has a moderate pitch to the south. South pitching metal trends (especially pyrite) have been recognised previously (e.g. Zaw, Huston & Large 1988, Lutherburrow verb. comm.) but no structural control has been found either previously or in this study.

E lens is strongly pyritic throughout and has Cu-rich zones both on its southern margin and at isolated areas 100–150 m further north. Pb/Zn ore is patchy

and only dominant on the northern margin. The level plans here are particularly instructive. For example on 16/2 sublevel there is a strong Cu-rich base to the lens (Fig. 11). The pyrite zone extend throughout the lens in discrete areas closely linked to high Cu Pods in the base of the lens. In some cases Cu-rich pods extend to the top of the E lens. On 16/1, 16/2 and 17/1 levels the distribution of metals is consistent with the lower of a number of stacked lenses. Here the hydrothermal system has continued after further sedimentation to deposit metals on the seafloor but is stripping Pb/Zn from the lower lens. While this is a model-based interpretation of the metal distribution it is consistent with the reported geology. In such a stacked system the centres in the upper lenses should be related to the Pb/Zn depleted zones below. In their present geometry the centres in G lens do not correlate well with those in E lens except to the extent of the concentration along the southern margin of the lenses. A reverse displacement of 100 m between G and E lens is sufficient to explain the difference with the Cu-rich zone at 14 level in G lens originally formed on top of the Pb/Zn depleted centre at 16 to 15 level in E lens. This also brings the lower margins of the lenses into line.

GEOCHEMICAL TRACERS

A major problem in a detailed model for the Rosebery Mine is the ambiguity in logged position of the footwall. Away from the alteration zone there is less problem but in the main centre the alteration makes the distinction very difficult. One possibility is that immobile trace elements may discriminate the two rock types. To assess this possibility I considered the data base from Rosebery reported by Naschwitz (1985) and Naschwitz & Van Moort (1991). The least mobile elements Al_2O_3, TiO_2, P_2O_5, Zr, Y and Nb were transformed into log ratios (Aitchison 1986) and the result was subject to discriminant analysis using the program DISCRM of Davis (1973). The host and footwall are clearly discriminated at the 99% confidence level using these elements (Table 1). In practise it is clear from these results that the discrimination can be made at almost the same level by using the Ti/Zr or Ti/Y ratios (Fig. 12). The footwall compositions have a small range of compositions. Most of the host sequence analyses are quite separate but five analyses fall in the footwall area perhaps reflecting smaller bodies of coarser volcaniclastic.

For completeness the the host-rock hangingwall and hangingwall footwall were tested using the same elements and in each case highly significant discrimination was possible. The discrimination is well displayed in the Log Zr/Nb vs log Y/Ti diagram (Fig. 13). While the host sequence is fairly variable and overlaps partly into the footwall compositions the hanging wall volcaniclastics have higher Zr/Nb ratio.

The geochemical data available from Rosebery suggest that estimates of the position of the footwall boundary can be substantially improved even in moderately altered areas by application of trace element ratios such as Ti/Zr. A major step forward in the structure of the mine would be to test logged footwall positions in 17 to 19 levels between E lens and H lens.

Table 1. Host footwall discrimination based on Davis (1973)

Variable	Constant	Prot. Added
Log (TiO_2/Al_2O_3)	3.89	41.9
Log(P_2O_5/Al_2O_3)	0.92	17.7
Log(Zr/Al_2O_3)	-3.32	11.9
Log(Y/Al_2O_3)	-6.31	28.6
Log(Nb/Al_2O_3)	0.04	-0.1

F test based on 5° and 108° freedom
F= 15.18
(At 1% confidence to reject hypothesis of discrimination F<3.2)

SUMMARY

1. The position and significance of reverse faults has been demonstrated in the central part of the mine. The restoration of lenses resulting from this analysis suggests the original lens configuration was complex with G lens being stacked on top of E/D lens and partly fed by fluids transmitted through E lens.
2. In order to advance this model it is necessary to improve the reliability of identification of the footwall/host boundary in the central part of the mine. One possibility is the use of a geochemical tracer such as Ti/Zr ratio which has potential to accurately identify the boundary independent of alteration. In particular the geometry of footwall lithologies above E lens is an important constraint on structural models which has not received enough attention.
3. The localisation of ore lenses is related to a large number of centres. The structural work here has emphasized the tendency for such centres to define lines which pitch at 90° in the ore position. The present exploration emphasis on down dip extensions is strongly supported. The only strong linear element which dies rapidly down dip is the major zone a 50 m N and despite the clear termination of E/G lenses below 19 level some more distant down dip extension are worth investigating. The secondary linear trend pitching moderately south has received attention recently but no direct structural control on this direction has been found.
4. The possibility of small growth faults controlling mineralisation (Berry 1990) is partly supported by this study. Two examples are closely related to mineralisation but a third in F lens is near to a mineralising centre defined by Cu-pyrite but does not control its distribution. The pattern of host sequence thickness may be a measure of extensional fault geometry but this pattern is still elusive.
5. The metal zoning and structure have been related together. Classic VHMS style metal zonation occurs in F lens and to some extent in A/B lens. E/G lenses are a stacked system formed against a growth fault. The stratigraphically higher H lens is separate and sourced further down dip (although possibly along the same trend). The continuation from G to F lens at 15 level suggests a drape fold. H lens is eroded off over this structure suggesting it may have originally been less asymmetric in metal zonation than it now appears.

ACKNOWLEDGEMENTS

I am indebted to the Pasminco Rosebery staff for the strong support they have given this project and especially to Jim Farquahar for help with the level plans. Mr Aung Pwa kindly made available an Excel version of the Natschwitz (1985) database.

REFERENCES

Aitchison J. 1986. *THE STATISTICAL ANALYSIS OF COMPOSITIONAL DATA*. Chapman & Hall, London: 416pp.

Berry R.F. 1989. The structure of the Rosebery Mine Sequence. Unpublished report to EZ Rosebery 15pp.

Berry R.F. 1990. Structure of Rosebery deposit. Unpublished AMIRA report: 17–26

Brathwaite R.L. 1972. The structure of the Rosebery ore deposit, Tasmania. *Proc. Aust. Inst. Min. Met.* 241: 1–13.

Brathwaite R.L. 1974. The geology and origin of the Rosebery ore deposits. *Econ. Geol.* 69: 1086–1111.

Davis J.C. 1973. *STATISTICS AND DATA ANALYSIS IN GEOLOGY*. John Wiley & Sons, New York: 550 pp.

Natschwitz W. 1985. Geochemistry of the Rosebery ore deposit. Unpublished PhD thesis, University of Tasmania.

Naschwitz W. & van Moort J.C. 1991. Geochemistry of wallrock alteration, Rosebery, Tasmania, Australia. *Applied Geochemistry* 6: 267–278.

Solomon M., Vokes F.M. & Walshe J.L. 1987. Chemical remobilisation of volcanic-hosted sulphide deposits at Rosebery and Mt. Lyell, Tasmania. *Ore Geology Reviews* 2: 173–190.

Zaw K 1991. The effect of Devonian metamorphism and metasomatism on the mineralogy and geochemistry of the Cambrian VMS deposits in the Rosebery-Hercules district, western Tasmania. Unpublished PhD thesis, University of Tasmania.

Zaw K., Huston D.L. & Large R.R. 1988. Ore metal distribution, zonation and structural relationship at Rosebery, western Tasmania. Unpublished report to EZ Co., Australasia.

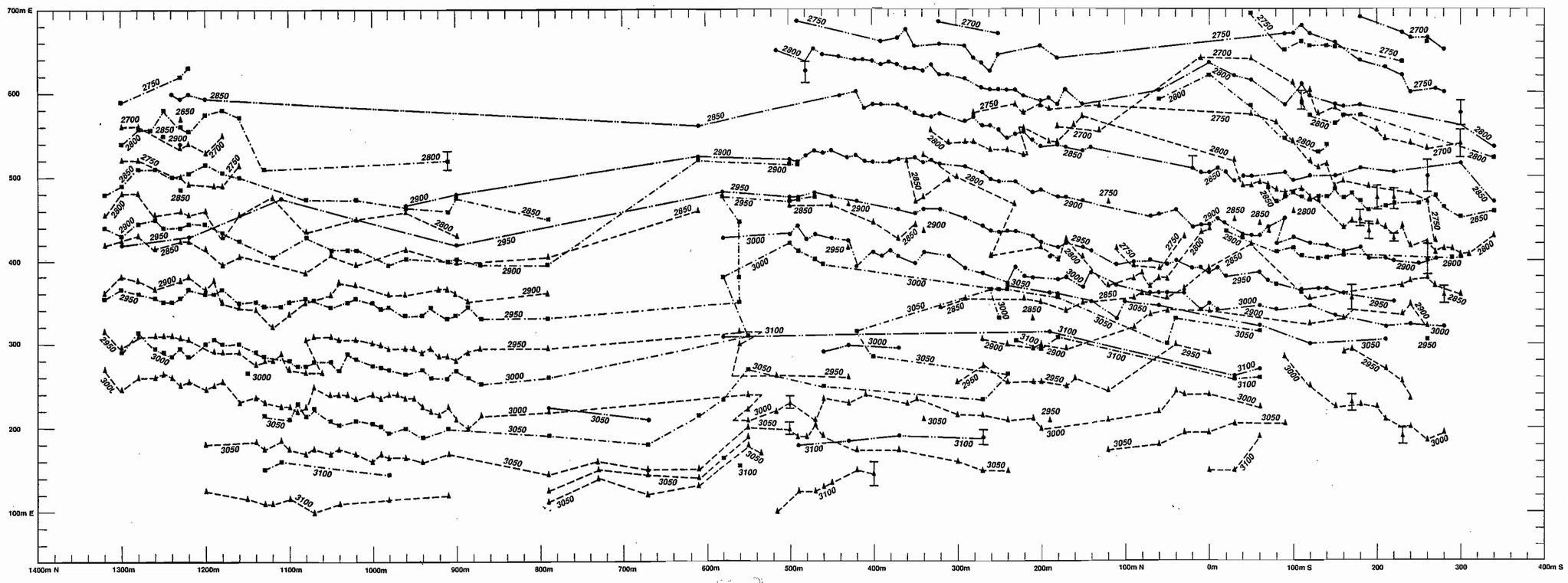

Fig. 1 Structure contours at 50 m intervals for three surfaces in Rosebery mine. Contours based on interpretation of 1:1000 drill sections.
Footwall -host contact: triangles joined by dashed lines.
Host-black shale contacts: squares joined by dot/dash line
Lower contact of hanging wall volcaniclastics: circles joined by dash-double dot lines

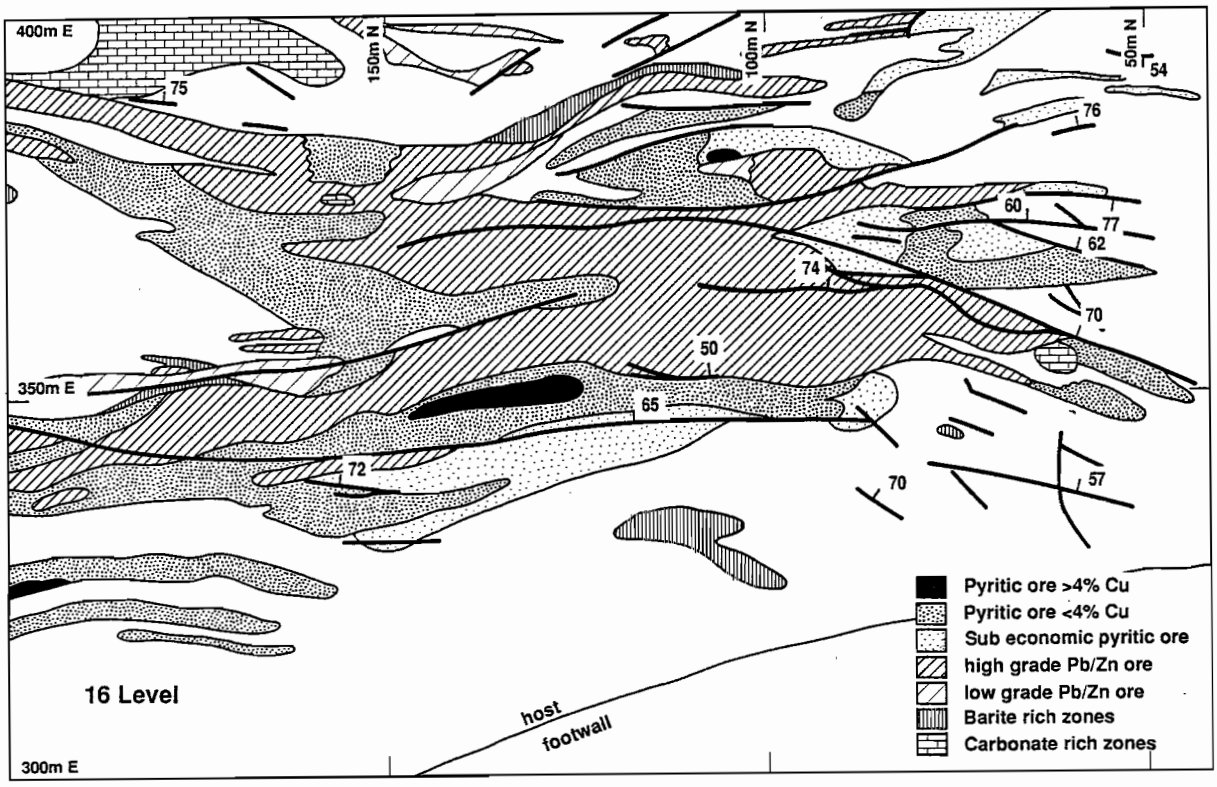

Fig. 2 Section of 16 level plan showing intense and complex faulting at the eastern termination of E and G lens. Most faults dip 50–70° E.

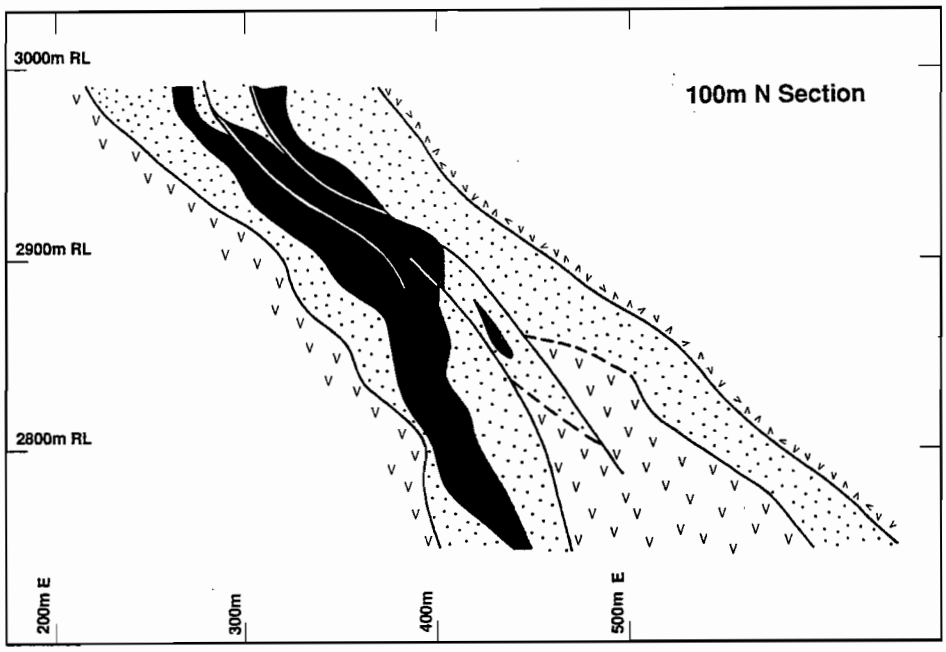

Fig. 3 Cross section at 100 m N from 14 to 19 level based on level plans. Legend as in Fig. 7.

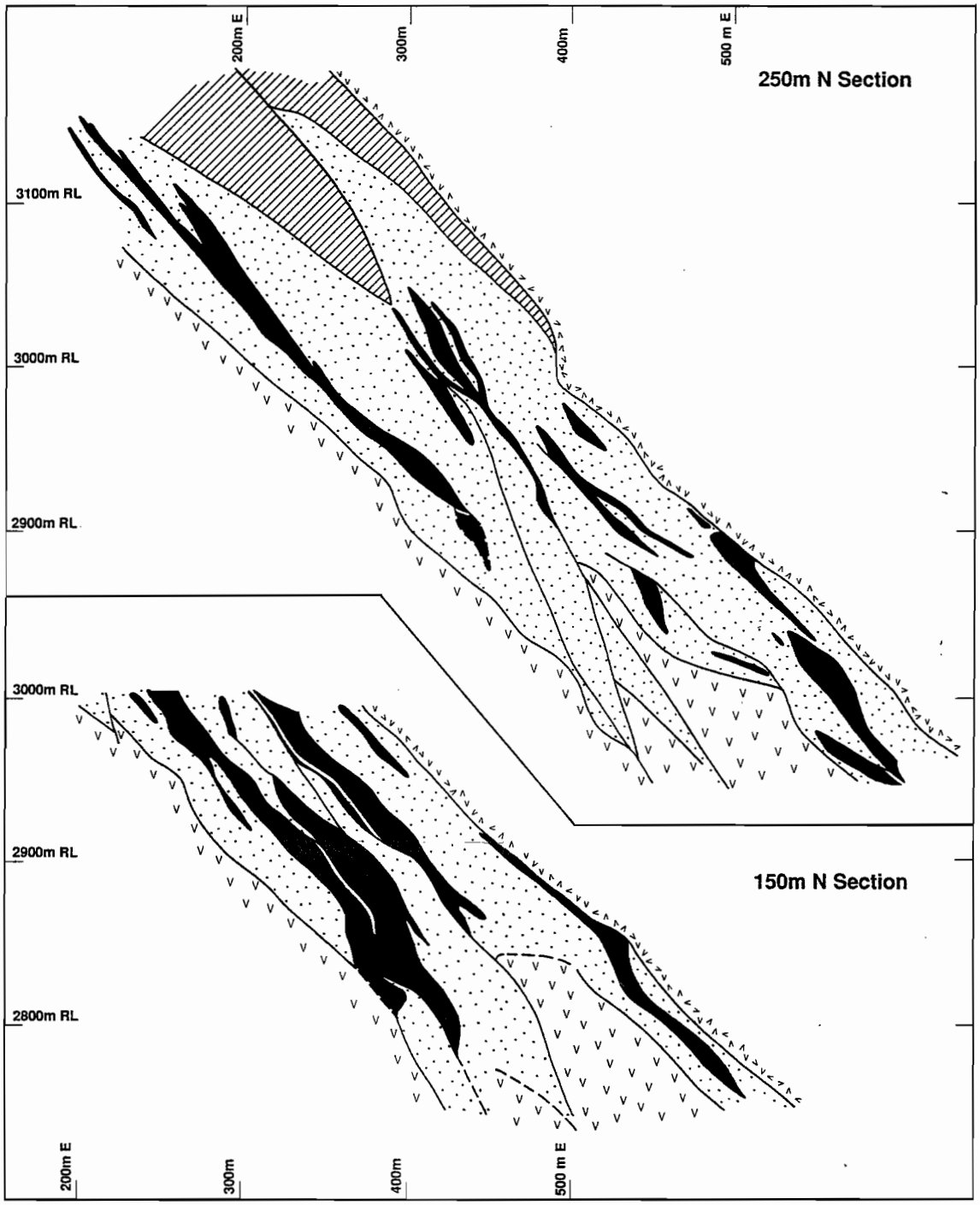

Fig. 4 Cross sections at 150 m and 250 m N based on 14 to 19 level plans. Section above 3000m RL is from drill sections. Legend as in Fig. 7.

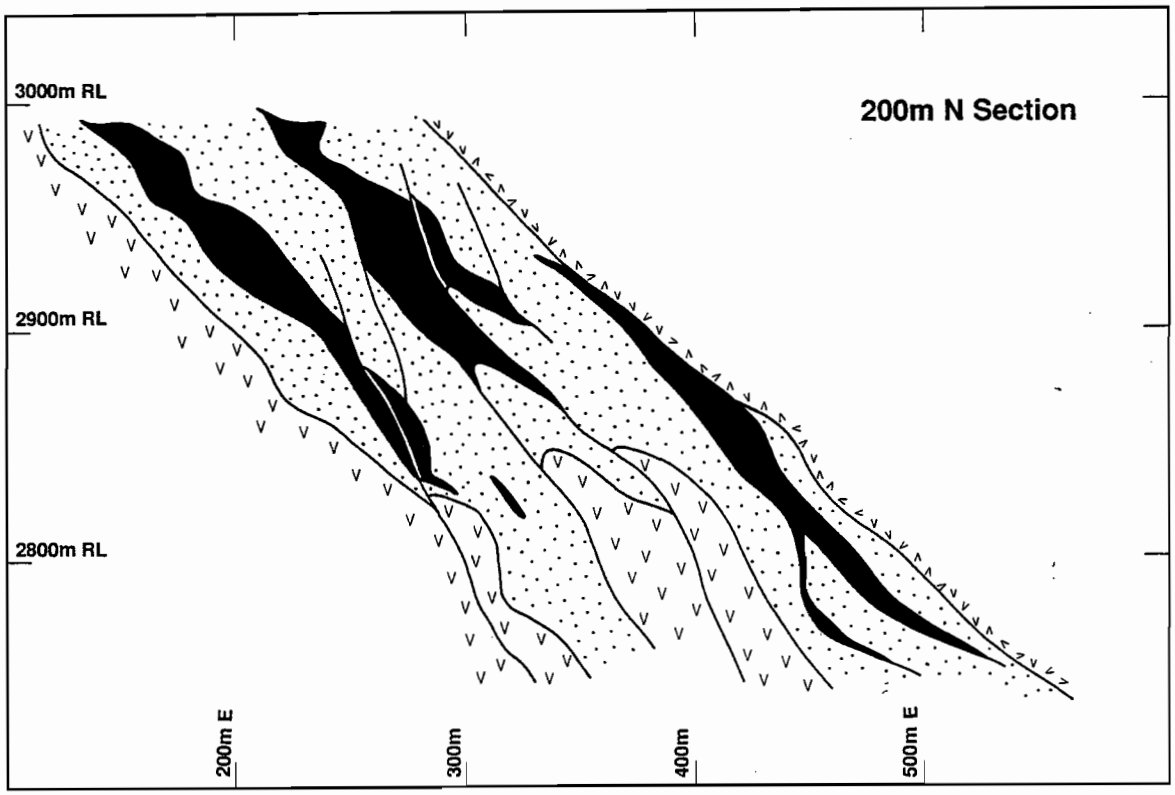

Fig. 5 Cross section at 200 m N from 14 to 19 level based on level plans. Legend as in Fig. 7.

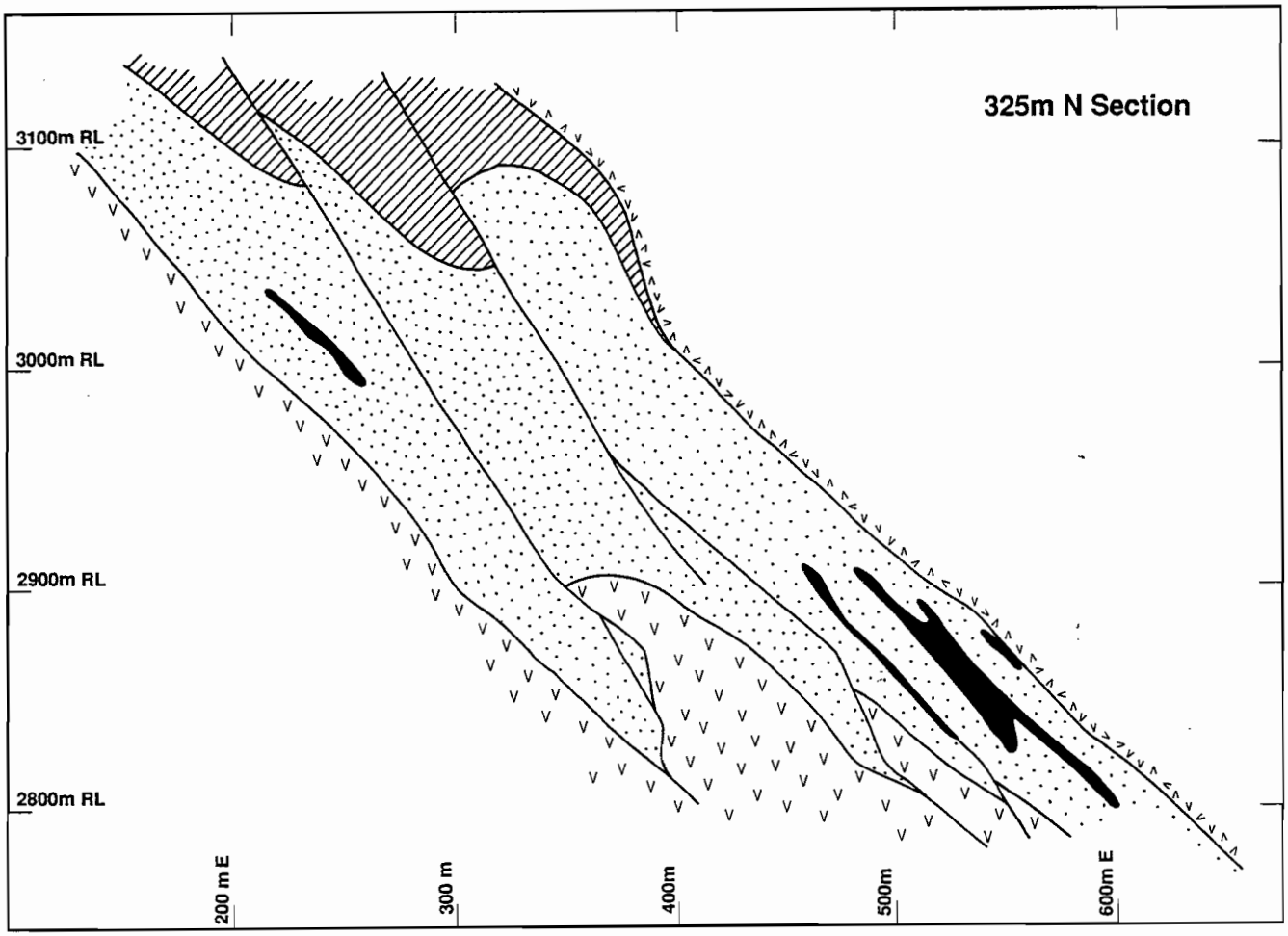

Fig. 6 Cross section at 325 m N from 14 to 19 level based on level plans. Section above 3000 m RL is from drill sections. Legend as in Fig. 7.

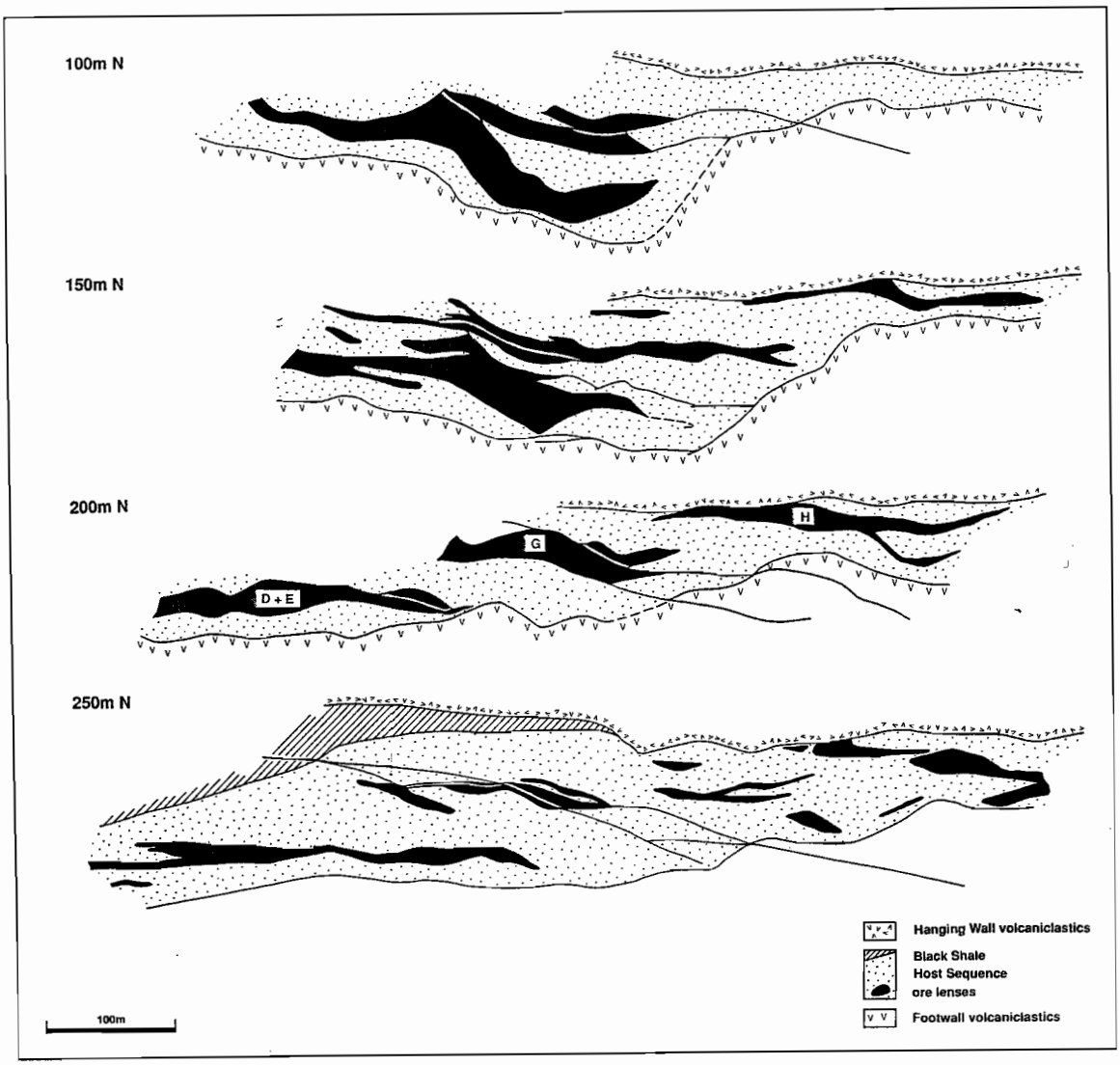

Fig. 7 Restored section based on Figs 3, 4 and 5 using the footwall position as the primary constraint on fault movement. Areas of units are maintained. Construction was from the hangingwall down.

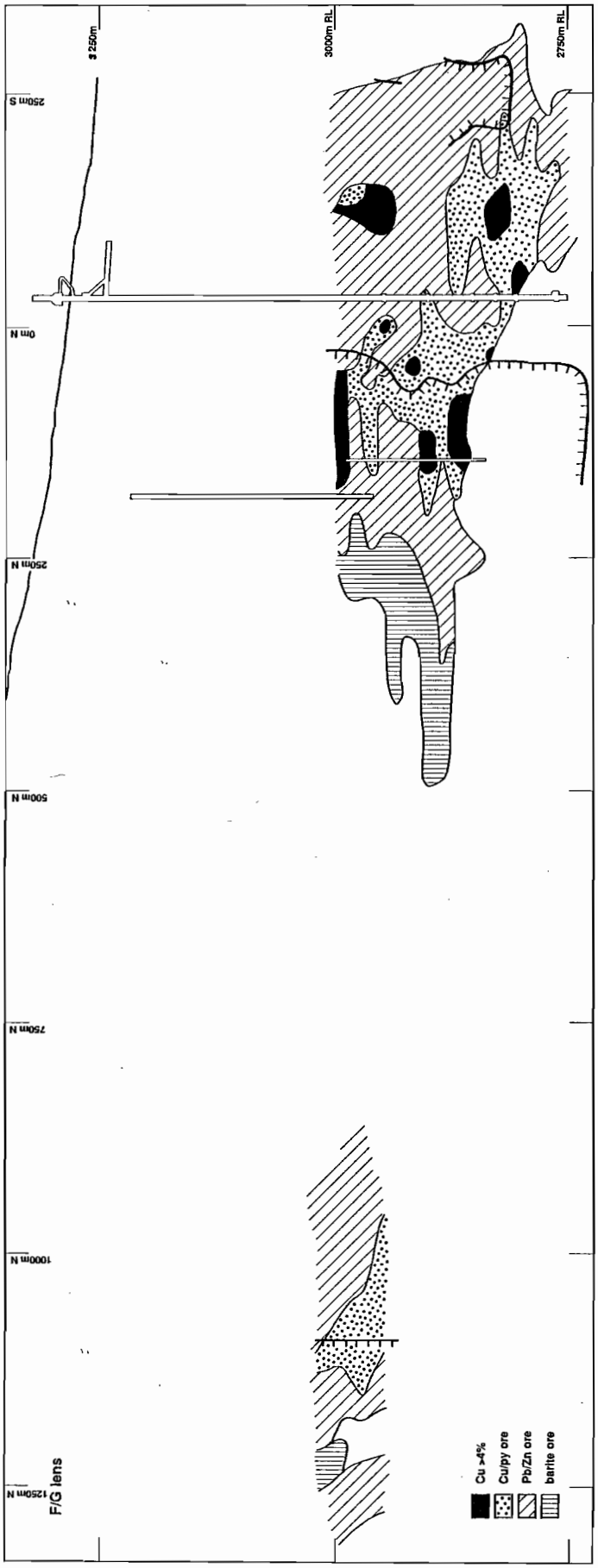

Fig. 8 Long section for F, G and A/B lenses based on a simplistic interpretation of level plans. Thick hatched lines show positions of syn-depositional normal faults with hatching on downthrown side.

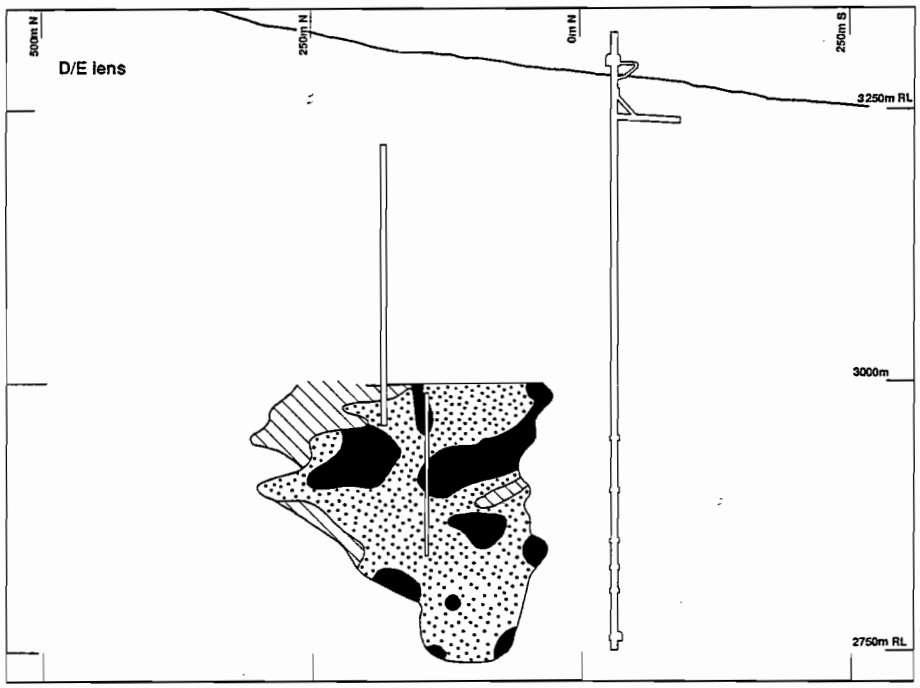

Fig. 9 Long section for D/E lens based on a simplistic interpretation of level plans. See Fig. 8 for legend.

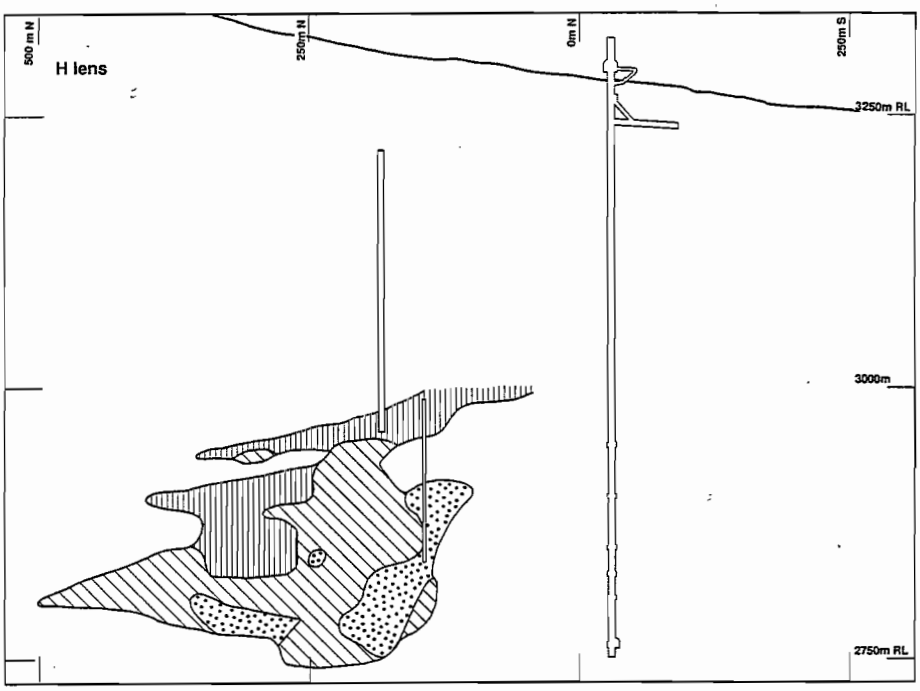

Fig. 10 Long section for H lens based on a simplistic interpretation of level plans. See Fig. 8 for legend.

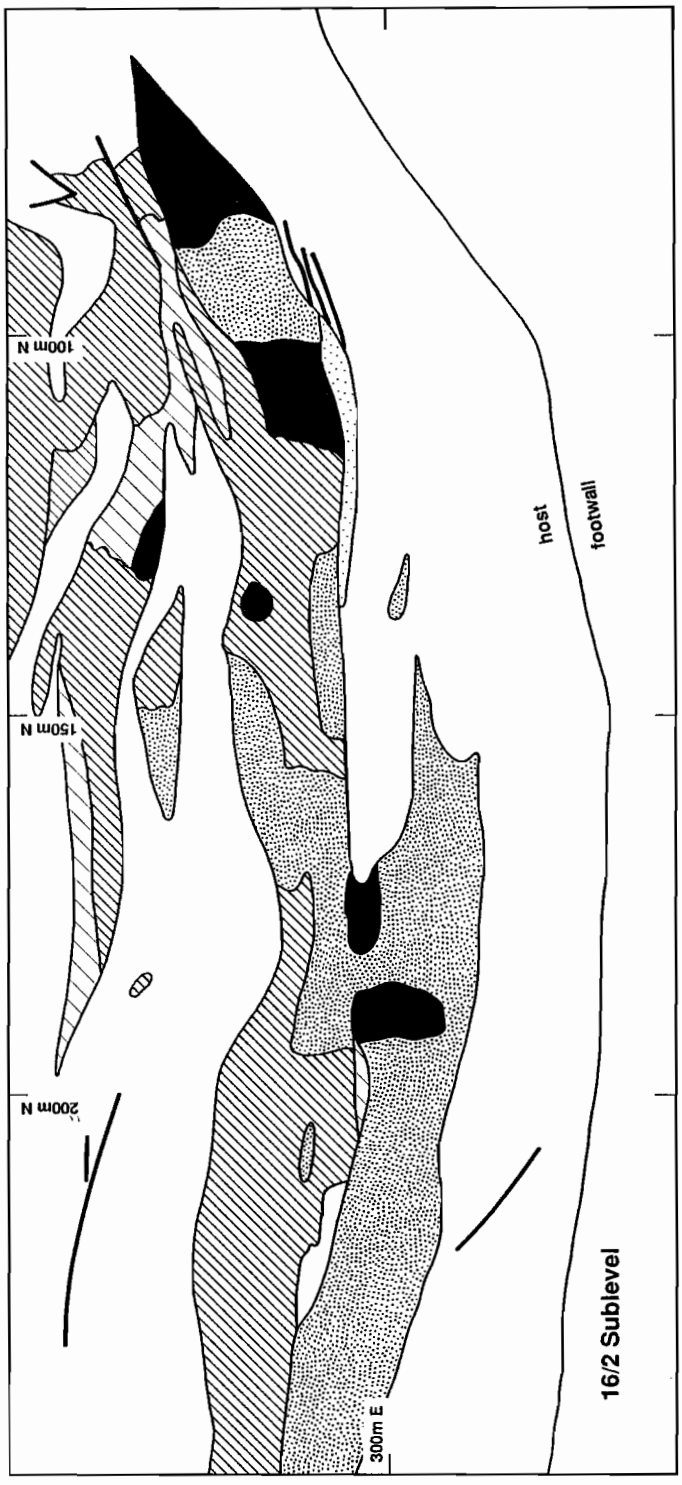

Fig. 11 Extract from 16/2 level plan showing the intense Cu-pyrite zone at 175m N which penetrates right through E lens supporting a model of stacked lenses in this part of the mine. See Fig. 2 for legend.

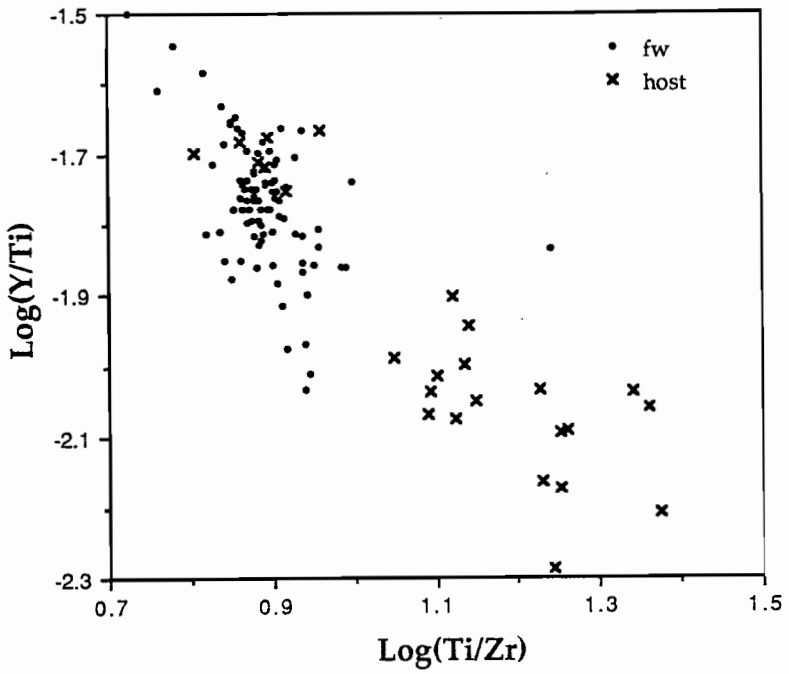

Fig. 12 Immobile trace element diagram. Footwall (dots) and host sequence (crosses) compositions from Rosebery. Data are from Naschwitz (1985).

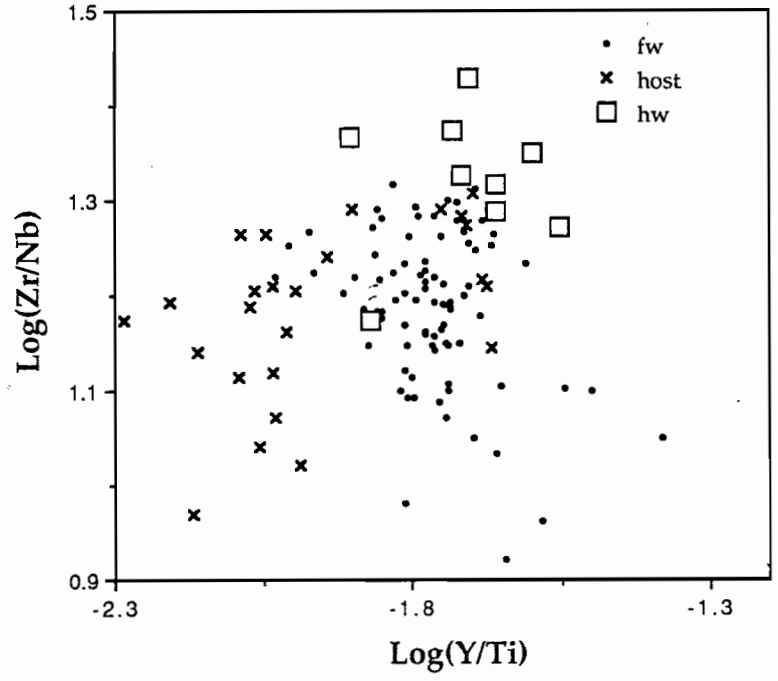

Fig. 13 Immobile trace element diagram. Footwall (dots), hanging wall (squares) and host sequence (crosses) compositions from Rosebery. Data are from Naschwitz (1985).

Appendix 1

Foliation–boudinage control on the formation of the Rosebery Pb–Zn orebody, Tasmania: Discussion

R.F. Berry
Centre for ore Deposit and Exploration Studies

INTRODUCTION

Aerden (1991) has put forward a model for Rosebery ore genesis which conflicts with the weight of structural, geochemical and isotopic evidence which demonstrate a subhorizontal pyrite bands, intense rotational deformation of the ore with the development of a fine mylonitic foliation, and a patchy post-kinematic recrystallisation. The first stage of comformable ore lenses is exemplified in the northern Rosebery ore body where there is very limited Devonian faulting.

Syn-tectonic quartz carbonate veins are common throughout the mine. These are closely related to faults which are oblique to the cleavage and with drag of the cleavage indicating reverse movement. The faults were active during S_3 cleavage development as they produced strongly cleaved zones and the veins in the fault zones are folded and boudinaged consistent with continued flattening on the cleavage. The vein systems indicate syn-tectonic mobility of silica and carbonate and may suggest remobilisation of the ore. However these veins are variably mineralised depending on their environment. In barren host sequence they have no sulphide phase. In banded sphalerite ore they contain galena and sphalerite. In pyritic ore, they contain chalcopyrite. This is strong evidence that sulphides have not been transported by this fluid movement. These vein systems do not contain economic concentrations of base metals.

Where the boundaries of the ore lenses are not faulted the asymmetric nature of the alteration is apparent (Green et al., 1981; Naschwitz, 1985; Huston & Large, 1987; Naschwitz & van Moort, 1991). Some of the ore lenses are truncated sharply at the low angle unconformity at the top of the host sequence.

In summary, while Devonian syn-kinematic fluids have produced quartz– carbonate veins throughout the mine, all the available evidence suggests that they did not introduce significant quantities of metals. Evidence from the southern portion of the mine (e.g. Solomon et al., 1987) suggests that granite related Devonian fluids have removed metals from the Rosebery ore lenses. The major mineralisation is pre-kinematic, conformable and has an asymmetric alteration pattern consistent with a syn-genetic origin.

SPECIFIC COMMENTS

While the foliation boudinage structures reported by Aerden (1991) are common throughout Rosebery and especially in the area from 0 m N to 300 m N, they are not related to mineralisation. Rather the extensive quartz carbonate veining which is found in these zones is essentially barren of sulphides. These structures are very common in a horizontal direction, sub-perpendicular to the stretching direction, but I have not observed any vertical examples. As such it is unexpected that the mineralised zone, representing in this model the largest and strongest of the foliation boudinage structures, is essentially elongate down dip.

The model for ore localisation suggested by Aerden (1991) implies that the major mineralisation in the central part of the mine (about 50 m N on the mine grid) is the result of strong extension in both vertical and horizontal directions at this locality. This conclusion is totally incompatible with the well defined thickness distribution of the host sequence in the vicinity of the mineralisation (Fig. 1). In this region the host sequence for the mineralisation is dramatically thickened. There is no evidence from the sur-

rounding lithogies of knecking in either horizontal or vertical direction at the ore position as suggested in Fig. 12 of Aerden (1991).

The microstructural evidence for mineralisation at Rosebery are totally ambiguous with respect to the age of formation. The textures shown in Figure 9 of Aerden (1991) indicate that sphalerite is stable and growing during S_3. There is no evidence for the source of the sphalerite which I argue is remobilised from within diffusion range of a few mm (e.g. Etheridge et al., 1984). The use of the word "replacement" in this context is misleading.

The metal zonation within the mine is complex and the suggestion of a simple zonation from Cu-rich down dip does not do justice to the very complex zoning which varies dramatically from place to place in the ore. There are a number of centres and zoning can only be understood in a local context of a single ore lens. The metal zoning is at least as supportive of a syn-genetic ore body as it is of the foliation boudinage model discussed here.

Aerden (1991) dismisses the fault model of Berry (1990) on the basis that faults of the correct orientation have not been observed. I agree that faults steeper than cleavage are rare and unlikely to be significant. However I totally disagree with the cleavage distribution shown in Aerden (1991, Fig). The average dip of S_3 in the mine is 65° not 45° as suggested in this section. There are many faults with dips of 75°. For example, in Figure 5 of Aerden (1991) a fault parallel to cleavage is shown steepening to 75° while still parallel to cleavage. There are a large number of faults with dips around 75° in the host sequence near the major structure which offsets the ore lenses at 0–400 m N.

The deformation style of Rosebery Mine is shown well in sections between E and G lens (Fig. 3). There is a gradational contact through chlorite pyrite alteration to pyritic ore and then into banded sphalerite rich ore. In 16 mezzanine level at 400 m N this then changes sharply into a conformable sequence of siliciclastics. A minor fold occurs within this sequence and then it is cut off by a fault with drag folding against the ore horizon. The ore is again conformable overlain by the less altered siliciclastics of the host sequence. Within a few metres the level of deformation in this sequence increases with a zone of fold tightening up against the next major reverse fault which again repeats the ore horizon. A very similar style of faults related to stratigraphic repetition is shown in sublevel 15/2 at 500N. The mesoscopic structures observed in the mine strongly support repetition of the ore horizon by steep reverse faults subparallel to the dominant cleavage.

ACKNOWLEDGEMENTS

The research reported here has been made possible by the support of Pasminco mines and of AMIRA. The isopach map shown as Figure 1 is a simplification of an unpublished Pasminco long section.

REFERENCES

Aerden D. 1990. Formation of a massive sulphide orebody by syn deformational host rock replacement in a ductile shear zone, Rosebery, Tasmania. *Geol. Soc. Aust Abstracts* 25: 174–175.

Aerden D.G.A.M. 1991. Foliation-boudinage control on the formation of the Rosebery Pb–Zn orebody. Tasmania. *J. Struct. Geol.* 13: 759–775.

Berry R.F. 1990. the structure of the Rosebery Mine Sequence, western Tasmania. *Geol. Soc. Aust. Abstracts* 25: 278–279.

Brathwaite R.L. 1972. The structure of the Rosebery ore deposit, Tasmania. *Proc. Aust. Inst. Min. Met.* 241: 1–13.

Brathwaite R.L. 1974. The geology and origin of the Rosebery ore deposits. *Econ. Geol.* 69: 1086–1111.

Etheridge M.A., Wall V.J. & Cox S.F. 1984. High fluid pressure during regional metamorphism and deformations: implications for mass transport and deformation mechanisms. *J.G.R.* 89: 4344–4358.

Green G.R. ,Solomon M. & Walsh J.L. 1981. The formation of the volcanic-hosted massive sulphide deposits at Rosebery, Tasmania. *Econ. Geol.* 76: 304–338.

Gulson B. L. & Porritt P.H. 1987. Base metal exploration of the Mount Read Volcanics, Western Tasmania: lead isotope signatures and genetic implications. *Econ Geol.* 82: 291–307.

Huston D.L. & Large R.R 1988. Distribution, mineralogy and geochemistry of gold and silver in the north end orebody, Rosebery, Tasmania. *Econ. Geol.* 83: 1181–1192.

Naschwitz W. 1985. Geochemistry of the Rosebery ore deposit. Unpublished PhD thesis, University of Tasmania.

Naschwitz W. & van Moort J.C. 1991. Geochemistry of wallrock alteration, Rosebery, Tasmania, Australia. *Applied Geochemistry*, 6: 267–278.

Solomon M., Vokes F.M. & Walshe J.L. 1987. Chemical remobilisation of volcanic-hosted sulphide deposits at Rosebery and Mt. Lyell, Tasmania. *Ore Geology Reviews* 2: 173–190.

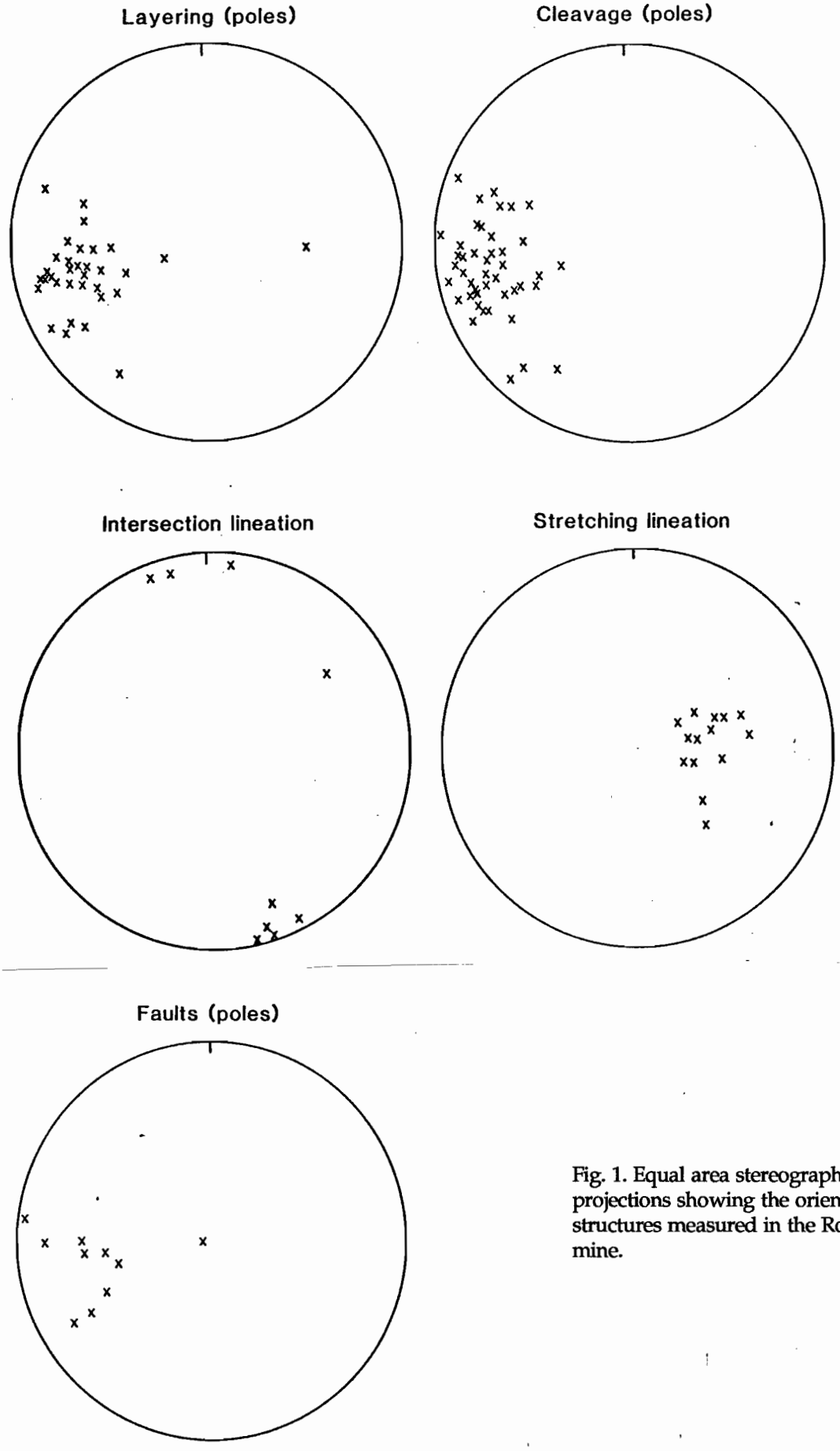

Fig. 1. Equal area stereographic projections showing the orientations of structures measured in the Rosebery mine.

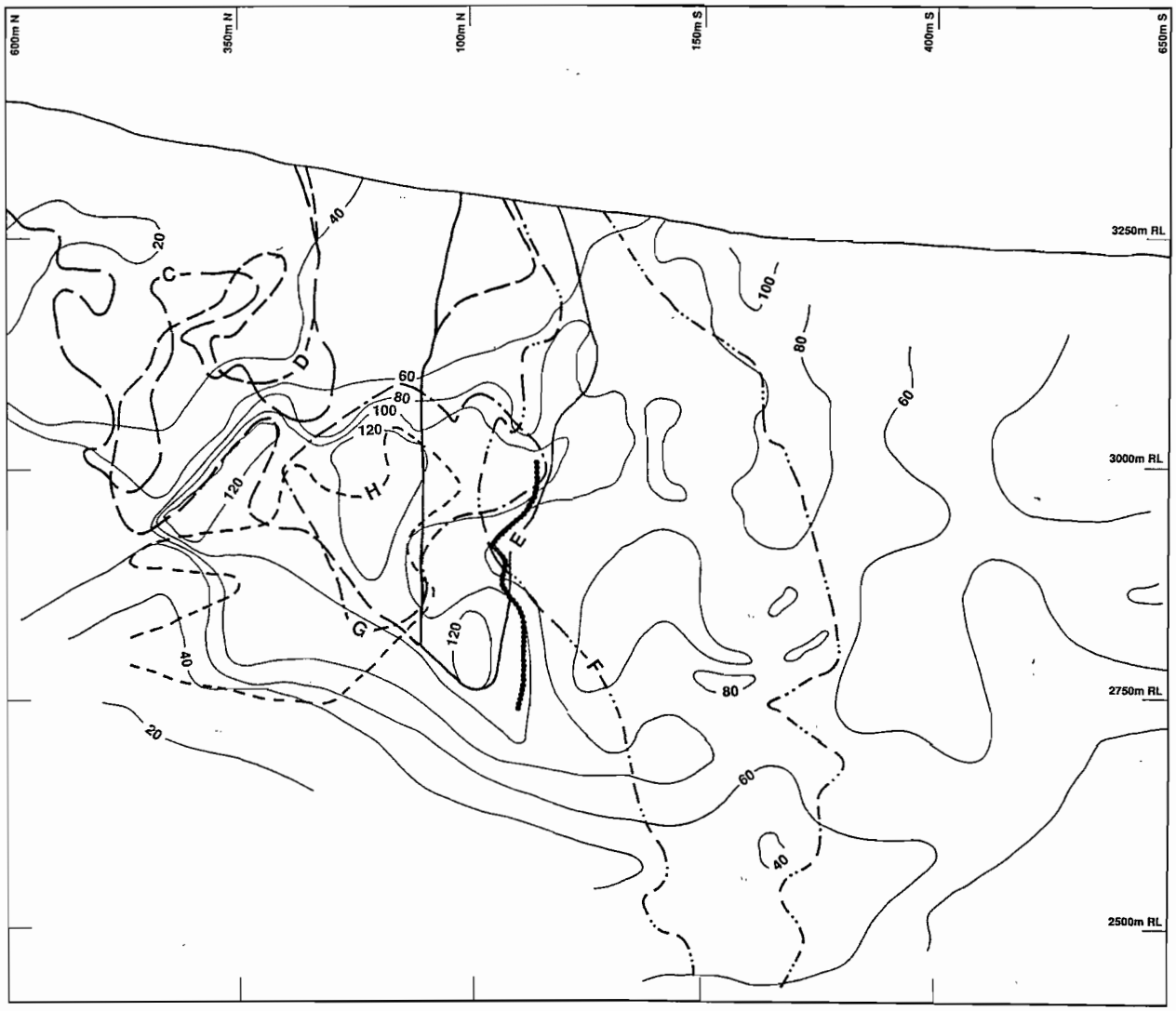

Fig. 2. Isopachs of the host sequence in the Rosebery orebody.

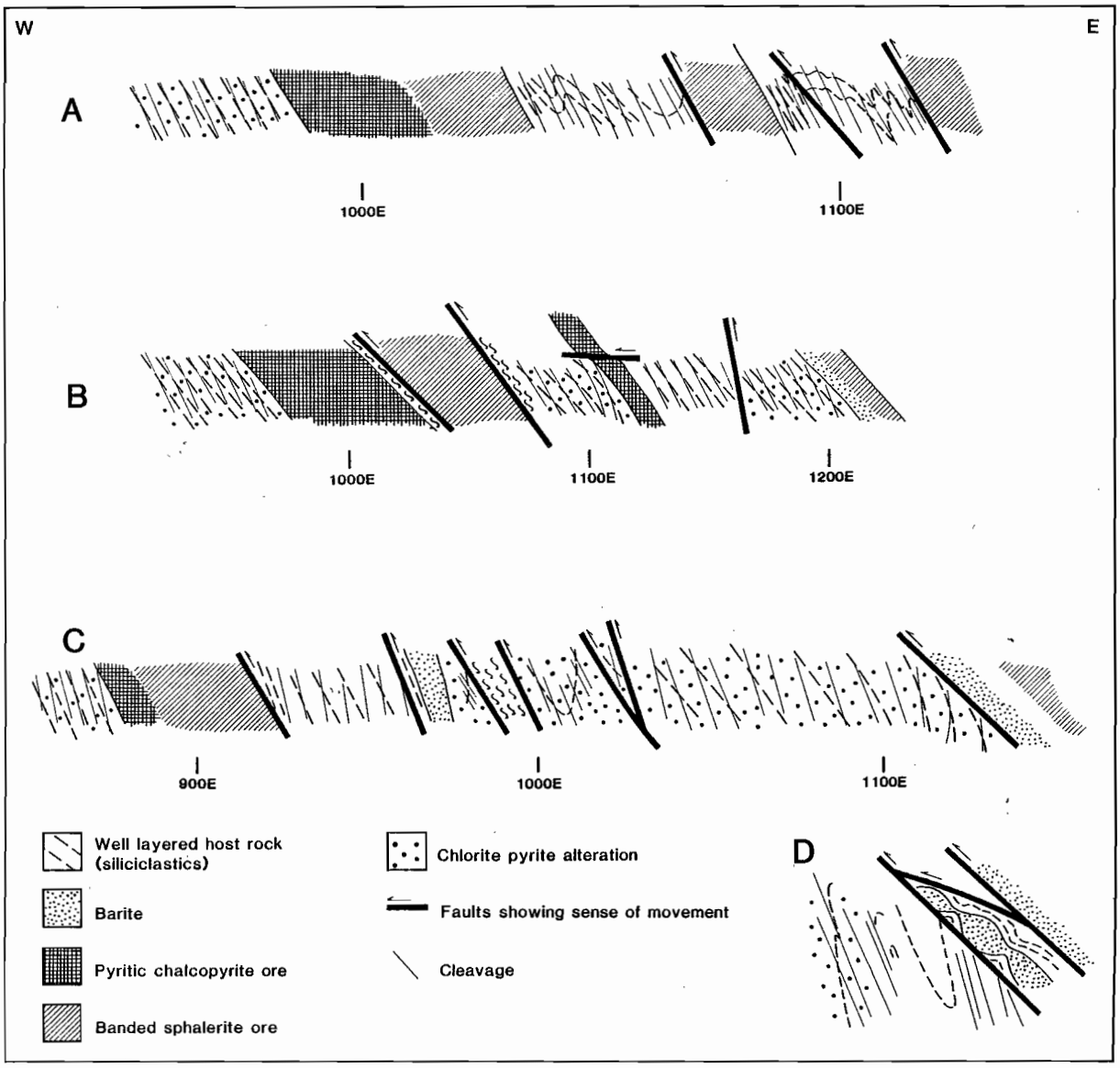

Fig. 3. Sketches of geology on crosscuts from E to G lens. (A) at 16 Mezzanine level 120m N. (B) at 16 sublevel 2, 225m N. (C) at 15 sublevel 2, 150m N. (D) at 15 sublevel 2, 245m N

Victoria Pass to Queenstown Regional Section

R.F. Berry
Centre for Ore Deposit and Exploration Studies

ABSTRACT

A regional section from Queenstown was studied from exposures near the Lyell Highway. The structural style deduced was used to construct three regional NNE trending sections and an E–W along My Lyell. The sections emphasized the importance of high angle reverse faults in generating the Devonian structure. Shortening across the Linda Zone was about 8 km. This overprints the east directed earlier Devonian structures of the Great Lyell and King River Faults. The E–W section provides useful constraints on Cambrian tectonic models which are taken up in the Mt Lyell section of this report.

INTRODUCTION

A week was spent in the field determining the structural style of the Linda Valley and along the Lyell Highway to Victoria pass. The western section is poorly exposed except at the eastern end of the Linda Valley. The next section is dominated by Bell Shale which has been largely ignored in previous studies. Finally the structural complex area of the Nelson Valley and Victoria Pass has good exposures along the highway but this is largely along the major reverse faults and does not give a good view of the structural style. The area is covered by the Queenstown 1:25 000 (Corbett et al., 1989) and Lyell 1: 50 000 (Calver et al., 1987) scale maps. The geological interpretation below depends heavily on the lithological distribution and structures shown on these maps.

The last event in this area is the strong reverse faulting along the Linda Zone. Thus the first stage was to draw sections along NNE directions across the structures in this area. Subsequently a domain analysis of the Bell Shale correlate was used to locate major structures which predate the WNW striking reverse faults of the Linda trend. The east west section along the line through Cape Horn–Mt Lyell–King River Valley was chosen to largely lie on one block of the later structure.

STRUCTURAL STYLE — BELL SHALE CORRELATE

The slates of the King River Valley have a strong slaty cleavage (Fig. 1) which largely strikes NW but there are discrete zones of W strike, especially near the major faults. In the Linda Valley the dominant cleavage strikes W and and earlier N to NNW striking cleavage is visible locally within the Owen Conglomerate. Bedding defines a diffuse great circle distribution indicating a dominance of the WNW fold tend but supporting complex fold interference patterns. The presence of discrete zones of overturned bedding is widely recognised. A good example was exposed on the old Lyell Highway at 901E 405N (Fig. 2). At this point the overturning is related to NE directed thrusting. The bedding/cleavage intersection is also of critical interest in this area. Over most of the slates the intersection plunges north but in a narrow zone along the King River it plunges to the south. The weak stretching lineation in the slaty cleavage is nearly vertical throughout so this is not related to refolding but rather implies an earlier generation of fold.

DOMAIN ANALYSIS

Based on the variations observed in bedding and bedding cleavage intersection the area of the Bell Shale correlate was sub-divided (Fig. 3). The zone of south plunging bedding cleavage intersection lies along the King River. The close association with east dipping and facing Florence Quartzite correlate is interpreted here as evidence of a pre-cleavage drag fold along the King River Fault (Fig. 4). The distribution of this zone is moderately well constrained on the basis of the Lyell 1:50 000 map sheet. East of this zone the area of north and south dipping limbs was used to define major fold closures (syn-S_2). The western zone has dominantly north dips until north of the Eldon River junction. In contrast, across most of the area south dips dominate except in the SW. The interpretation here is of a transfer fault between the south dipping reverse faults of the Linda Zone and the north dipping reverse faults of the northern margin of the Comstock Valley. The southern section of this fault is associated with overturned bedding and shallow west dipping cleavage. The thrust recognised on the old Lyell Highway (Fig. 2) is very close to the transfer fault and is shown here. Thrusts inferred from the sections (Figs 5, 6, 7) have been added to keep Bell Shale correlate thickness below 3 km. The position of thrusts west of the transfer fault is poorly constrained and only suggested positions are shown.

The remainder of the structural map represents the major faults considered in this study. Major movements are shown where some evidence is available but most of these faults have a number of movements. The general view is then of a major rigid body (Owen Conglomerate) acting as an indenter and distorting the strain field.

LINDA VALLEY

The western end of the Linda Valley is well exposed and easily accessible I represents a microcosm of the structures occurring along the western margin of the King Valley. Interestingly, there is very little evidence of north south faulting. The area is dominated by north side up high angle reverse faults often as axial plane thrusts (Fig. 9) especially along Linda Creek. These faults have extensive quartz veins and localised chloritic alteration on them similar to Owen Conglomerate near the Great Lyell Fault. The are overprinted by a dextral wrench movement (Fig. 1) similar to that reported at Mt Lyell.

REGIONAL INTERPRETATION

Linda Zone

Three sections were drawn across the Linda Zone to show the nature of the structure (Figs 5, 6, 7). Some assumptions are needed in drawing these sections. In line with the limited data on fault dips, an average 70° dip was assumed for reverse faults. The thickness of the section from the Gordon Group to the Florence Quartzite correlate can be inferred from the maps available, but the Bell Shale correlate appears to be very thick. If there are no major faults other than those shown on the Lyell 1:50 000 map the Bell Shale must be 6 km thick. This contrasts with the thickness measured elsewhere of about 1 km. In drawing the sections here a thickness of 3 km was assumed. While this is still to thick compared to measure sections, it only requires one additional reverse fault and the position of the structure is relatively well constrained. If a 1 km thickness is assumed, then several thrusts need to be identified and there is not sufficient data available to constrain these structures at present. The sections were drawn using the kink method which produces parallel folds. This is a poor assumption for the strongly cleaved rocks of this area but there is insufficient data for a more sophisticated approach. The sections were drawn bearing in mind the restrictions of restorable sections but are too short to check if these restrictions have been met.

The major feature of section I (Fig. 5) is the strong northward transport direction combined with the backthrusting within the Victoria Pass area. The consistent northward dips in the Bell Shale correlate require an additional reverse fault to keep the stratigraphic thickness to a reasonable amount.

The second section (II) has a thrust out syncline missing from section I. The section is drawn with the Gordon Group acting as a decollement although there is no specific evidence for this. Both section show about 8 km of shortening which is equivalent to a 40 % shortening. This is compatible with the cleavage development in the slates.

Comstock Valley

A third section (Fig. 7) was drawn across the Linda and Comstock Valleys. Both are synclinal structures with high angle reverse faults on the limbs. The North Lyell Fault is anomalous in these sections because of the normal fault movement implied from the steep southern dip. No other faults of this type are known and thus all other faults are assumed to be high angle reverse. Some of these may be normal. The thickness of Owen in the Comstock Valley is limited by geophysical data in the eastern segment of the valley

which suggest a maximum thickness of 2 km. No minimum thickness can be obtained from this data.

Cape Horn–King Valley Section

Based on the NNE sections and the structural map (Fig . 3) a structural section was selected along Mt Lyell which avoids most of the WNW striking faults. This section has a number of interesting features. First a major fault (the King River Fault) is inferred with a size and history very similar to the Great Lyell Fault. Between the Great Lyell Fault and the King River, the thickness of Owen Conglomerate is relatively well constrained. The Owen Conglomerate is thick in the west and thins over the thickest Tyndall Group section. To the west of the GLF the position of Cape Horn and Comstock represent extreme limits to the Lyell mineralisation. A string of similar bodies is projected into this position. The Great Lyell Fault a Cape Horn is presumed to cut out the Haulage unconformity which is thus shown on the uplifted block. The structure at Marble Bluff has been projected beneath the King Valley Fault as the best available example for how the CVC is truncated against Precambrian metamorphic rocks.

SUMMARY

The Victoria Pass to Cape Horn regional section is dominated by two generations of high angle reverse faults. The first generation structures are the Great Lyell Fault and the King Valley Fault. The second generation structures are north direct thrusts of the Linda Zone. The Linda Zone faults probably continue through to the Firewood Siding Fault. Both these structures are essentially Devonian in age. Cambrian structures along this line are considered in the Mt Lyell section.

Comstock and Linda Valleys are faulted synclines in which the intensity of faulting increases towards the thickest part of the Owen Conglomerate. The King River Fault has generated syn-S_2 quartz vein similar to the Great Lyell Fault suggesting it also trapped metamorphic fluids.

REFERENCES

Calver C.R. et al. 1987. *Lyell,* Tasmania. Tasm. Dept. Mines Geol. Atlas 1:50 000 map series.

Corbett K.D. et al. 1989. *Queenstown,* Tasmania. Geol. Surv. Tasm. 1:25 000 map series.

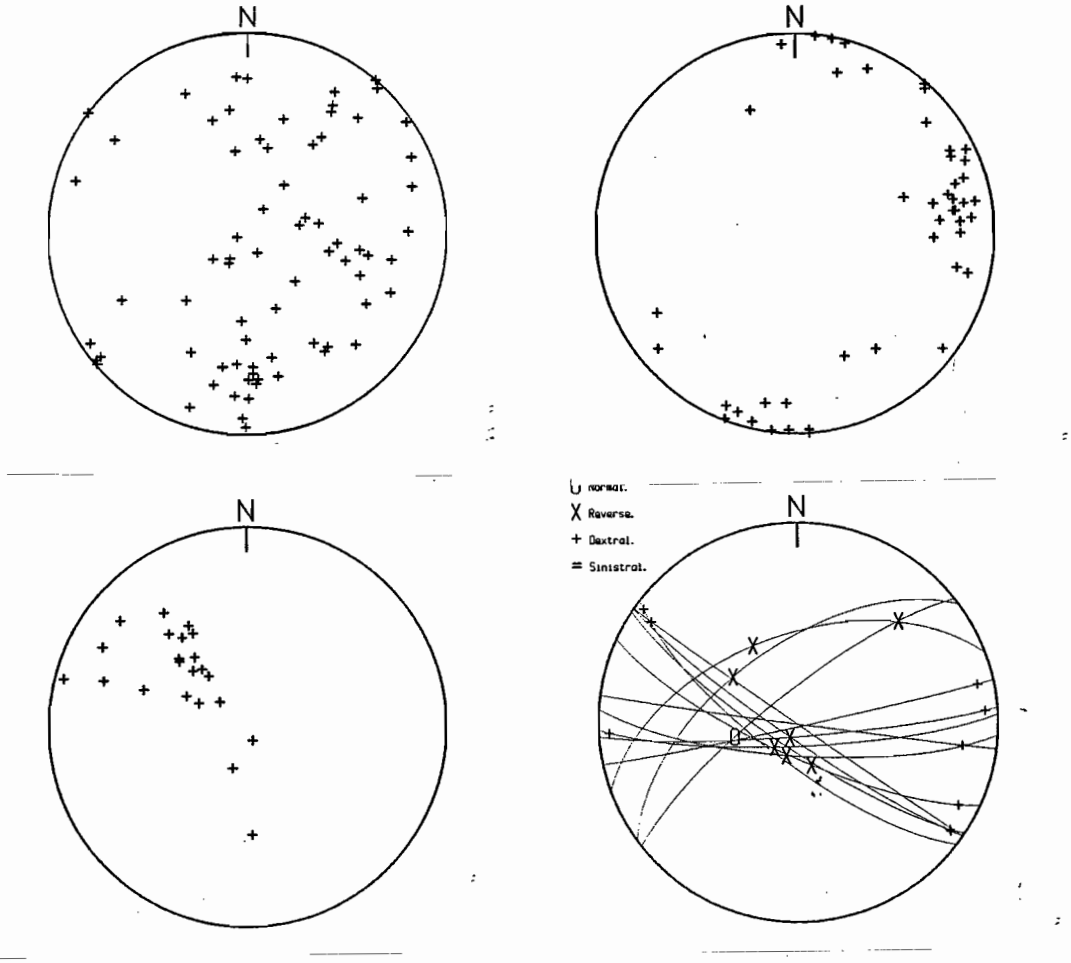

Fig. 1 Stereographic projection of structures east of Mt Lyell. (a) poles to bedding, (b) poles to slaty cleavage, (c) bedding/ cleavage intersection, (d) faults from the Linda valley and near the old King River Bridge.

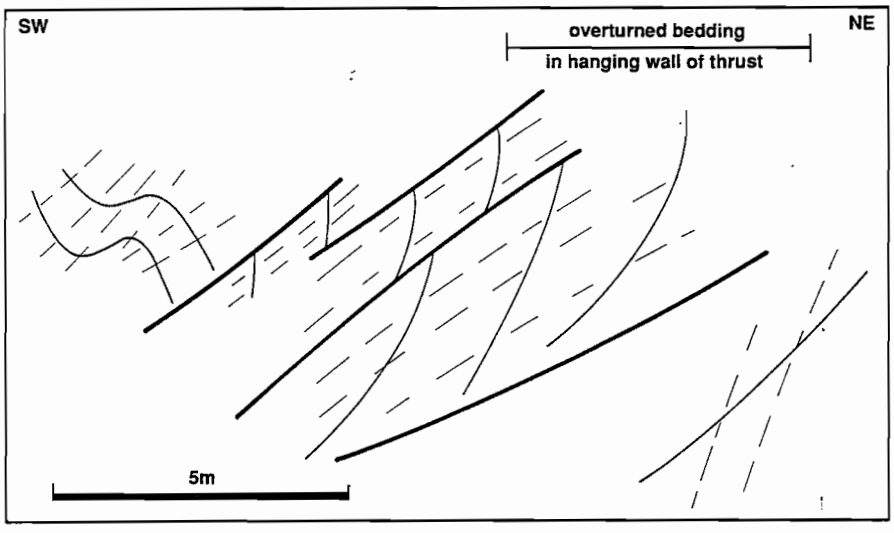

Fig. 2 Thrust fault in slates on the old Lyell highway at 901E 405N. Fault movement towards 010°.

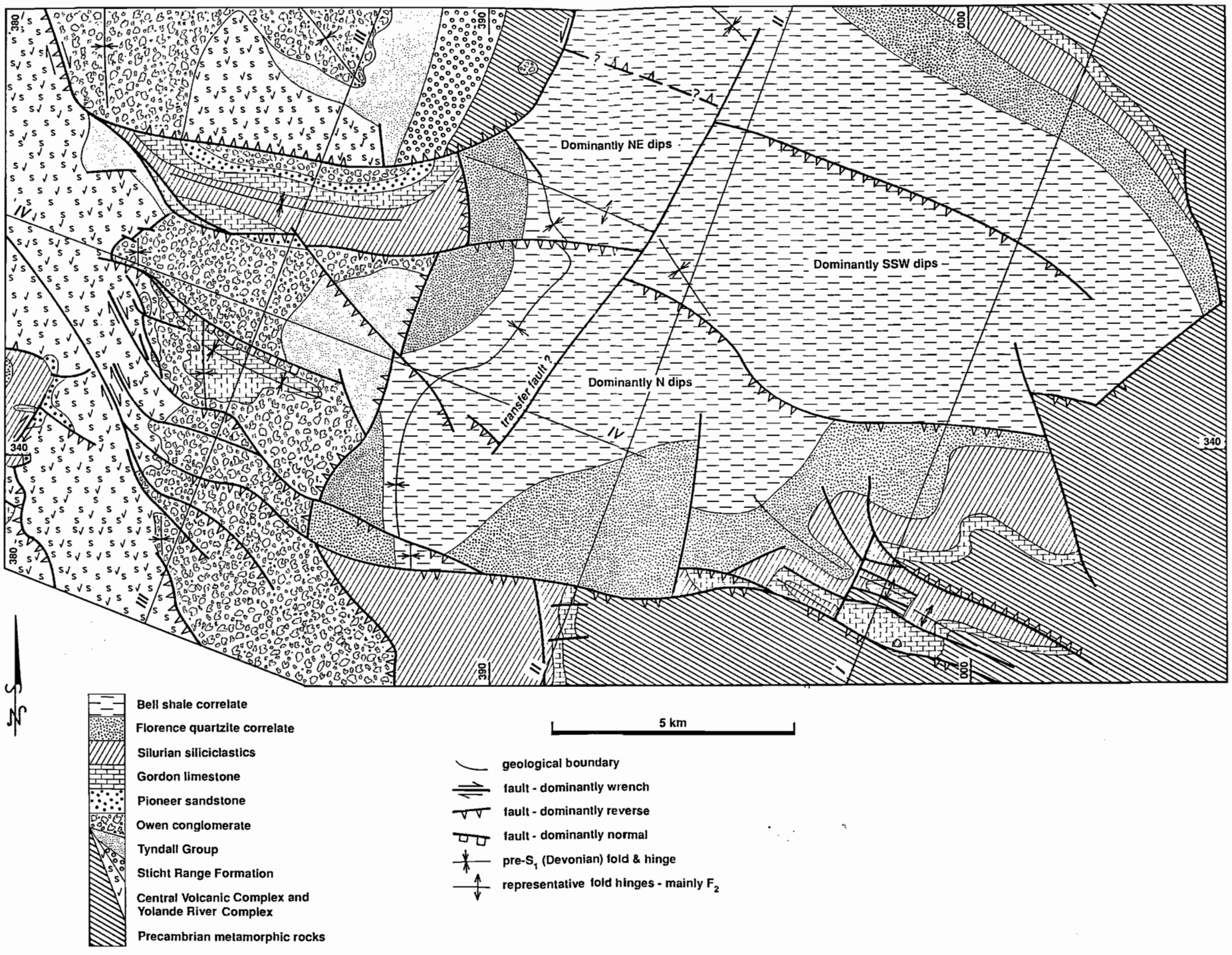

Fig. 3 Structural interpretation of part of the Lyell 1:50 000 map (Calver et al., 1987). Structures within Bell Shale correlate are from domain analysis and from the sections shown assuming maximum thickness of the Bell shale correlate of 3 km.

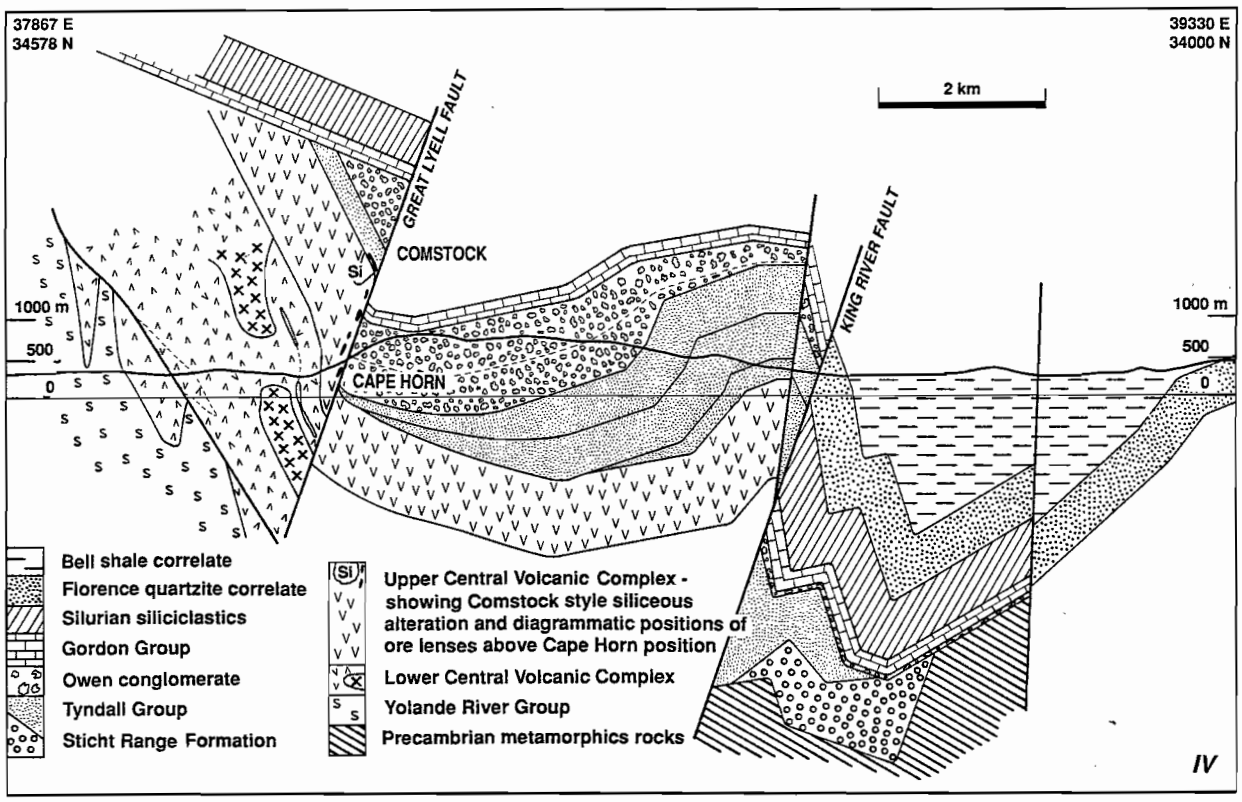

Fig. 4 Cross section from Glen Lyell Fault across Cape Horn and Mt Lyell to the King Valley. Position of section shown on Fig. 3 as IV. Legend as on Fig. 3

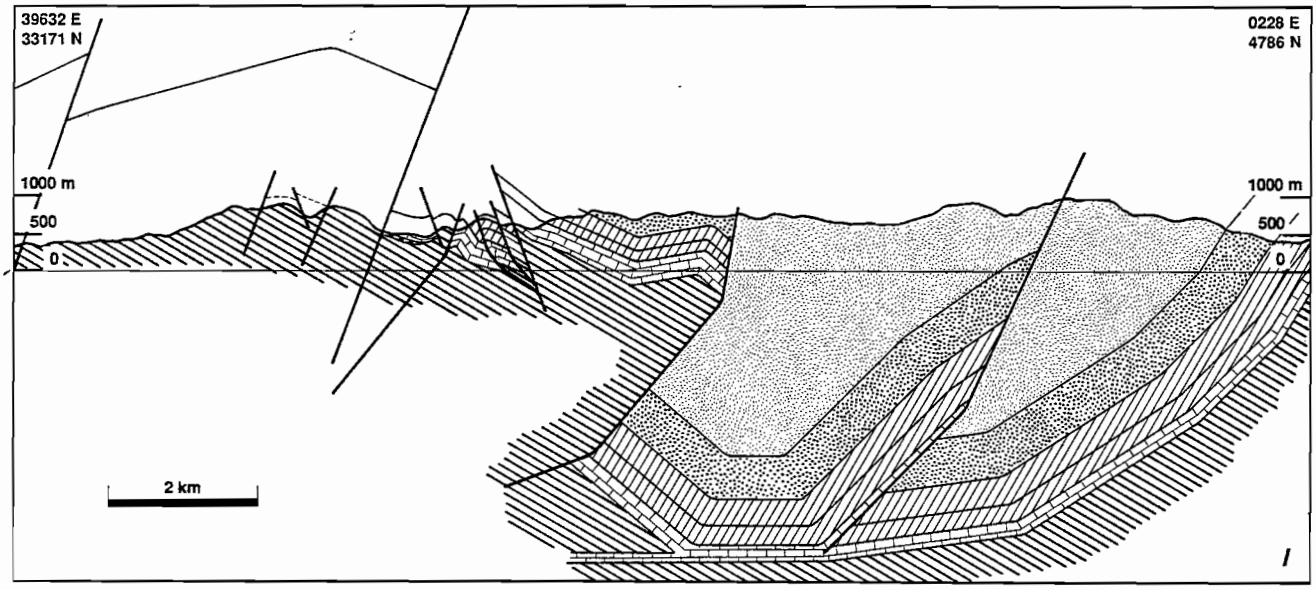

Fig. 5 NNE trending cross section through Victoria Pass. Position of section and legend shown on Fig. 3.

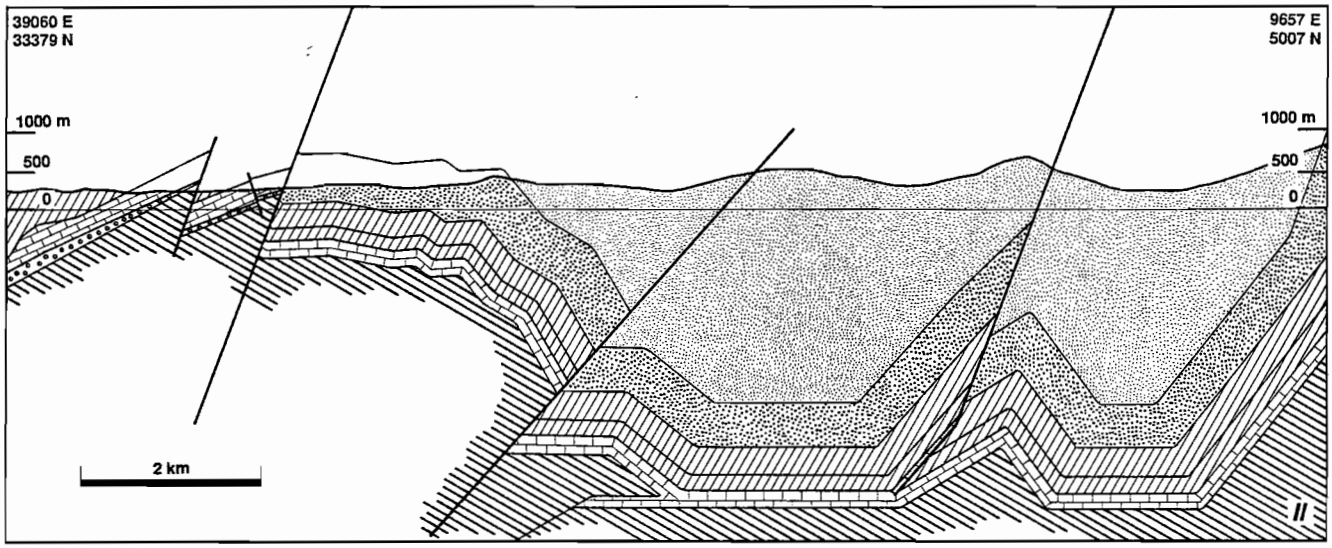

Fig. 6 NNE trending cross section through Linda Zone at the Princess River. Position of section and legend shown on Fig. 3.

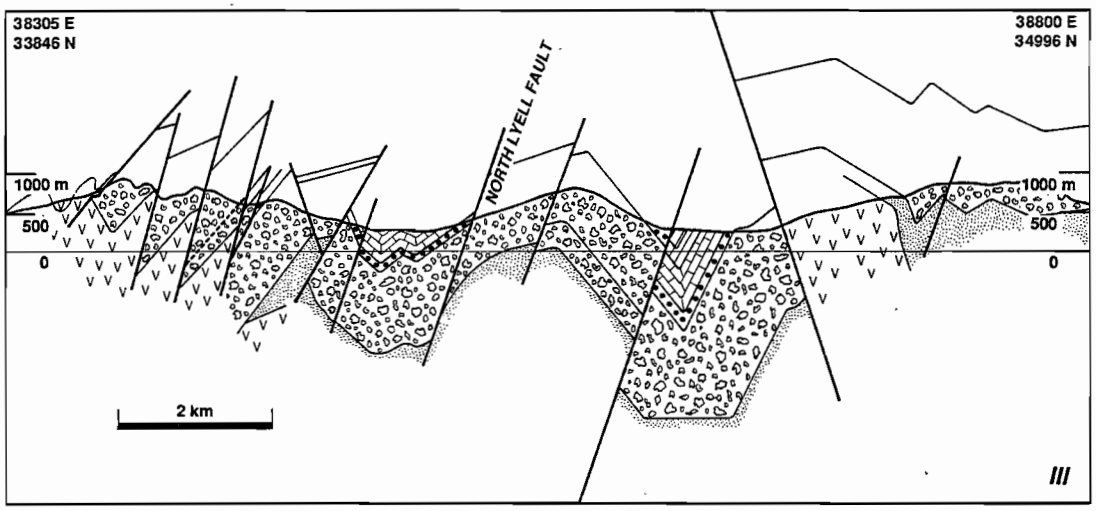

Fig. 7 NNE trending section along the main range of Owen Conglomerate. Position and legend as on Fig. 3.

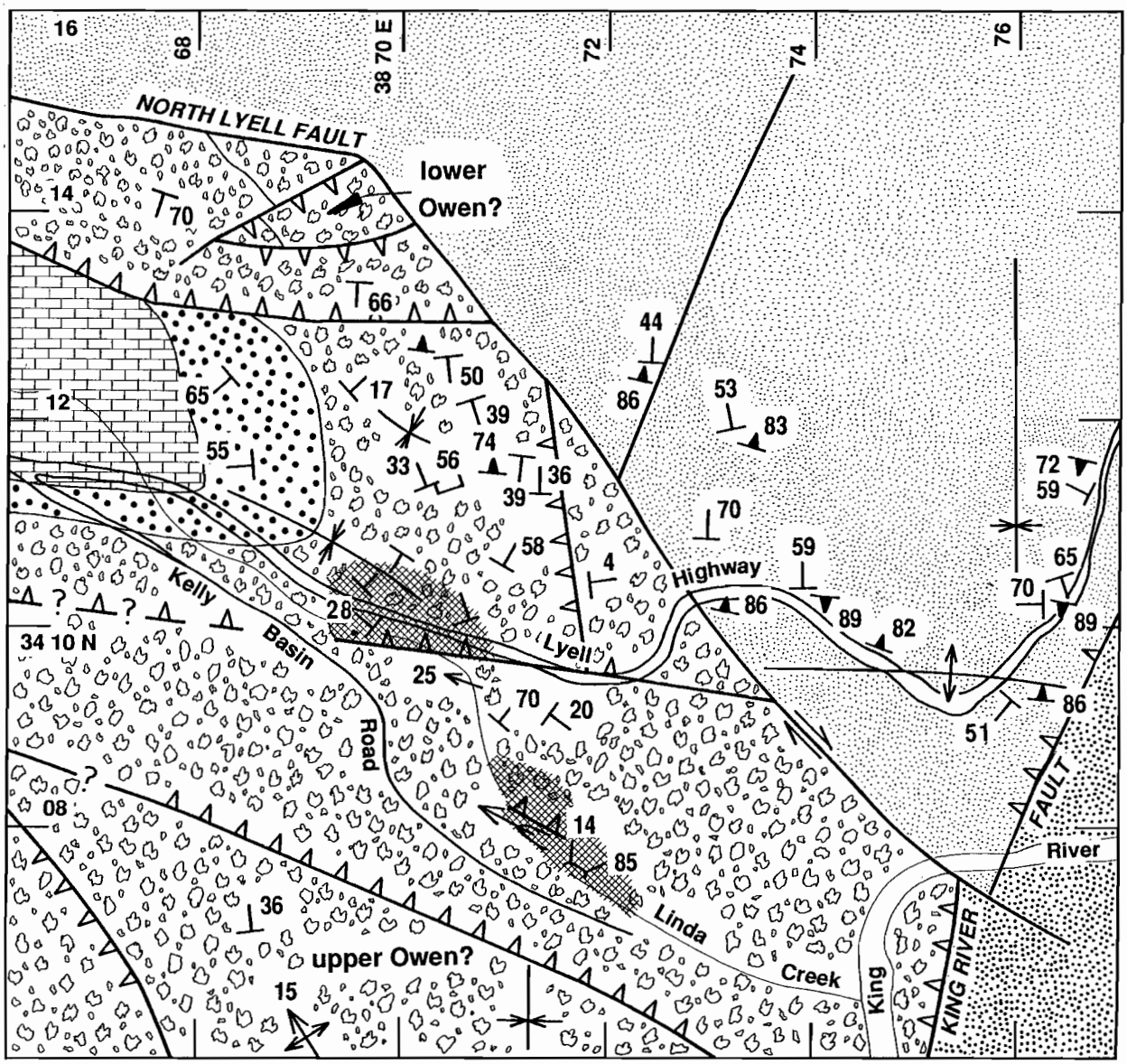

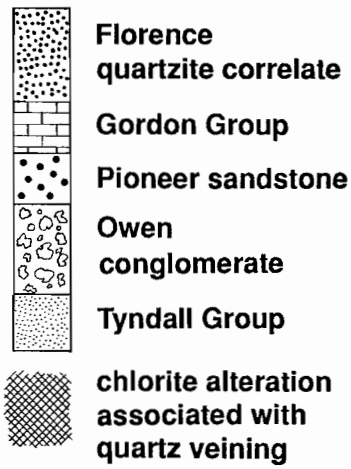

Fig. 8 Interpretation of the geology at the eastern end of the Linda Valley. Modified from Corbett et al., 1989.

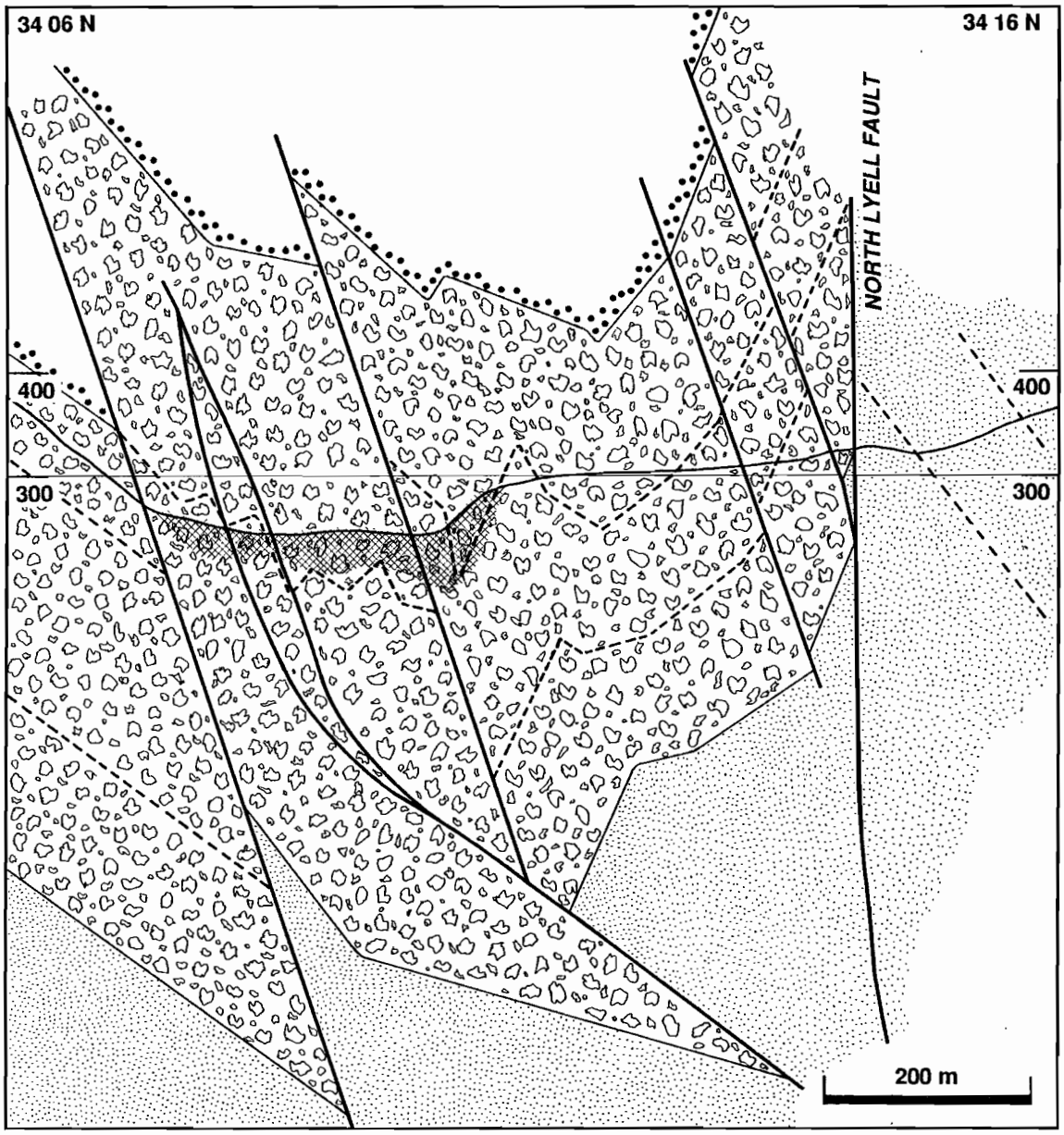

Fig 9 N trending section across Fig. 8 at 820E.

Mt Lyell Mine Leases

R.F. Berry
Centre for Ore Deposit and Exploration Studies

ABSTRACT

Further work on the Lyell Leases confirms the very simple east facing structure NE of the Glen Lyell Fault. The contrast in structure with the folding and faulting south of Queenstown strongly supports the existence of a Cambrian transfer fault along the Firewood Siding Fault and its extension to the east in about the position of the Owen Fault. The syncline recognised by Corbett et al. (1989) along Whip Spur probably continues between Comstock and Mt Sedgwich. The Tyndall Group postdates the initial formation of this syncline. Although it has been effect by tightening of the structure in the Devonian. Circumstantial evidence for a Cambrian thrust event is slowly accumulating.

The Razorback/Blow structure is the result of a series of W to SW side up fault starting with a shallowly dipping structure and gradually getting steeper until the last fault is subvertical. The additional data collected now supports a model of

(i) Haulage unconformity
(ii) east direct thrusting (age uncertain)
(iii) N–S folding (Devonian)
(iv) NNW cleavage (S_1)
(v) shallowly dipping NE directed thrusting
(vi) upright F_2 folds and high angle reversed faults (NW strike) and
(vii) dextral wrench faulting

The Haulage Unconformity is related to relatively shallow dips to the east. There is no evidence for overturning during the Cambrian. The age of the North Lyell mineralisation requires more work. Both S_1 and S_2 are visible in the altered Owen Conglomerate. The alteration does penetrate into Pioneer Sandstone and possibly into Gordon Limestone but the intensity drops of sharply at the contact suggesting that either the alteration is nearly finished at "Haulage time", two stages of alteration are required or some cryptic compositional control is restricting the effects of alteration.

INTRODUCTION

Previous reports have defined a complex structural history. The Devonian fault history involves N-S folds along high angle reverse faults followed by NNW cleavage and related reverse faults and finally a WNW cleavage with closely relate faulting which has three stages (a) NE direct thrusting (b) NE directed high angle reverse faults which are synchronous with upright folds and strong S_2 cleavage and (c) a brittle style set of dextral wrench faults largely post cleavage. This pattern is more complex than most area of western Tasmania because of the complexity of the Linda Zone deformation. The relative age of N striking reverse faults and S1 is the opposite of that found at Rosebery and Tullah.

The structure of the East Queen River and near the Iron Blow have been investigated in the light of the ongoing AMIRA project activities and especially in regard to the regional structure from Victoria Pass to the Glen Lyell Fault. A brief investigation was made of the East Queen River area to confirm the existing structural database. Further work in the Razorback/ Iron Blow area was carried out to support the structural interpretation.

Further work on the constraints on the North Lyell alteration were carried out by Mr I. Hart and will be reported elsewhere.

The structure west of the Glen Lyell Fault awaits the more detailed consideration of data collected from Strahan to the Queen River and is not reported here. The interpretation of this section depends on additional structural data south of Queenstown and will be completed along with the Mt Darwin section.

EAST QUEEN RIVER TO CAPE HORN

The section along the East Queen River provides an opportunity to check the structural relationships within the CVC. Cox (1981) interpreted the section east of the Glen Lyell Fault as a continuous east facing sequence and contrasted this with the facing west of the fault in Conglomerate Creek. This facing is supported by bedding data shown on the Queenstown 1:25 000 map. The consistent east facing contrasts with the section to the south of Queenstown and therefore required checking. I carried out traverses along the East Queen River and on a creek section west of Western Tharsis (Fig. 1). There are few reliable stratigraphic facing indicators in these areas. A relatively good east facing was obtained on the Comstock road west of Cape Horn. Along the East Queen River, four low reliability facings were obtained all supporting an east facing. No evidence was found which suggested a reversal of stratigraphic facing in this area. The structure is a consistent steep dip to the east cut by numerous sub-vertical west side up faults. I only found evidence of late brittle dextral movement on the Glen Lyell Fault. The other faults are brittle ductile with a steep stretching lineation (Fig. 2). The effect of these faults on the section is small but they effectively thin the section. The CVC across this zone has an apparent thickness of 3 km which should be a minimum estimate.

The extension of the North Lyell Fault into the CVC has always been contentious. A major E–W fault was mapped by RGC geologists cutting the end of the major massive intrusive body at about 4430N. This fault boundary is exposed in the small creek at 8145E 4436N. It dips steeply north (c.f. steep south dip of North Lyell Fault) and has a north side up movement during D_2. Despite this it is the only possible extension of the North Lyell Fault found. The difference between these two structures is taken up by the shear zone exposed at ML 547 (Fig. 16 of Berry 1991). Since both faults probably started out vertical (as transfer faults) the present dip probably reflects the differences in F_2 fold patterns east and west of the edge of Cape Horn.

A section (Fig. 3) was drawn at 8380 N across the Lyell alteration zone and out to the Glen Lyell Fault. The Glen Lyell Fault shows an apparent W side down movement due to late brittle dextral offset, but other NNW striking faults in this region have small west-side up movement. Some of these are east dipping which gives an overall normal movement. The rapid thinning of the Owen Conglomerate in this area is emphasized by the difference between measured bedding and drill hole information on the position of the GLF. The alteration zone is very wide and a direct line between Western Tharsis and Royal Tharsis ore bodies produces the projected ore position on this section. While Tyndall Group rocks are exposed under Owen north of the North Lyell Fault, they are missing from the boundary on the western margin of Owen Conglomerate on Tharsis Ridge. The regional section (Berry this volume) along Mt Lyell suggests that the major thickness of Tyndall Group lies west of the thickest Owen Conglomerate in this region. Tharsis Trough is shown as a complex interaction between west side up faults, one of which predates the D_1 folds.

An important feature of this map is the distribution of Tyndall Group. The exposures in the SW corner of the map are probably south of the Firewood Siding Fault extension but indicate the Jukesian unconformity has cut out the whole CVC sequence at this point. Corbett et al. 1989 shows a west facing bedding in the CVC south of Mount Sedgwick suggesting a synclinal closure between Comstock and the Beatrice prospect. The Tyndall Group is shown as having a major high angle unconformity of this point. The mapping evidence along the south side of Mount Sedgwich indicates the Tyndall Group postdates this fold phase. The simple interpretation of this structure is shown in Fig. 4 for the structure at the time of Pioneer Sandstone deposition. This pattern will be discussed further below.

IRON BLOW AND THE RAZORBACK

The Iron Blow fault pattern is dominated by steep west dipping reverse faults overprinted by dextral movement (Fig. 5). At the Razorback, an early steep reverse fault pattern (correlate with D_1) is overprinted by southeast reverse faults and finally by dextral faulting . These striations support a composite D_2 event where SW–NE compression starts as high angle reverse faults and changes late in the history to brittle style dextral faults. This change is consistent with a rapidly uplifted block moving into a shallower, and therefore less constrained, structural position.

The faults at the Blow (Fig. 6) largely correlate with the early D_2 style and orientation.

There are several important structural features in this area. In the northern part of the Blow pit pyrite bands occur both as conformable and crosscutting vein sets. The crosscutting veins strike 340°, implying extension towards 250. This contrasts with the orientation of sandstone dykes within the volcanics west of the Owen Conglomerate (Fig. 7), which support a N–S extension. These relations suggest a different stress pattern during mineralisation in the Blow and that which was underway during Owen Deposition.

To the NNE of the Blow, the GLF is exposed as an apparently conformable contact with no evidence of strain. Pebbles project from the base of the lowest

sandstone and are not truncated. The 5 m of volcanics immediately beneath this surface are blocky and lack distinct bedding but there is no direct evidence of faulting. They may reflect a thin layer of Tyndall Group. The Haulage unconformity is exposed here and the Owen Conglomerate wedges out to less than 5m from the Lyell Schists. The Haulage unconformity has a low angle, about 20°, and the level of strain suggests this is the result of flattening so that the original angle was more like 40°. The Haulage syncline should be exposed on the ridge to the north but is faulted out as is the Pioneer Sandstone although the offset seems to be small (Fig. 8). On the section A–B this fault surface is interpreted as flattening under the corridor of Lyell schists between the Razorback and this point. A problem here is that the offset of the GLF on this fault is much greater than the offset of the Pioneer sandstone which suggests this fault was active in the Cambro-Ordovician. The section could be changed to make the difference less, assuming the Haulage syncline was originally only just above the present Razorback as suggested from the map distribution of east facing beds (Fig. 7).

The Razorback is a sample of Owen Conglomerate from east of the Haulage syncline (based on the structural style) which appears anomalous at this position west of the known position of the Haulage fold in the block immediately east (Fig. 7). This reflects the removal of Haulage structures by the shallow thrust fault shown in section A–B. This interpretation is supported by very low angle thrust planes exposed on the top of the Razorback (Fig. 5).

The exposure in the south end of the Blow pit (Fig. 9) contains both F1 and F_2 folds. The major synclinal structure is exposed on one of the benches. Two cleavages are clearly visible in this hinge. S_1 is a spaced cleavage which is approximately parallel to the axial plane of this "Haulage syncline" while the S_2 cleavage is clearly overprinting the major structure and produces the kink fold which trends at a high angle to the GLF. The Haulage syncline projects towards the GLF in a way that suggests it will be truncated by it just below the present waterline (350m above sealevel). The structure at the Razorback may be reproduce below this level.

The Razorback Fault (Fig. 7) is near vertical. It has a strong west side up movement. All other faults in the area are truncated indicating this is a very late stage fault. This view is supported by the absence of alteration or folding along the fault. The movement is nearly dip slip. The structural differences between the Razorback and the Blow, especially with regard to the position of the Haulage syncline support the offset section of the Gormanston Fault as shown in Fig. 7 although there is no outcrop at this position. This is also compatible with the small window of Lyell schists to the east of the Blow which correlates with embayment of the Owen Conglomerate at the Blow.

The cross fault at the SE end of the Blow is an early near vertical fault striking 250° It has been folded during D_2 giving the complex shape of the GLF at the southern end of the Blow pit.

THARSIS TROUGH/RAZORBACK

The structure of both the Tharsis Trough and the area west of the Razorback have been interpreted as the result of interaction of an early thrust with later high angle reverse faults. The age of this thrusting has a substantial significance for the age of mineralisation. If this structure is early it may be the cause of the Haulage unconformity much as suggested by Arnold (1985). The alternative is that it postdates the Haulage. Faults of this orientation are common along the western margin of the Owen conglomerate. They have been recognised both north (Margaret Fault) and south (8400E 3700N) of Mt Lyell (Corbett et al 1989). where they are unrelated to mineralisation. In both cases there is a spatial relation to N trending folds like the Haulage syncline. A very similar upturn was reported from the Farrell Range by Berry (1988). In none of these cases has an unconformity been found. The relationship of these faults to the Haulage is weakened by the recognition of N trending pre-S_1 folding in the Bell Shale correlate in the King Valley (Berry this volume).

The section at the Razorback has been drawn as if the movement on the thrust shown is pre-Pioneer Sandstone but this is not required by the presently observed structure. At this stage the age of this structure must remain ambiguous.

LARGE SCALE STRUCTURAL CONSTRAINTS

1. The strength of evidence supporting a series of unconformities in the Lyell area during the Cambrian is overwhelming. The CVC is restricted to a synclinal position cutting out underneath the Tyndall Group both near Marble Bluff in the east and near Queenstown in the west (Fig. 4). The Tyndall Group itself thins over the CVC suggesting an onlap relationship. A similar feature occurs in the thickness on the Owen conglomerate except the thickest development of Owen Conglomerate is further west on both sides of the CVC.
2. It was argued in Berry (1990) that the North Lyell mineralisation was pre-Pioneer. Further work (Hart this volume) on the North Lyell alteration is suggesting that this is much more extensive than suggested earlier and weakens this position

dramatically. Further work is being carried out to see if any differences are found between the styles of alteration in the North Lyell field and that in the Pioneer sandstone.

3. Further work on the Haulage unconformity has failed to find any perfect exposures of the Haulage unconformity which support a steep east dip or any zone of overturning during Pioneer Sandstone deposition.
4. The nature of the GLF in the Lyell area can now be seen as a strong onlap relationship complicated by strong faulting and folding, most of which substantially postdates the deposition. Owen Conglomerate style sedimentation is typical of syn-orogenic sedimentation. There are many examples of foreland conglomerates (very similar in depositional style to the Owen Conglomerate) which are related to thrusting. Woodward et al. (in prep) have suggested this style of deformation for northern Tasmania in the Late Cambrian.

The major feature of this type of conglomerate is that the sediment is derived from the upthrust block. To fit this model properly, the thrusting should be directed to the west so that the Tyennan block is uplifted. This may be consistent with the section shown in Fig. 4. Here the first syn-orogenic sediment is the Tyndall Group as it is stripped of the metamorphic rocks and the Owen Conglomerate represents a second stage. The accumulation further west is consistent with a system where erosion is slower than thrusting. In this model, the Haulage is a minor unconformity representing the ongoing loading of the basin as the thrusting top the west continues. this loading could produce either normal or reverse faults in the syn-orogenic sediments.

One advantage of this model is it explains the presence and orientation of sandstone dykes better. It also fits some of the other evidence in the belt for a latest Cambrian thrust event (e.g. the 500 Ma K/Ar date on the Arthur Lineament, the thrust geometry in the Miners Ridge area, thrusting proposed for Sorell Peninsula, evidence for early deformation on the Howards road section).

This represents the most favoured model at the moment but there is not enough critical data to reject the alternatives. A major problem with this model is that the evidence for early west directed thrusting within the CVC is hard to find and the extension of this structure to the north through the Lake Murchison area has not been recognised. These problems disappear in a more complex wrench model.

REFERENCES

Arnold G.O. 1985. Mt Lyell 1985: an exploration perspective. Unpublished report to Gold Fields Exploration.

Berry R.F. 1989. The history of movement on the Henty Fault zone: an analysis of fault striations. *Aust. J. Earth Sci.* 36: 189–206.

Berry R.F. 1990. Structure of the Queenstown area and its relation to mineralisation. Interim report. Unpublished AMIRA Report 1 for P291: 27–68.

Berry R.F. 1991. An excursion guide for the Mt Lyell Mining Lease with emphasis on the Great Lyell Fault, Haulage unconformity and North Lyell alteration. Unpublished AMIRA Report 2 for P291: 1–22.

Corbett K.D. et al. 1989. *Queenstown*, Tasmania. Geol. Surv. Tasm. 1:25000 map series.

Cox S.F. 1981. The stratigraphic and structural setting of the Mt Lyell volcanic-hosted sulfide deposits. *Econ. Geol.* 76: 231–245.

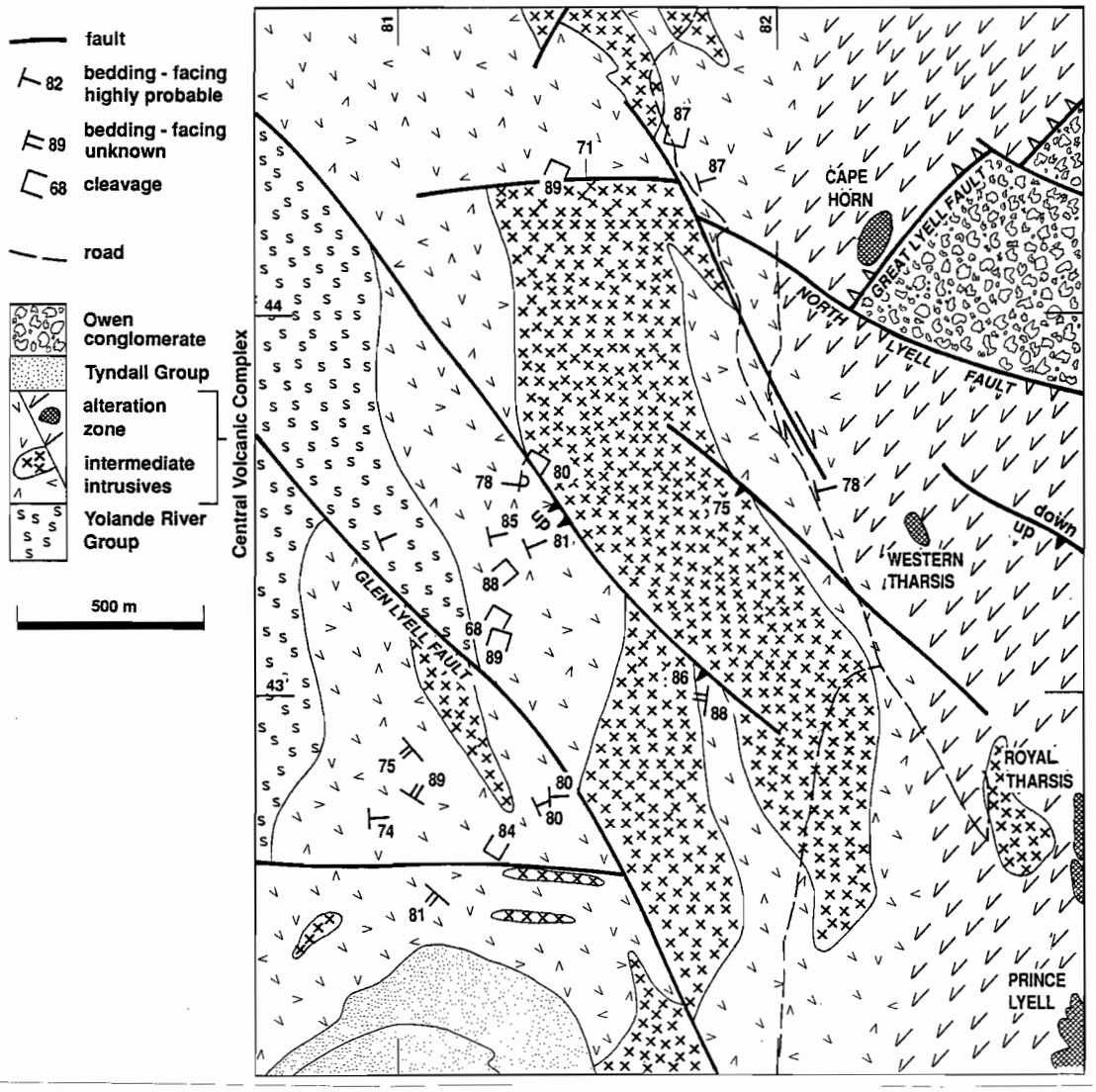

Fig. 1 Geology of the East Queen River area. Geology slightly modified from Corbett et al. (1989).

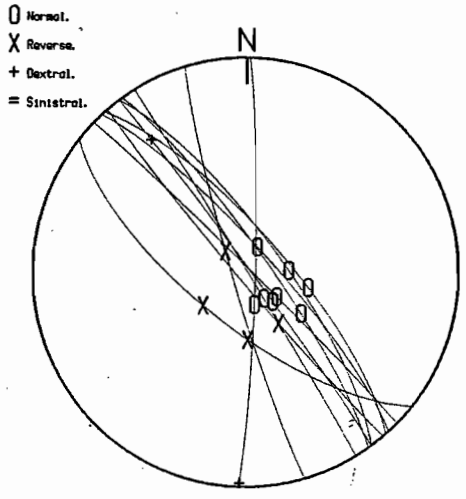

Fig. 2 Stereographic projection showing west side up fault orientation in the East Queen River area.

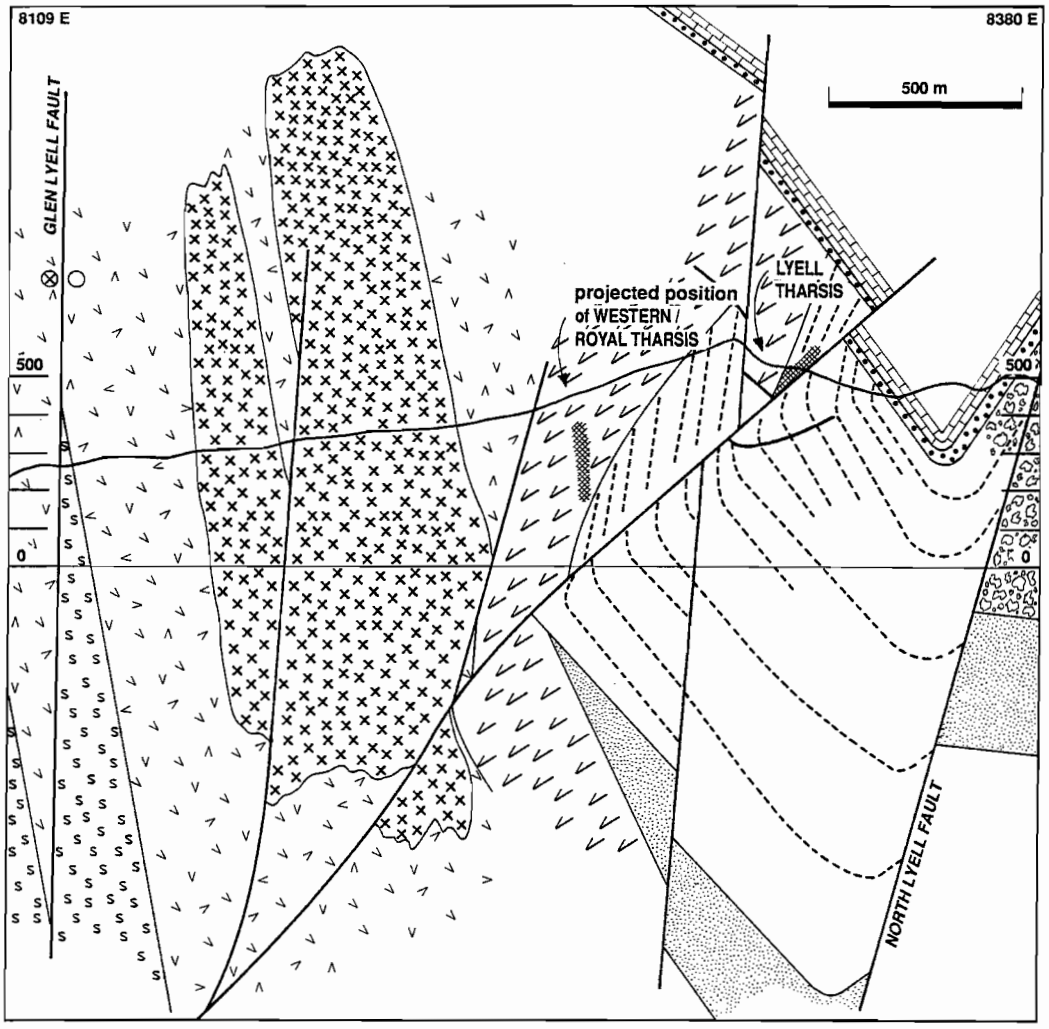

Fig. 3 Cross-section along the line 4305 N from the Glen Lyell fault to the North Lyell Fault.

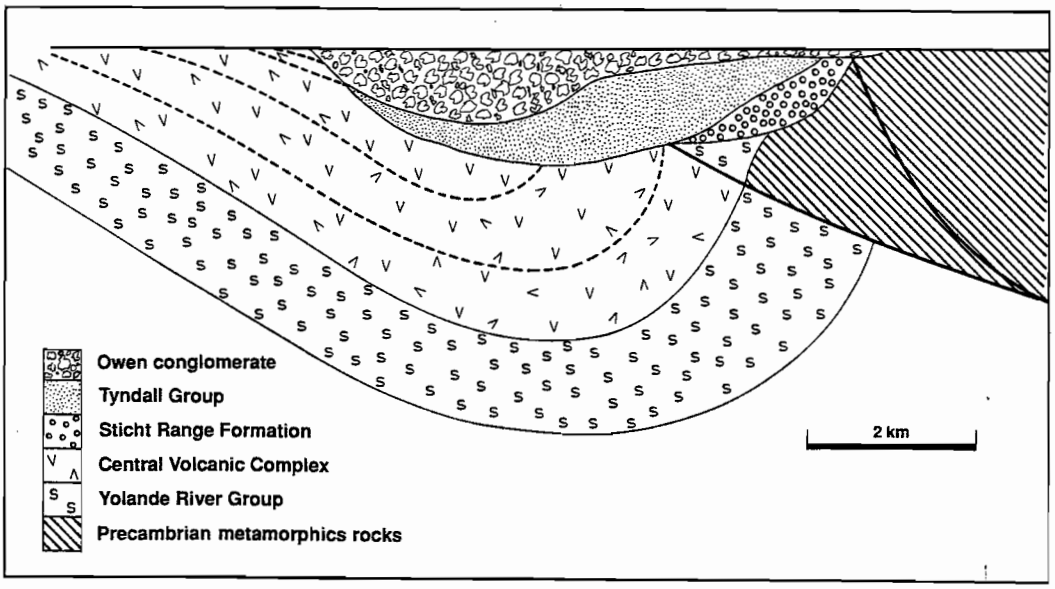

Fig. 4 Cartoon of an E-W section from Queenstown to the King River prior to Pioneer Sandstone deposition.

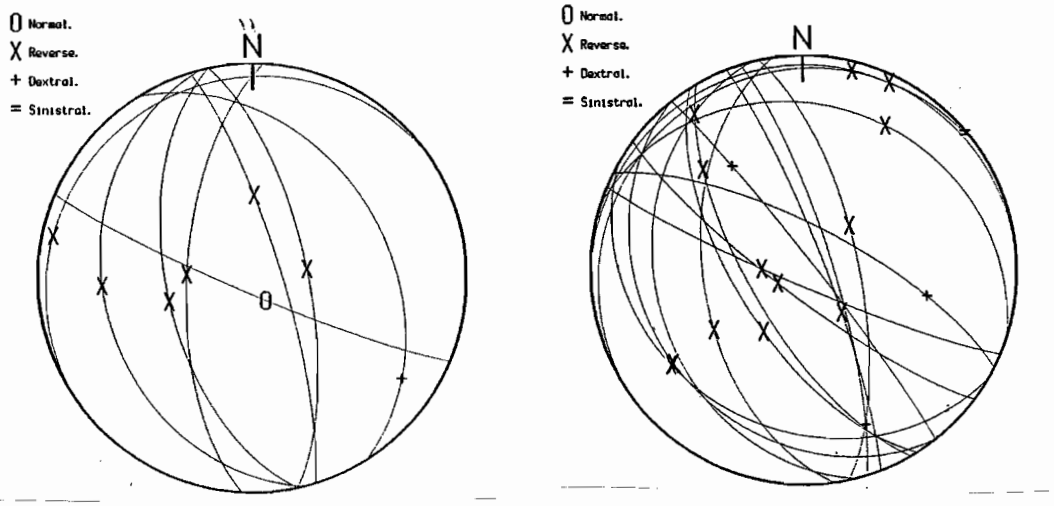

Fig. 5 Stereographic projections of the (a) syn-S_1 and (b) syn-S_2 fault near the Razorback.

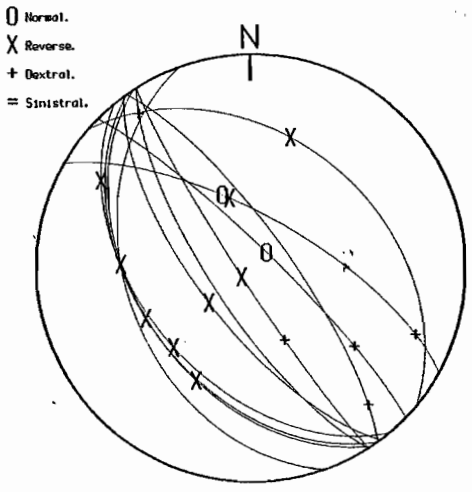

Fig. 6 Stereographic projection showing west side up fault orientation at the Blow.

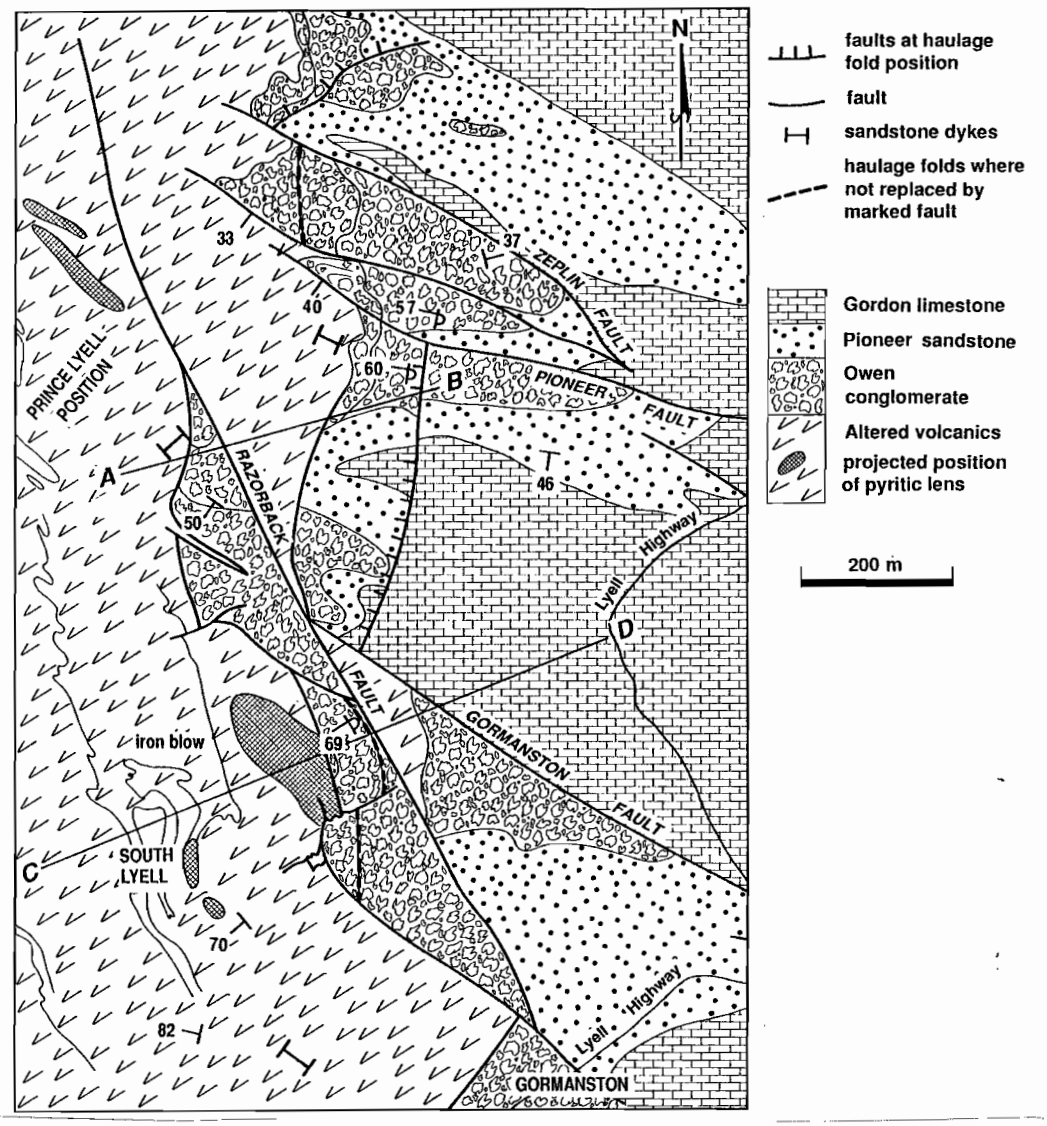

Fig. 7 Geology of the Razorback/Blow area. Geology slightly modified from Arnold (1985).

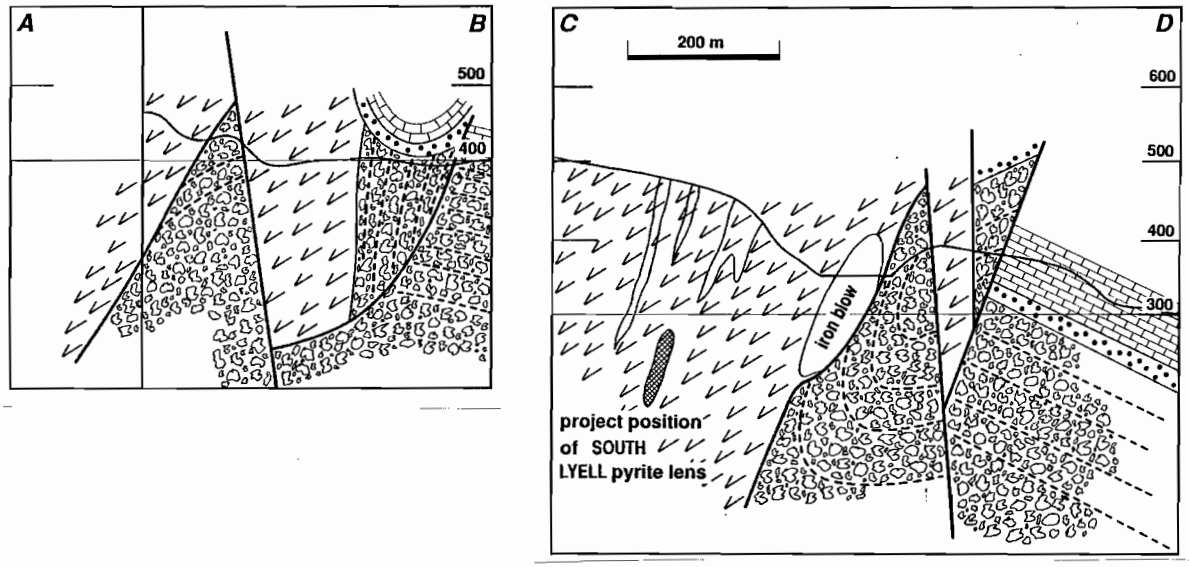

Fig. 8 Sections through (a) the Razorback and (b) the Blow based on Figs 7 & 9 and Arnold (1985).

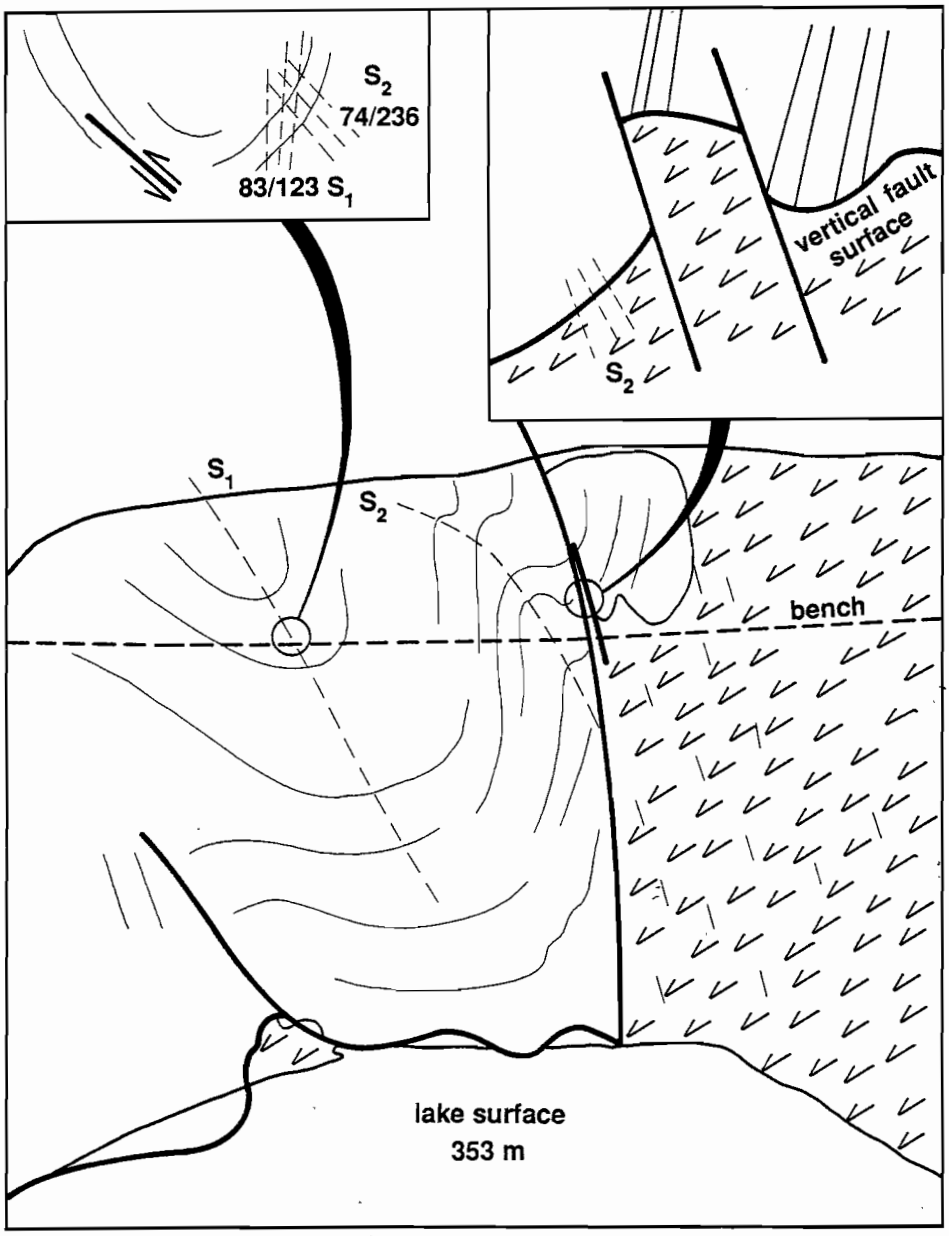

Fig. 9 Structure in the Owen Conglomerate at the south end of the Blow based on geology along the upper bench.

The Zeehan–Red Hills–Lake Selina Traverse — A domain approach to the analysis of structural data

R.A. Keele
Centre for Ore Deposit and Exploration Studies

INTRODUCTION

Previous structural work in the region has focussed on the relative timing of movements on the Henty Fault (Berry, 1989). An early phase of dip-slip movement was followed by strike-slip movement during at least two phases of Devonian movement (D_1 & D_2) corresponding to gross changes in the regional compressive stress field from E–W to N–S.

This study has concentrated on the spatial relationships between individual domain blocks — defined by unique structural style, orientation and litho-stratigraphic association — along the Zeehan–Red Hills–Selina traverse. Rather than focussing directly on fault structures — which may be poorly exposed and often confusing in their interpretation — the emphasis has been on the kinematics of the entire block. The aim has been to work out which block was moving which way and when, and to relate these movements to known mineralisation.

The structural work is presented in the form of an interpreted map, a series of cross sections and a detailed analysis of 14 structural domains.

The map is based on field data gathered from four separate traverses (Fig. 1), as well as the existing geological data base of the region (Elliston, 1950; Blisset, 1962; Pitt, 1962; Rubenach, 1967; Both and Williams, 1968; Corbett and Lees, 1987; Berry, 1989). The actual compilation was made on the 1:25 000 topographic maps of the Lands Dept and made use of mapping by K.D. Corbett and A.V. Brown which has been compiled by the Geological Survey of Tasmania.

The cross sections (Figs 2–5) are drawn as close as possible to the traverses in the field and therefore are a reasonable factual representation of the geology there. The sections, although balanced to a first approximation, are in a form where they can be combined into a single balanced section across the Dundas Trough as and when required.

The domain analysis is presented in the form of a map (Fig. 6) and a series of stereonets (Figs 7 and 8). The stereoplots have been subdivided into *fold data* and *fault data* , thus effectively separating them into the ductile and brittle fields, respectively. Transport directions have been inferred from the fault data. In some domains (e.g. domain 3) the data are too many to analyse effectively as a single domain and further sub-domains will be required; the movement directions on shear fractures and faults have been omitted for the sake of clarity.

The bulk of the raw data is appendixed; firstly, as a plan showing structural stations, i.e. locations of the measurements in the field (Appendix 1) and secondly, as an Excel spreadsheet listing the AMG coordinates of the stations and the structural readings (Appendix 2).

ANALYSIS OF DOMAINS

Since each individual domain has a unique structural style, typically dependant on the litho-stratigraphic associations, each section begins with a brief summary of the rock types present. The structural data is discussed with reference to both *fold* and *fault* data — individual structures being described in detail where they have a bearing on the tectonic evolution of that block, or any of its neighbours.

Domain 1 — West Yolande River Anticline (Anthony Road)

A small triangular shaped area on the southern edge of the regional section line, consisting of folded and thrusted, distal fine to medium grained volcaniclastic sediments of the Yolande River Sequence, comprises this domain (Fig. 1). Its

northwestern boundary is the South Henty Fault (SHF), whilst its northeastern boundary is defined by an E-directed reverse fault on the western flanks of the Yolande River Anticline. The other boundary is unspecified, however, there is evidence to suggest that this domain continues, with minor modifications, as far south as Queenstown.

The folds in this domain plunge very gently to the south (Fig. 7).

Domain 2 — East Yolande River Anticline (Anthony Road)

This domain covers the main part of the N-plunging Yolande River Anticline. Lithologies are identical to those in domain 1 and a prominent felsic porphyritic lava has enabled the structure of the anticline to be reconstructed with some degree of certainty (Fig. 2).

Overall, the structure is a folded and thrusted N-plunging anticlinorium whose eastern limb is squeezed up into the vertical against a 1 km wide fault zone comprising strongly altered CVC and fine grained sandstones. The metamorphic grade increases marginally towards this fault — on the basis of observed quartz and phyllosicate textures — indicating that the W-directed thrust has been brought up from lower crustal levels along a fault with an indicated movement of at least 1 km.

The thrusting on the E-limb of the Yolande River Anticline is interpreted to be D_1 in age, whereas the main axis is interpreted to be D_2, for the following reasons (noting that the two events are coaxial with each other):

- a NW trending fracture cleavage (S_2) was observed to cut a rotated NNE trending slaty cleavage (S_1) in the hinge region;
- bedding–cleavage intersections plunge more steeply in the hinge than on the limbs, i.e. 70 to 80 as opposed to 35 to 50. Clearly, the hinge region had been steepened, or rotated, more than the limbs during this subsequent fold event;
- tectonic transport on the E-limb of the fold, as measured by quartz fibres and slicks on reverse shears, is due westward, i.e. +55 towards 280; whilst in domain 1 this direction is +30 towards 068.

Movement directions on the E-limb of the anticline are consistent with D_1 transport, whilst movement directions in domain 1 are consistent with NE–SW shortening during D_2.

Domain 3 — CVC/Tyndall/Newton Creek Sandstone (Anthony Road)

This domain forms a conformable sequence of E-facing CVC, Tyndall Group volcaniclastics and Newton Creek sandstones that lie between the South Henty and the Great Lyell Faults. The southern boundary is a fault zone separating the Yolande River sediments from the CVC. Lithologies comprise minor rhyolites (always in faulted positions), andesites, black shales, siltstones, sandstone, conglomerates and quartz felspar-phyric lava flows.

The folds plunge moderately to the S (Fig. 7); the data shows, however, an almost identical pole of rotation for the cleavage (47 towards 164), indicating that cleavage orientations are controlled by similar processes that affected bedding, i.e. regional folding, cleavage refraction or shearing, or a combination of these.

The intensity of shearing/jointing/faulting and cleavage development increases markedly towards the tip of the wedge, which is the locus for a number of splays off the Henty Fault. As well as the better known South Henty and the Great Lyell Faults, there are at least two bedding-parallel faults splaying off the same point, one at the top and the other at the base of the Tyndall Group.

The Tyndall Group volcanics are folded and faulted along their base. The shales at the base of the Tyndall Group near Howards anomaly are tightly folded (pers. com., R. Gibson, 1991). Form surfaces in the TGV permit much of the lower and upper contacts to be faulted; for example, bedding trend lines are truncated on both sides of the Tyndall Group, in such a way as to suggest that the Great Lyell Fault and the structure at the base of the TGV formed a fault duplex with a right-hand sense of displacement (Fig. 1). Only a small amount of the upper contact of the Tyndalls has been preserved, the rest — including much of the overlying Newton Creek Sandstone Member — has been removed by movements on the Great Lyell Fault.

Within the underlying andestites, easterly trending NW-directed thrusts are exposed at the base of a thick porphyritic lava flow in the Newton Creek spillway; they not only accounts for the lack of strike continuity of this unit, but also reqiure that the base of the Tyndalls volcanics is a transfer fault zone They are identical to the thrusts north of the Henty Fault which fit a sinistral wrench geometry (Keele, 1991; Figs 3 & 4) .

The base of the CVC in this domain has been altered and ductilely deformed to sericite–quartz ± pyrite schists similar to the mineralised zones at Mount Lyell. The fault surface which is exposed in the east side of the Anthony Road is a vertically dipping graphite shale horizon which gives an east-block-up sense of movement; this is supported by

kinematic indicators from nearby shear bands in the altered volcanics.

Quartz fibres in domain 3 also indicate that the overall transport direction in this domain was to the NE, i.e. opposite in sense to, and away from, that in domain 2.

The strata are overturned adjacent to the Great Lyell Fault with clear indications that the Tyndall volcanics are locally thrust up over the Newton Creek sandstones (Fig. 2); although elsewhere in the northern part of the wedge, the sandstones are seen to rest conformably on the Jukes Breccia. Fold plunges are moderate to the S (contrast this with domain 2) and a multiplicity of shear joints and fractures record both dip-slip and strike-slip movements; sinistral as well as dextral movements are recorded on NNW–SSE striking shear fractures — due to E–W shortening during D_1 followed by N–S shortening during D_2.

The complex and variable nature of the stress field at the northern end of the wedge is demonstrated by an exposure of the Great Lyell Fault on the north side of the Anthony Road. A change from reverse dip-slip movements (D_1), through oblique-slip reverse movements — involving curved tips to the quartz fibres — to dextral strike-slip (D_2), illustrates that the stress field was changing whilst movement occurred on the Great Lyell Fault.

Domain 4 — Owen Conglomerate (Anthony Road)

This domain comprises all Owen Conglomerate east of the Great Lyell Fault. Three units in the Owen are present — the lower Newton Creek Sandstone, the middle silicic conglomerate and the upper cross-bedded sandstone with minor pebble beds (Fig. 2).

Overall folding in the Owen is open to close in style with sub-horizontal plunges predominant, athough individual folds may plunge up to 30° from the horizontal in either a north or south direction. In detail, each of the above units of the Owen Conglomerate has a unique style of deformation attached to it:

Newton Creek Sandstone: folds are open to close and plunge towards the south;

Siliciclastic Conglomerate: this unit occupies the vertical limb of a flatly north plunging monoclinal fold which, when combined with data from secton 4, is seen to be the upward projection of the underlying Red Hills Shear Zone displaying east-block-up senses of movement on multiple bedding surfaces.

Upper Owen: folding is much simpler and more open in style plunging gently to the north or south.

Fault data indicates that reverse, and sinistral, movements on steep E-dipping shears are the norm for this domain (Fig. 8). The quartz fibres in the underlying volcanics (domain 5) are related to the shearing in a predictable way and indicate that the deformation east of the Great Lyell Fault is considerable more brittle than that west of it, and is largely controlled by reactivation along bedding surfaces when they become rotated to the vertical.

Domain 5 — Red Hills

This domain comprises all the Central Volcanic Complex and Tyndall Group volcanic rocks east of the Great Lyell Fault that lie unconformably below the silicic, or Middle Owen Conglomerate, unit (Fig. 5). It therefore excludes the volcanic rocks wedged between the South Henty Fault and the Great Lyell Fault which are seen to lie conformably beneath the Owen Conglomerate. The angle of the unconformity varies from 65 at Red Hills to 90 at the Anthony Dam site where horizontal silicic conglomerates rest directly on vertically dipping Tyndall volcanics in the keel of a gently N-plunging syncline.

Fold data in this domain indicate steeply plunging lineations and minor fold axes, implying vertical movements on faults.

The fault data indicates E-block-up, dip-slip movements on N–S shear joints and some E–W horizontal striae due to an unspecified equatorial transport. The similarity in striations between domains 4 & 5 implies that both the Tyndall volcanics and Owen Conglomerates east of the Great Lyell Fault have behaved as a single cohesive rock mass during the penetrative phase of regional deformation; in fact for the purposes of this structural analysis domains 4 and 5 could easily have been treated as a single entity.

Domain 6 — CVC West of Henty Fault

This domain comprises all the CVC rocks west of the Henty Fault and thus forms a wedge of rhyolitic to rhyodacitic volcanics that pinches out to the south against the fault. Other lithologies include: minor black shales, silstones, mineralised host rocks, and basalts and dolerites of the Henty Dyke Swarm which are emplaced into the felsic volcanic pile. The dykes are probably high-level sub-volcanic sills rather than dykes mainly because the vesicles lie preferentially on the western or inferred upper sides of the bodies, and as such can be useful as a form surface like any other.

Fold data — as opposed to individual folds which are rare in this domain — indicate that a moderately S-plunging fold axis can be defined by this more generalised form surface which includes bedding, banding in the volcanics and the mafic-felsic contacts referred to above. However, the cleavages measured

in this domain, which include individual S & C foliation pairs, form a statistically significant axis of rotation with a similar orientation as bedding (Fig. 7); the tendency for the poles to smear out along a girdle is best explained as a result of shearing. The lineations reflect both this pole of rotation and the inferred movement directions perpendicular to it.

The fault data, collected mostly from within several hundreds of metres of the Henty Fault, is consistent with reverse (and slightly dextral) senses of movement on NNW to NNE trending shears (Fig. 8). If this is translated into the dip-slip phase of movement on the Henty (Berry, 1989), then this wedge of volcanics is moving up and out towards the NE, supporting a "pop-up" escape mechanism during D_1 compression. Note how the cluster of quartz fibre directions on the stereogram corresponds to the majority of movement directions.

An important element in this domain is the low to moderate-angle D_2 thrusts which generally strike ENE–WSW and have an important effect on the outcrop patterns. The best example — two smaller ones of which were inspected in the Henty Canal during the field trip — is located at the south end of the domain and thrusts volcanics northwards over the Jones Creek shale; this had the effect of concealing, and thereby, terminating outcrop of this unit which cannot be traced any further to the south. Such thrusts logically originated as splays off the North Henty Fault; however, there is also evidence further north at Mt. Hamilton and Hercules, that they may be generated in response to differential (or possibly oblique?) movements along NNW trending faults or shears, suggesting that these thrusts may not only be localised around the Henty Fault but may be found anywhere in the CVC.

Domain 7 — White Spur Formation (Howards Road)

This domain comprises the entire White Spur Formation which wedges out northwards between the converging Rosebery Fault and the CVC. On structural grounds the western boundary of this zone is taken to be one of the thrust splays off the Roseberry Fault; stratigraphically, it is the highest or most westernmost occurrence of coarse grained quartz-rich wacke/tuff/flow markers in the formation. The southern boundary of the domain is the North Henty Fault.

The contact between the WSF and the CVC is perceived to be partly original and partly faulted; at the north end, where W-facing White Spur Formation is in direct contact with E-facing, highly altered footwall volcanics, it is sheared; here the contact is a collapse zone within the hinge of an anticline which can be traced all the way back to the North Henty Fault (Fig.1). At the southern end, adjacent to the Henty Fault, there is further evidence of faulting along the contact whilst on the other hand the contact is largely intact in the White Spur canal.

The folding in this domain is unique in that gently N and S plunging open folds are interspersed with domains of steeply plunging bedding/cleavage intersections (Fig 3). The best example of one such steeply plunging zone occurs adjacent to the North Henty Fault, where the limbs of a fold open out and steepen into near parallelism with the fault surface, the fold dieing out in the process. This implies that the folds developed at the same time as the fault was active.

The cleavages measured in domain 7 have been rotated about a vertical axis as a result of strike slip movements on the fault; since the orientation of this axis corresponds to the steeply plunging bedding/cleavage domains and spatially such zones are best developed adjacent to the NHF, the field data supports the North Henty being a strike-slip transfer zone during folding. As a consequence, no offsets of folds would be expected on either side of the fault.

The fault striations and quartz fibres in this domain give reverse senses of movement — with a westward transport direction — on N–S shears; such kinematic indicators are consistent with the western boundary of this domain being a splay off the Rosebery thrust. However, there are a some faults, particularly along the eastern boundary, that give an eastward transport direction, implying either a certain amount of back thrusting within the block or, more likely, that these structures are appropriate to the neighbouring domain 6 rather than domain 7. Shears with strike-slip movements are also found along the eastern margin indicating, overall, that the White Spur/CVC contact is a zone of thrusting and strike-slip transfer movements.

Domain 8— Middle Dundas Formation (Howards Road)

This domain is in the shape of a four-sided figure bounded to the north by the Rosebery Fault, to the east by the Roseberry thrust splay (described above), to the south by the North Henty Fault and to the west by the Cambro-Ordovician boundary wrench fault (Fig. 1).

Lithologies consist almost exclusively of shales, silstones and fine grained sandstones from the middle part of the Dundas Formation. Included within this domain, although not observed in the field, are the coarse grained volcaniclastic sandtones, gritstone and conglomerates of the upper part of the Dundas Formation, now thought to be the lateral equivalent

of the Owen Conglomerate in the western half of the Dundas Trough.

The folds within this domain comprise W-verging, doubly plunging, non-cylindrical close to tight folds, some of which have axial plane hinge faults (Fig. 3). Every fold closure is accompanied by a change in plunge of the bedding/cleavage intersections on each limb, which can be summarised thus: *the W-limbs of the anticlines (or E-limbs of the synclines) plunge to the north, whilst the E-limbs of the anticlines (or W-limbs of the synclines) plunge to the south.* A feature, therefore, of this style of folding is that although the folds verge to the north, the map view shows that the bedding has a strike direction that varies in a tight range from N–S to NE–SW (Fig. 1). Whilst such folds can be produced by rotation of the limbs on hinge faults, it is likely that the initial folds pre-dated the Devonian compression, and may be Cambian in age. The doubly plunging configuration is due to Devonian compression being slightly oblique to the initial fold trends and rotation occurring during a further tightening of the limbs when the cleavage and the overturned, thrusted limbs formed.

The fault data indicates that, apart from some minor thrusting in one of the anticlinal hinges, the domain is kinematically dead. The few quartz fibre measurements, however, indicate that this block was pushed towards the SW during Devonian deformation, indicating that the North Henty Fault — and its extension to the west, the Little Henty Fault — is a high-angle reverse fault that brought older strata on the north side into contact with younger strata on the south side. It is also implied that the dextral wrench fault on the boundary between the Ordovician and Cambrian strata is an accomodation or transfer structure that allowed the Cambrian rocks to fold independently of the Ordovician and younger cover sequences. If this is so, then the unconformable bedding and cleavage trends observed between the Cambrian and Middle Ordovician sequences in the SW corner of domain 8 — at the Howards Rd turn off — is due as much to later deformation than to an unconformity.

Domain 9 — Upper Dundas Formation (Dundas Road)

Medium to coarse grained sediments of predominantly volcanic origin, from the Red Lead Conglomerate to Misery Conglomerate members of the upper Dundas Formation, make up the stratigraphy of this domain. In contrast to the previous domain, the contact between the upper units of the Dundas Formation and Ordovician Moina Sandstone is conformable (Fig. 4).

The structure is simple with bedding surfaces dipping (and facing) to the west, with rare E-verging open style folds being present. Folds trend NNW and plunge gently south, although the presence of steep bedding/cleavage intersections and the vertical 'rotation' axis of the cleavage, suggests a significant influence from strike-slip faulting along the boundary of the adjacent Razorback Serpentinite body (pers. comm., D. Selley, 1991).

Domains 10 & 11 — Henty Fault Wedge

The rocks in this domain comprise sediments, tuffs, basaltic volcanics and serpentinites after dunite, peridotite and pyroxenites which have lithological affinities to the base of the Western Sequence south of Queenstown. From a structural point of view domain 10 and 11 should probably be treated as one, however, the presence of a thrust at the base of preserved slice of steep W-dipping oceanic crust — with dunites passing up into pyroxenites and basalts at its top (pers. comm., R. Poltock, 1991) — tends to suggest that these domains are two distinct blocks (Fig 1).

Both bedding and cleavage are steeply dipping and rotated about a near vertical axis in the wedge, as would be expected adjacent to a strike-slip fault system where the folds formed initially in a subvertical orientation, rather than having arrived at this position as a result of refolding about horizontal axes.

The fault data suggests that this is a wedge of Western Sequence which has been faulted up between the CVC/White Spur/Dundas Formations on the northern side of the Henty Fault and CVC/Tyndall Group volcanics on the southern side of the Henty Fault, by sinistral strike-slip movements. The continuation of the North Henty Fault through the Wedge — as a steep E-directed thrust/reverse fault at the base of the ultramafic unit — allows a remarkable continuity of structure at least as far south as Lynchford, a distance of 20 km.

Domain 12 — Ordovician-Silurian-Devonian strata south of the Little Henty Fault

Sediments from Ordovician to Devonian in age are folded into a series of large amplitude, shallow NW-plunging folds. The Zeehan Syncline has lost its identity south of the Little Henty Fault — the folding having degenerated into a series of anticlines-synclines with stable wavelengths of 1–1.5 km (Fig. 1). This indicates that the LHF acted as a transfer during the first phase of Devonian deformation, causing the wavelengths of the folds on either side of the fault to be different and thus no correlation of individual folds need be expected.

The evidence for faulting along the Ordovician–Cambrian boundary on the eastern side of domain 12, can be summarised as follows:

- 5 km right-hand offset on the North Henty Fault;
- cataclastic fault breccias in the Gordon Limestone unit;
- variably oriented bedding in the Gordon limestone with steep dips locally dominant;
- inferred SSW transport direction in the Cambrian sediments of domain 8, whereby movement is transferred on to this fault from the Rosebery Thrust via an E–W strike-slip zone along the northern boundary of domain 8.

Domain 13 — Ordovician–Silurian–Devonian strata north of the Little Henty Fault

The main structure here is the NNW trending Zeehan Syncline which is a regional fold depression developed in strata that range from Ordovician to Middle Devonian in age (Figs 1 &4). Fold plunges range from gentle to steep NNW, depending on relative positions within the synclinal depression. Cleavage orientations vary from NNW to NE depending on their proximity to cross faults; this is due to a change in regional maximum stress direction from NE–SW to NNW–SSE at a late stage in the development of the Zeehan Syncline. The structure is dominated by two fault-controlled bulges on the flanks of the central portion of the syncline — the eastern one being controlled by the cross-trending Brickfields Fault, and the western one being the focus of structural complexity around the Zeehan mineral field. NNE and WNW trending brittle conjugate shears, seen in the Bell Shales within the centrally thickened part of the syncline, have helped to accomodated a 18–22% axial shortening of the Zeehan Syncline during the later part of the Tabberabberan Orogeny.

Thrusting occurs on the southwestern limb of the Zeehan Syncline in the vicinity of the Oceania Pb–Zn deposit (Fig. 1). The NE trending dextral Oceania Fault is a side ramp in a D1 thrust system that repeats part of the stratigraphy including the Moina Sandstone, Gordon Limestone and Crotty Quartzite Members. The Oceania Fault was probably a growth fault during deposition of the Gordon Limestone (Taylor and Mathison, 1990), because of the thinning of units towards the SE. However, the picture is not that clear cut because although the secondary recrystallised dolomite unit thins away from the fault, the main Gordon limestone does not — at least as far as its lower manifestation is concerned — being much the same thickness on either side of the fault. This implies that much of the 750 m dextral offset is related to the thrusting and is post-depositional. The thrust is terminated to the south by a E–W D_2 structure that pushes Ordovician rocks up to the north over Siluro-Devonian strata

Domain 14 — Precambrian and Eocambrian at Zeehan

This domain includes all rocks other than Ordovican–Silurian–Devonian strata west of the Zeehan Syncline.The lithologies comprise sandstones, shales, pyritic black shales, siltsones, quartzites of the Oonah and Success Creek Formations.

The contact between the Crimson Creek Formation and the unconformable overlying Ordovician sandstones is a faulted one, although the two domains share similar fabric orientations suggesting that the Devonian deformation had also affected the Precambrian. The main difference between the Oonah and the Palaeozoic rocks of the Zeehan Syncline is the lack of a penetrative cleavage in the former — the only cleavage observed being a weak axial planar fracture cleavage in the fold hinges. Although these folds plunge to the E (in contrast to the folds in the syncline) their axial surfaces parallel the orientation of some of the cleavages related to the D_2 event, suggesting the possibility that the the basement rocks have been subjected to a weak late-stage Devonian deformation.

Tectonic transport as deduced from Devonian extension directions

The Devonian compression has produced widespread quartz veining of extensional origin throughout the district, particularly in the altered volcanic assemblages. These veins tend to have moderate dips; in time they are close to the last brittle event to occur in the Devonian because they are not significantly deformed. The vein fibres themselves were measured — and not the poles to the veins, since this allows for oblique extension where the fibres grow at an angle to the walls — giving an orientation for the *least principal stress* (σ_3) during regional deformation.

Two basic assumptions are made in this analysis: firstly, that the fibres represent the bulk transport direction in the rock, and secondly that the movements on all shears/faults that accompanied this transport were reverse. Both assumptions appear to be valid because the quartz fibres do correspond to the dip-slip movement directions measured on a multiplicity of shear/fault surfaces (e.g. domains 2, 3, 6 & 7) and almost without exception all movements recorded were reverse, particularly in the Henty Fault area.

The quartz fibres have been averaged and plotted

on the domain map. The direction of the arrows on the map represents the direction of tectonic transport during Devonian D_1 compression. The first point to note about the map is that the directions are in most cases sub-perpendicular to the averaged fold trends, as indeed would be expected (with the exception of domain 8); however, the following points are worthy of attention:

- lines separating domains of different movement polarities can be drawn on the map (Fig. 6);
- the lack of data in the western half of the map indicates a decrease in the intensity of the brittle-ductile style of deformation towards the west;
- through the process of *movement transfer*, strike-slip faulting in the district can be more readily understood;
- the kinematics processes in the rocks east of the Great Lyell Fault were different from those that occurred west of it.

Opposing transport directions

The best example of this is the line that separates the CVC from the White Spur Formation and the Yolande River Sequence. It is an axis across which the escape direction — during the "pop-up" between the Roseberry and Henty Faults — changes from easterly to westerly. Since transport was symmetrically *away* from this line these domain boundaries are extensional in nature, with the blocks on either side moving out and away from each other; consequently, faulting along this boundary would tend to be normal with thrusts and/or reverse faults lacking entirely . The evidence supports these conclusions — there are no thrusts or reverse faults along the CVC/WSF contact. Although normal faults were not recorded along this boundary, they should not be ruled out as a possibility. The domain 2/3 boundary, south of the Henty Fault, similarly has been involved in significant down block movements on steep faults, rather than thrusting and undoubtedly involved normal faulting in the now stripped off Ord–Sil–Dev strata.

The other significant change in polarity occurs on the western side of the belt. The axis of the Yolande River Anticline (domains 1 & 2) represents a compressional boundary as shown by a system of upward verging thrusts (Fig. 2); this sense of easterly transport continues into the Henty Fault Wedge; however, the reason this axis does not extend further north into the wedge is because the North Henty transfer allowed sufficient room for escape towards the east, obviating the need for any further folding there.

This eastward transport, particularly where it involves thrusting of ultramafics and the Crimson Creek correlates of the Western Sequence, south of Quennstown, may initially have started as a Cambrian thrusting event related to westward subduction in the Middle to Upper Cambrian (Crawford and Berry, 1991).

Strike-slip faulting and the transfer of movements — the North Henty Fault and the Cambrian-Ordovician boundary fault

The North Henty Fault is a D_1 transfer zone which separates W-directed thrusting in the Dundas and White Spur Formations — related to thrusting on the Roseberry Fault — from an earlier phase of E-directed high-angle reverse faulting/thrusting in the Yolande River Sequence. It defines a northern limit to the southern part of the Western Volcanic sequence (otherwise called the Yolande River Group). The shape of the Henty Fault Wedge, which comprises rocks of the Western Sequence, is controlled by the termination on the sinistral Henty wrench fault. The thin slice of sediments in the Henty Fault which continue north might provide one of the few reasonable bases for making any correlation of the Western Sequence with the Que-Hellyer sequences to the north.

Domain analysis predicts that the strike-slip movements would be greatest along the domain 7 boundary, whilst reverse movements — with southerly transport — would tend to occur along the domain 8 boundary. The South Henty Fault, on the other hand, is predicted to be a high-angle reverse fault, with little or no strike-slip component to the movement, especially along the domain 2 boundary.

A region of dextral strike-slip is also predicted for the southward continuation of the Rosebery Fault, particularly where it forms the boundary between domains 8 & 9. The 2.5 km offset on the North Henty Fault, assuming that the Little Henty is the same structure at the North Henty, supports this predicted movement.

Regional structural correlations in the Western Sequence

The Yolande River Anticline may be correlated with the Miners Ridge Anticline at Lynchford, some 20 km to the south, on the basis of similar structural styles and lithologies. The western limb of the Miners Ridge anticline has a basal thrust slice of basaltic to peridotitic (i.e.10–15% MgO olivine-bearing) rocks which have the similar compositions to the ultramafic rocks in the fault wedge (B. Dower, pers. com., 1991). This structure, which may have originated in the Cambrian, represents the most eastward expression of an E-directed thrusting event found along the

western side of the Dundas Trough. If this is so, the Henty Fault is the northward continuation of such a structure, a fact which may have important implications for the tectonic evolution of the West Coast terrain (Crawford and Berry,1991).

Role played by the Little Henty Fault in forming the Zeehan Syncline

The Little Henty Fault acted as a transfer fault during the formation of the Zeehan Syncline. It separates two distinct entities within the Ordovician–Silurian–Devonian sequences, one north of the fault where the Zeehan Syncline occurs, and another south of the fault where the syncline is absent. The fault was later re-activated as a high-angle thrust during a reorientation of the principal stress directions from E–W to N–S, at the close of the Tabberabberan Orogeny. The Zeehan Syncline formed during the first phase of this orogeny, subsequently suffering a 22% axial shortening during the second phase. The accompanying strain was accomodated by the following processes: folding in the Bell Shales, S-directed thrusting in Moina Sandstone to Crotty Quartzite stratigraphy on the SW limb of the syncline and wrench faulting on NNE to WNW trending conjugate faults.

The regional stress fields in Western Tasmania — a brief comparison with the rest of eastern Australia.

In Eastern Australia, the close of the Tabberabberan Orogeny was marked by a relatively stable N–S compressive stress field during the Carboniferous (Powell, 1984). In most places, even as far away as the Georgetown block in North Queensland, this stress field controlled the emplacement of volcanic rocks of Carboniferous age; however, during the Permian, the stress field began to shift to NW–SE (Mackenzie, 1987). Such a range in stress fields is mirrored by the structures of the Zeehan–Lake Selina section. The compressive stress directions in the Zeehan Syncline changed from NE–SW to NW–SE at a critical moment in the evolution of this synclinal depression; however, the extent to which this reflects a post-Devonian stress field or whether the changes happened at an earlier stage in Tasmania, is not certain. The WNW trending fault which bounds the Permian rocks NW of Zeehan, is a structure that also offsets the NE trending Brickfields–Waller Fault at Zeehan. The likelyhood that the Tabberabberan Orogeny was extended beyond the Devonian might seem a reasonable proposition in the light of such data (Goscombe, 1991).

Easterly thrusts in the CVC — an explanation for the abrupt termination of mineralisation?

Easterly trending thrusts — with a NNW transport direction — are widespread in deformed CVC rocks. They have been identified in the CVC rocks north and west of the Henty Fault and as far afield as Miners Ridge. Although one set of thrusts appears to splay off the Henty Fault — being a direct result of the strike-slip sinistral movements — a major wrench fault in the immediate vicinity appears not to be a necessary precondition for these thrusts to form. In time, they are equated with the D_2 longitudinal shortening of the Zeehan Syncline. Their significance lies in the fact that they can terminate stratigraphy almost at will, which is what has happened to the Jones Creek shale at its southern end. Further detailed mapping should reveal many more of these structures.

The Henty Gold Prospect — a regional perspective

The horsetail splay at the south end of the Henty fault is a classic fault termination which acted as an effective conduit for magmatic hydrothermal and/or metamorphogenic fluids during the active phase of faulting. The siting of the Henty Gold prospect is significant for a number of reasons:

- It is located at a splay that comprises two first-order structures, namely the Henty and Great Lyell Faults, and a number of second-order structures.
- The structural permeability of the fault bounded Tyndall–CVC–Newton Creek Sandstone wedge is higher than any other block in the region, and this permeability would be expected to be highest at the tip of the wedge. This would have considerably enhanced the flow of mineralising fluids through the system.
- The dip-slip motions of the North Henty Fault change to strike-slip at the splay. Strike-slip motions generally provide the most efficient, as well as rapid, escape mechanism for ponded fluids in the upper crust.
- The movement directions and mineral lineations in domains 3 & 6, the most important rock masses on either side of the prospect, plunge to the south, putting certain constraints on probable fluid pathways and possible ore shoot geometries.

Veining and stress patterns around overstepping faults in the Zeehan Mineral Field

The Zeehan fissure style of mineralisation (Both and Williams, 1968) is controlled by a system of WNW trending faults at the south end of the field (the Balstrup, Sylvester and Comstock Faults) and the Despatch & Montana Faults at the north end. They represent a series of overstepping faults with both releasing and restraining characteristics developed during D_1 and D_2 Devonian deformations (Fig. 9).

The first phase of movement on these faults (D_1) is an overstep with releasing characteristics causing normal movement on the NE-trending Waller Fault and a stress field that allowed NE–SW striking fissure veins to form. This phase coincided with the S-directed thrusting on the SW limb of the Zeehan Syncline at Oceania.

This was followed by dextral movements on the same, or a slightly different, set of faults during D_2 which reoriented the maximum principal stress direction (σ_1) from NE–SW to NW–SE and allowed the main northwesterly trending fissure veins to form. This stage also coincided with the axial shortening of the Zeehan Syncline. The Balstrup–Comstock left-stepping overlap was active at this stage; however, the effect was one of restraint rather than release and consequently the main vein fissures tended to shy away from the overlapping region, which instead was occupied by sulphides. There is some evidence to suggest that the mineral zonation boundaries are offset along minor faults set at a high-angle to the Waller Fault, indicating that the alteration was at least partially complete by this stage.

The left-stepping pattern of faults is maintained on the regional scale with the Balstrup and Tenth Legion Faults having the same overstepping geometry as the Balstrup/Comstock Fault system on the small-scale.

The Blue Mountain Volcanics and the Plaintain Garden FZ in Jamaica — A recent analogue of the Mt Read Volcanic Belt and the Henty Fault Zone?

There is considerable merit to be gained from comparing recent and ancient volcanic belts; one such recent volcanic setting is at the boundary between the North American and Carribean plates in Jamaica. The sinistral strike-slip, right-stepping Plantain Garden Fault Zone, with its associated Blue Mountain volcanic ediface, is remarkably similar in many ways to the Mount Read Volcanic belt (Fig. 10). The following points are important and are discussed briefly below:

- The dimensions and overall shapes of both are similar. If no distinction is made between volcanic and volcaniclastic rocks, then the overall shapes — partly defined in both by ultramafic rocks — are remarkably the same.
- In the recent volcanics the rocks dip away from the main fault zone. A similar effect is noted at the south end of the CVC where the beds face away from the HF; rather than having to invoke a separate folding event — for which there is not much evidence — such quasi folds can be shown to be produced by strike-slip faulting alone.
- The topographic highs occupy identical positions *vis-a-vis* the fault splays in both ancient and modern examples. Since the fault configuration in the recent example is a restraining bend, the volcanics have been uplifted and eroded to form the sinuous fan delta conglomerate deposits. These deposits would be equivalent to the Jukes Breccia, at the top of the Tyndall Volcanics.
- Both fault systems are sinistral strike-slip and their splays configurations are similar. The major difference between the PGFZ and the HFZ is that the latter appears to be a termination in a sinistral strike slip fault, and not a right-stepping bend as the other is. What is not obvious is whether the Henty Fault continues any further south than the fault wedge, and if it does what form would it be expected to have now?
- Obducted oceanic crust of Cretaceous age — with accompanying granitoid intrusions — forms an arcuate belt in the Carribean example similar to the faulted ultramafic bodies around Dundas. It should be noted that the Jamaican granites swing around into a similar orientation as the granite at Renison, and that the Federal Basset Fault has an analogue in the faulted termination of Cretaceous oceanic crust. The implications for the MRV is that a more thorough oceanic environment may have pertained, at least for a short time, during Middle to Upper Cambrian times. However, the essentially inter-cratonic setting of the MRV does suggest a fundamental difference between the two settings.
- An unique feature of strike-slip terrains is that they are capable of generating localised unconformities during the period of time the fault were active. Mann et. al. (1985) refer to two or possibly three unconformities during Miocene and Eocene times in Jamaica when compressional deformation and uplift started on the island. A similar problem is presented by the Dundas Trough where unconformities are known to occur at the base of the Tyndalls, the base of the siliciclastic Owen Conglomerate and the base of the upper Owen Conglomerate. Compression resulting from ongoing movements on a strike-slip system may account for these unconformities.

CONCLUSIONS

The structural data presented here has fulfilled one of the basic aims of the project which is to better understand the relationship between faulting and mineralisation in the West Coast of Tasmania. The two examples of mineralisation controlled by faulting — the Zeehan fissure veins and the Henty Gold prospect — are better able to be explained because of these regional studies. Such types of mineralisation would warrant further studies in order to firmly establish a link between local and regional structures.

The data on shear fractures and fibres in quartz veins has given an unique insight into the overall transport/movement directions during the Devonian deformation. Such data is relevent in piecing together the individual blocks of the jigsaw puzzle in order to reconstruct the pre-Tabberabberan geology. The domain approach will aid this process — which is more like a version of 3-D plate tectonics! — as more and more of the pieces start to fit into place. It is recommended that this approach be adopted in other areas.

The easterly thrusts in the CVC may have a bearing on exploration strategies for sulphide deposits, since they have the capacity to hide ore bodies. Blind ore positions may lie concealed beneath relatively thin covers of unaltered volcanics.

REFERENCES

Berry, R.F., 1989. The history of movement on the Henty Fault Zone, western Tasmania: An analysis of fault striations. *Aust. Jour. Ear. Sci.* 36: 189–205.

Blisset, A. H., 1962. One mile geological map series: the Zeehan sheet. explanatory report, Geological Survey, Tasmania.

Both, R.A., Williams, K.L. 1968. Mineralogical zoning in the lead–zinc ores of the Zeehan field, Tasmania, Part 1: Introduction and review. *Jour. Geol. Soc Aust.* 15(1): 121–137.

Crawford, A.J., Berry, R.F. 1991. Tectonic implications of Late Proterozoic- Early Palaeozoic Igneous rock associations in Western Tasmania (in press).

Corbett, K.D., Lees, T.C. 1987. Stratigraphic and structural relationships and evidence for Cambrian deformation at the western margin of the Mt. Read Volcanics, Tasmania. *Aust. Jour. Earth Sci.* 34(1): 45–67.

Elliston, J., 1950. Dundas Mineral Field. Unpublished BSc (Hons) thesis, University of Tasmania: 82pp.

Goscombe, B.D., 1991. Deformation of the Zeehan Tillite and re-evaluation of the Tabberabberan Orogeny in Tasmania. Division of Mines and Mineral Resources Rept. 1991/03: 20pp.

Guirard, M., Seguret, M., 1985. A releasing solitary overstep model for the late-Jurassic—Early Cretaceous (Wealdian) Soria strike–slip basin (Northern Spain). *In* Biddle, K.T., Christie-Blick, N. (eds): *STRIKE-SLIP DEFORMATION, BASIN FORMATION, AND SEDIMENTATION. Soc. Econ. Paleo. and Min. Spec. Publ.* 37, p.159–175.

Keele, R.A., 1991. A description of the Howard's Road traverse. In: Structure and Mineralisation of Western Tasmania: AMIRA Project P291, Rept No. 2.

Mackenzie, D.E., 1987. Geology, petrology, and tectonic significance of Permian and Carboniferous rocks of the western Georgetown Inlier, north Queensland. *BMR J. Aust. Geol Geophys.* 10: 109–120.

Mann, P., Draper, G., Burke, 1985. Neotectonics of a strike-slip restraining bend system, Jamaica. *In* Biddle, K.T., Christie-Blick, N. (eds): *STRIKE-SLIP DEFORMATION, BASIN FORMATION, AND SEDIMENTATION. Soc. Econ. Paleo. and Min. Spec. Publ.* No 37: 211–226.

Pitt, R.P.B., 1962. Geology of the Zeehan area. Unpublished B.Sc. (Hons) thesis, University of Tasmania: 117pp.

Powell, C. McA., 1984. Terminal fold belt deformation: relationship of mid-Carboniferous mega-kinks in the Tasman Fold Belt to coeval thrusts in Cratonic Australia. *Geology* 12(9): 546–549.

Rubenach, M. J., 1967. The Seperpentine Hill complex. Unpublished B.Sc. (Hons) thesis, Universtity of Tasmania: 141pp.

Taylor, S., Mathison, I.J., 1990. Oceana lead–zinc–silver deposit. *In* F. E. Hughes (ed.): Geology of the Mineral Deposits of Australia and Papua-New Guinea. Aus. I.M.M., Melbourne: 1253–1256.

Fig. 1 Geological map of the Zeehan-Lake Selina region. Geological interpretation is based on data from this study; Blisset,1962; Pitt, 1962; and mapping by K.D. Corbett and A.V. Brown compiled at 1:25,000 by the Geological Survey of Tasmania. ZMF= Zeehan Mineral Field, HGP = Henty Gold Prospect, OD = Oceania Pb-Zn deposit. BF= Balstrup Fault, BFF = Brickfields Fault, NHF = North Henty Fault, SHF = South Henty Fault, HF = Henty Fault, RF = Rosebery Fault.

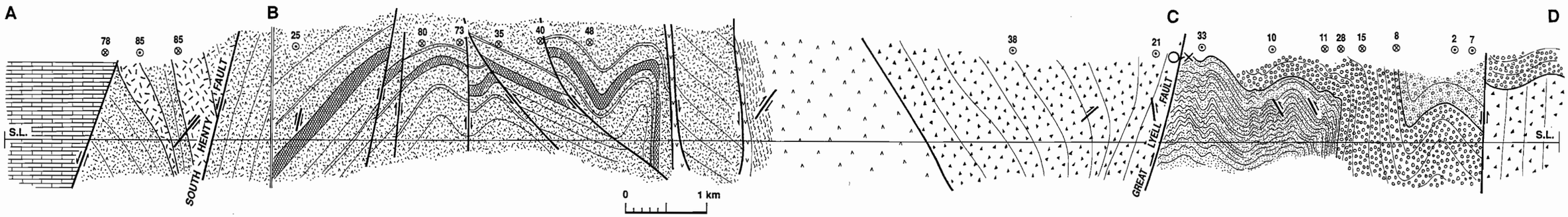

DEVONIAN

- bs Bell Shale
- fq Florence Quartzite
- as Amber Slate/Keel Quartzite/Austral Shale
- cq Crotty Quartzite
- gl Gordon Limestone
- ms Moina Sandstone

CAMBRO–ORDOVICIAN

- oc Upper Owen Conglomerate
- sc Siliclastic conglomerate
- nc Newton Creek Sandstone
- ud Upper Dundas Formation

CAMBRIAN

- md Middle Dundas Formation
- ws White Spur Formation
- tv Tyndall Volcanics
- CVa Central Volcanic Complex (andesite)
- CVr Central Volcanic Complex (rhyolite/dacite with host shale)
- yr/p Western Sequence Yolande River Group with porphyry flow marker

- Granite
- G/S Gabbro/serpentinite

- cc Crimson Creek Formation
- PЄ Precambrian

- ⊙ South plunging fold/lineation
- ⊗ North plunging fold/lineation
- ○ Movement out of page
- ╳ Movement into page

Fig. 2 Section line A–B–C–D; the Anthony road section. The Yolande River Group rocks are 55% shortened in the anticline, whereas the Owen Conglomerates are 28% shortened, implying that either a major detachment exists between these two sequences or that there is a change to higher strains within the Mt Read volcanic belt west of the Great Lyell Fault. The vertically dipping Newton Creek Sandstone and siliciclastic conglomerates lie above the down plunge projection of the Devonian shear zone in the underlying Tyndall/CVC (see fig. 5) implying that the Devonian deformation may account for most of the differences in shortening above and below the unconformity.

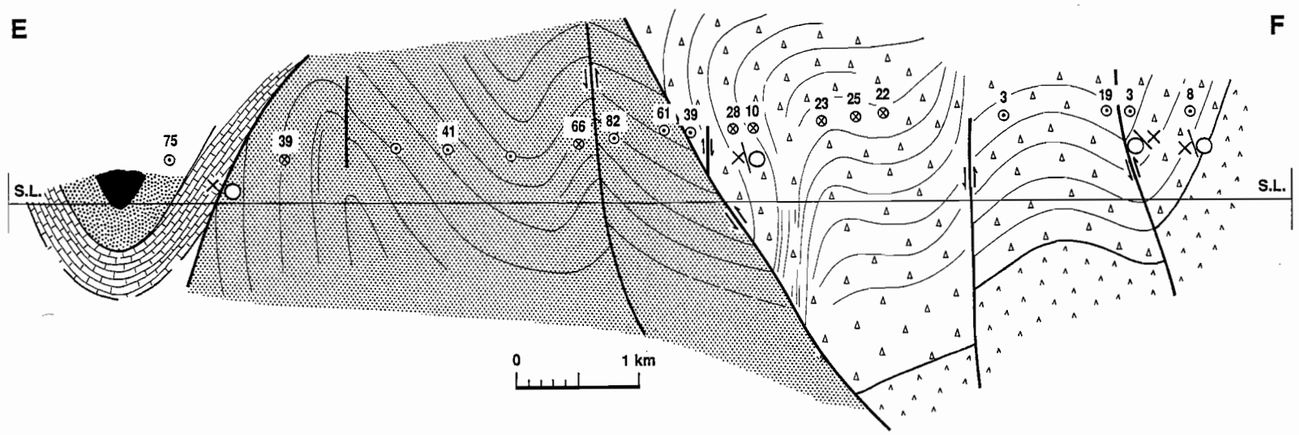

Fig. 3 Section Line E-F; Howards Road section

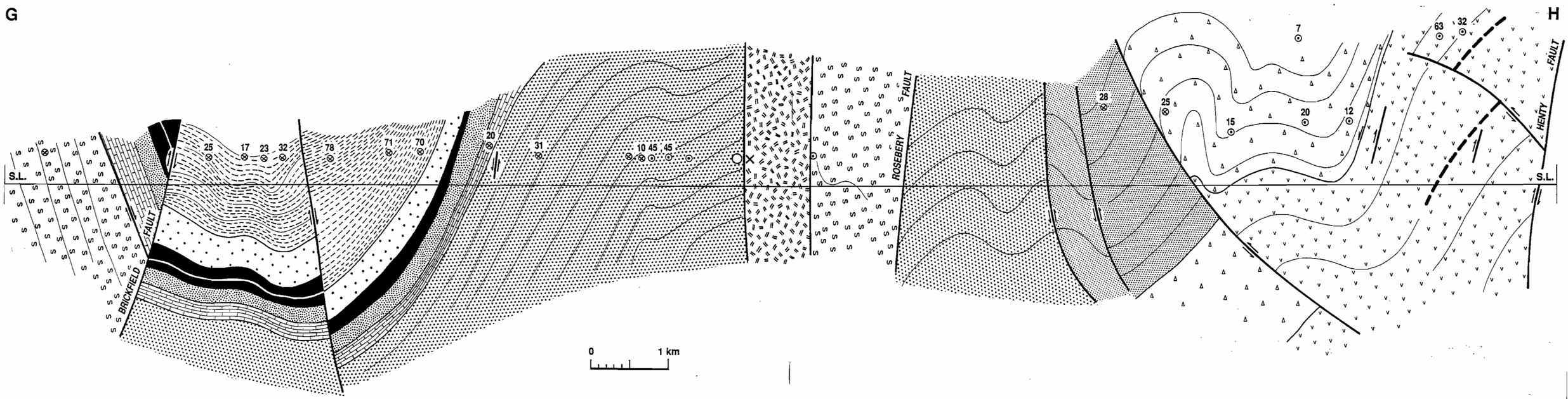

Fig. 4 Section G–H; Zeehan–Dundas Road–Henty Fault section.

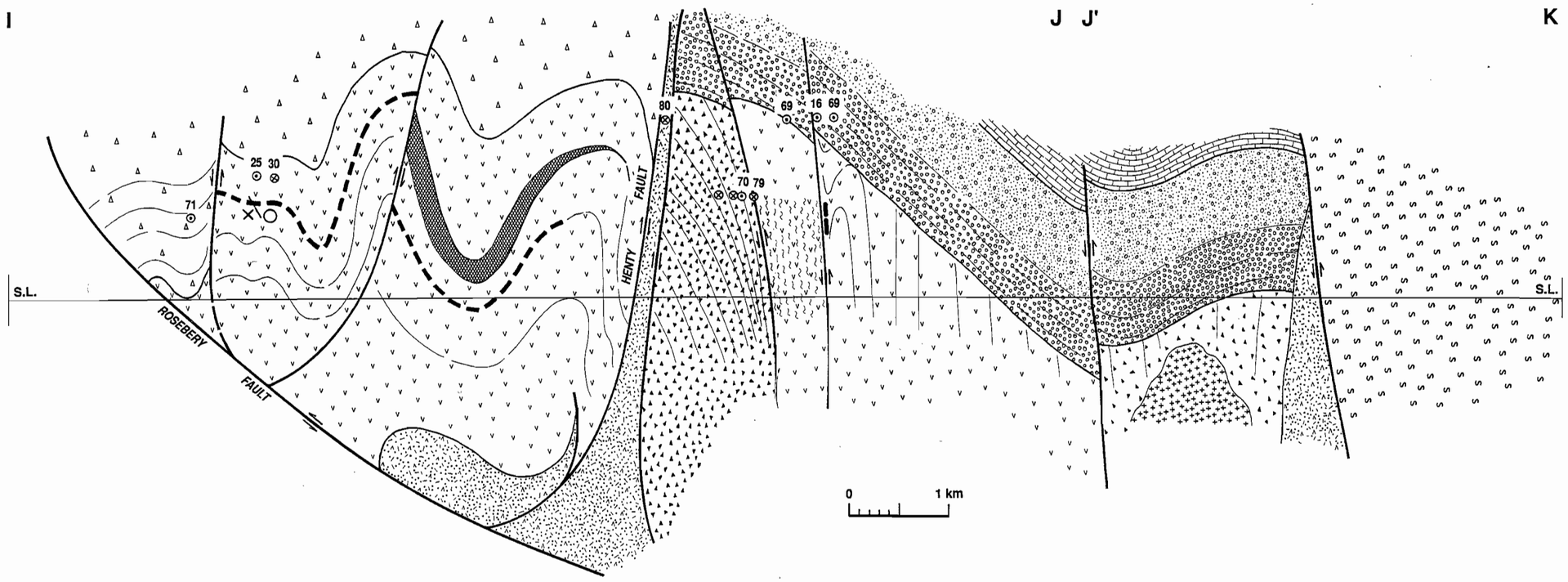

Fig. 5 Section I–J/J'–K; Mt Hamilton–Mt Read–Anthony Dam section. Bedding in the Tyndall Volcanics and CVC dips 40° E prior to folding of the Owen Conglomerate. The increased angle between the Tyndall Volcanics and Owen Conglomerate to 90° may be explained by increased deformation in the hinge of the syncline of the Anthony dam site.

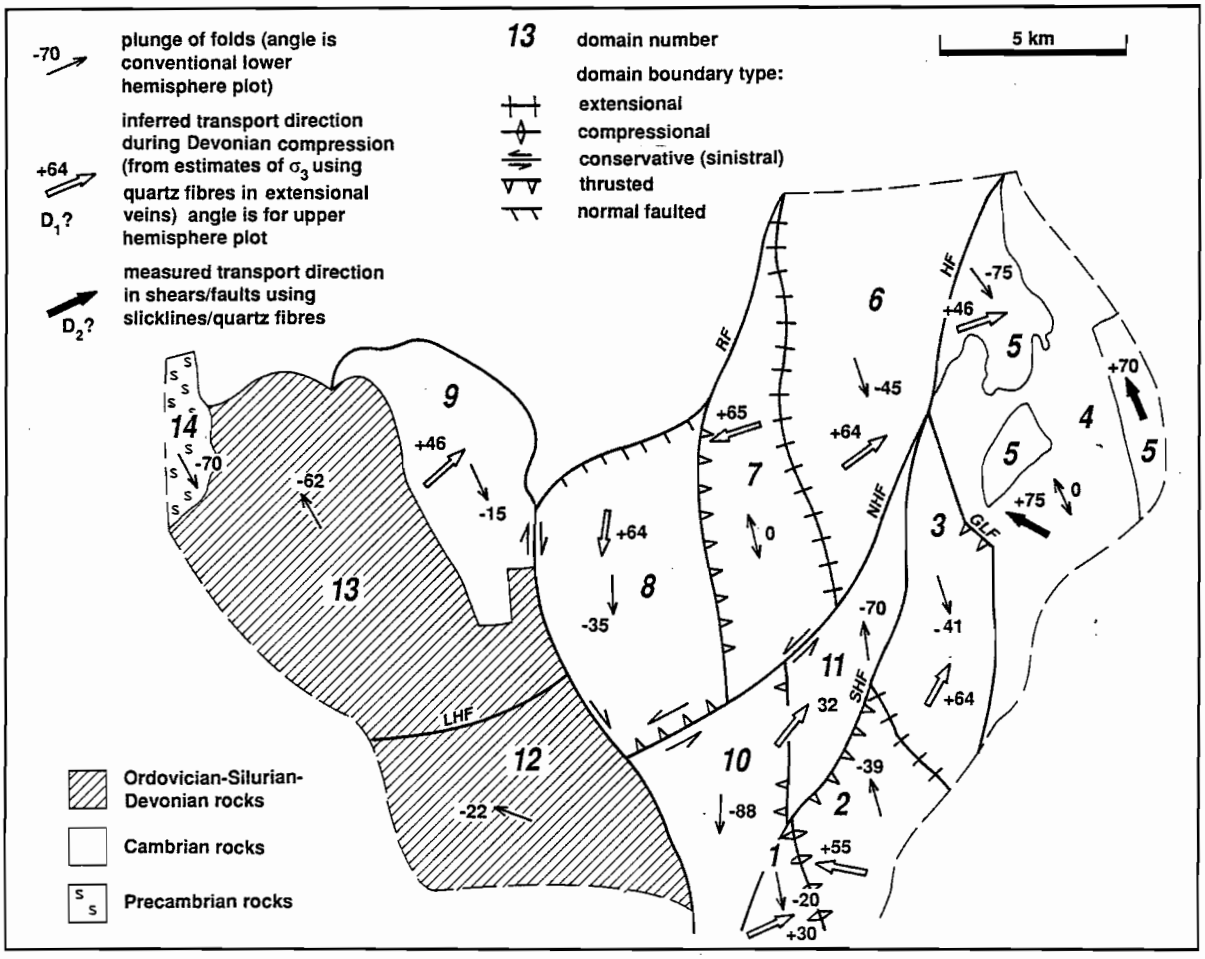

Fig. 6 Domain map of the Zeehan-Lake Selina region. For explanation, see text.

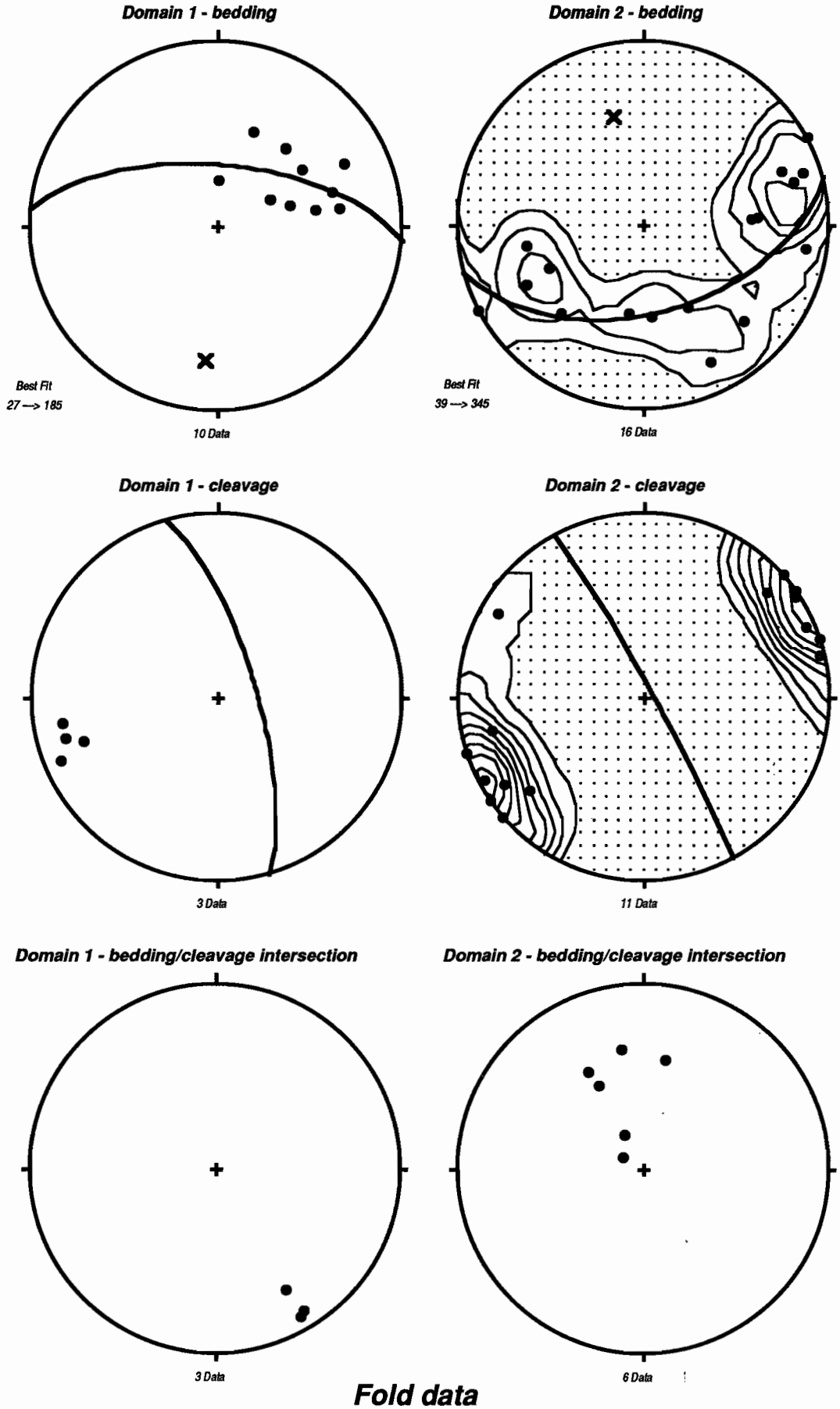

Fig. 7 Stereoplots of domain fold data

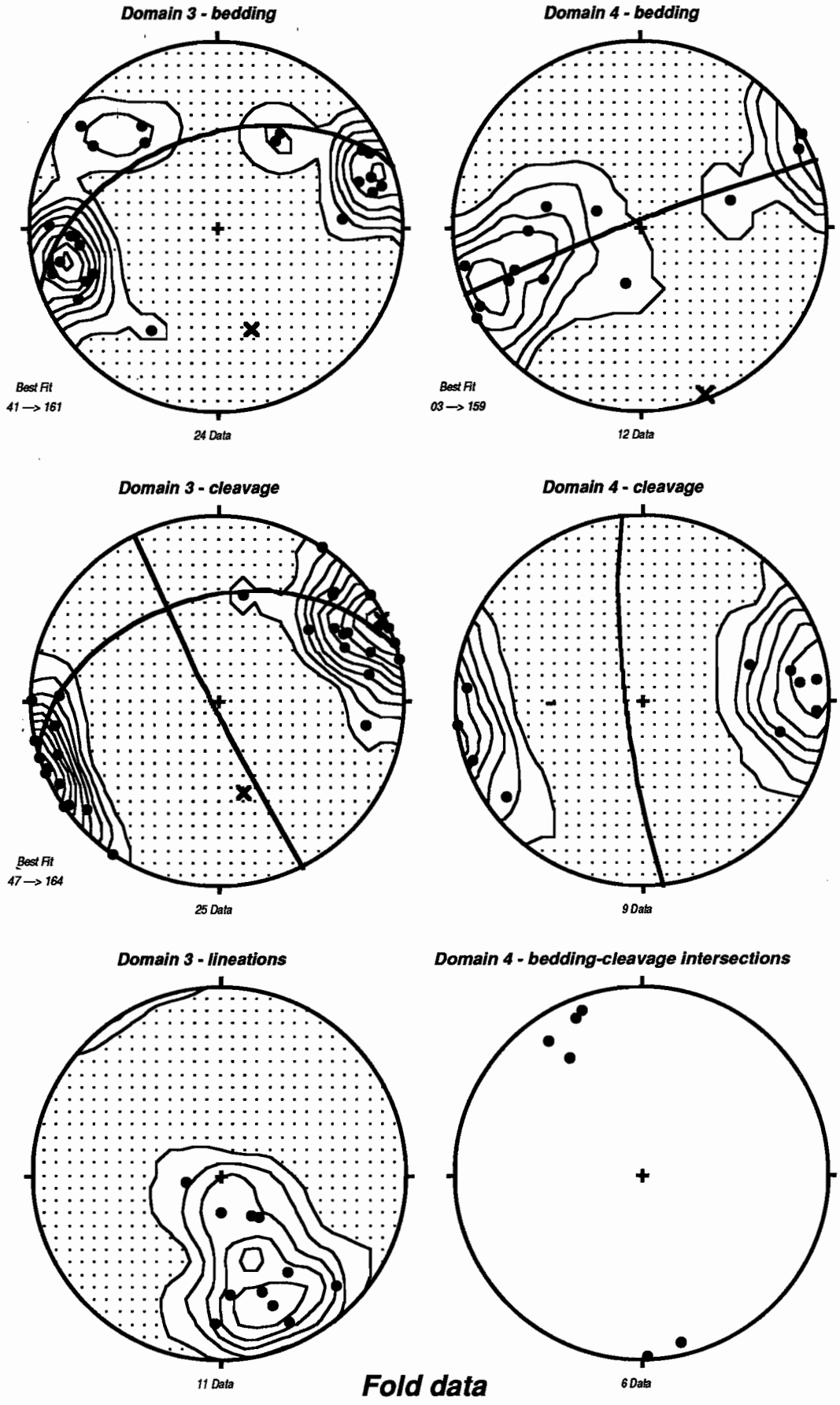

Fig. 7 cont. Stereoplots of domain fold data

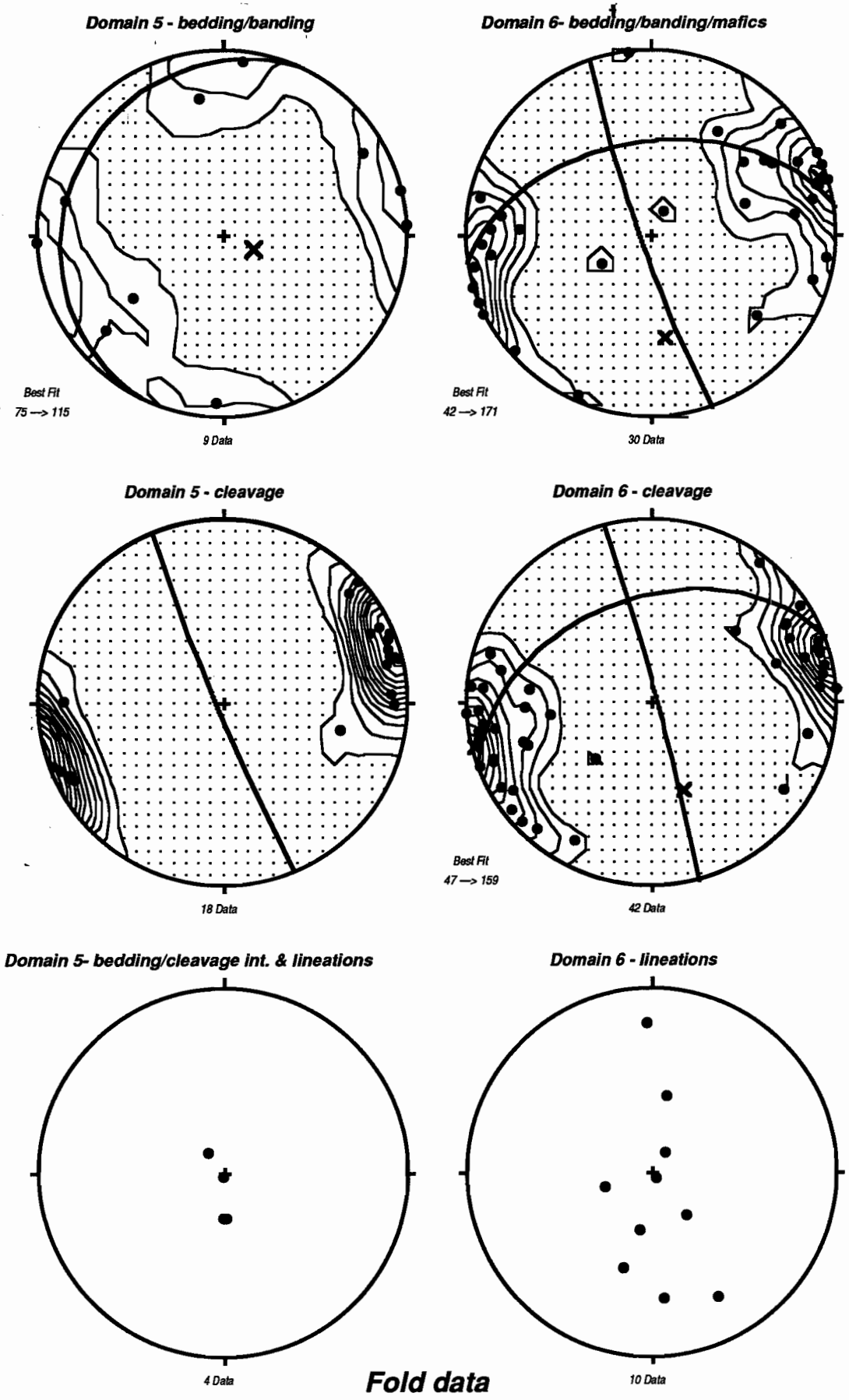

Fig. 7 cont. Stereoplots of domain fold data

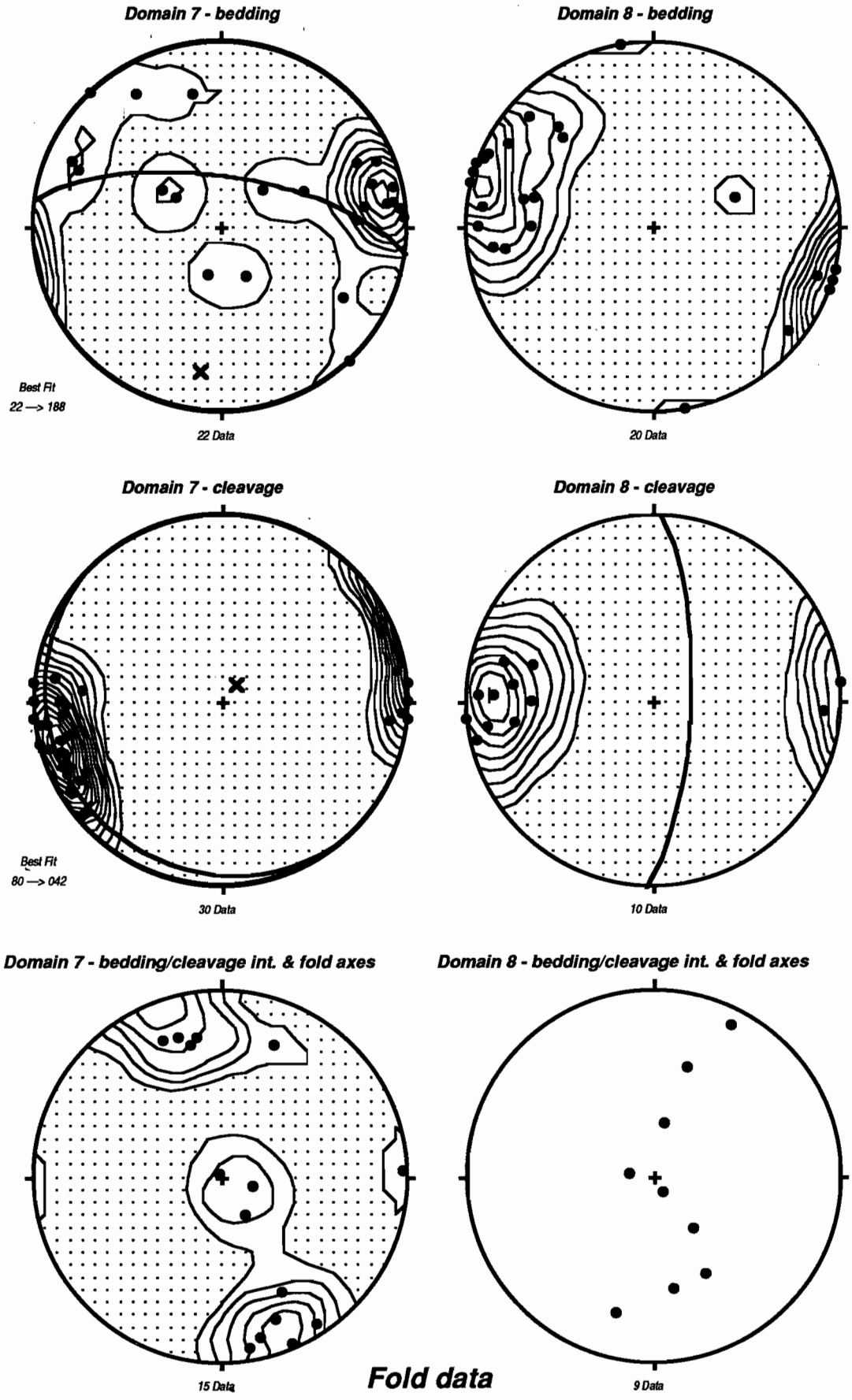

Fig. 7 cont. Stereoplots of domain fold data

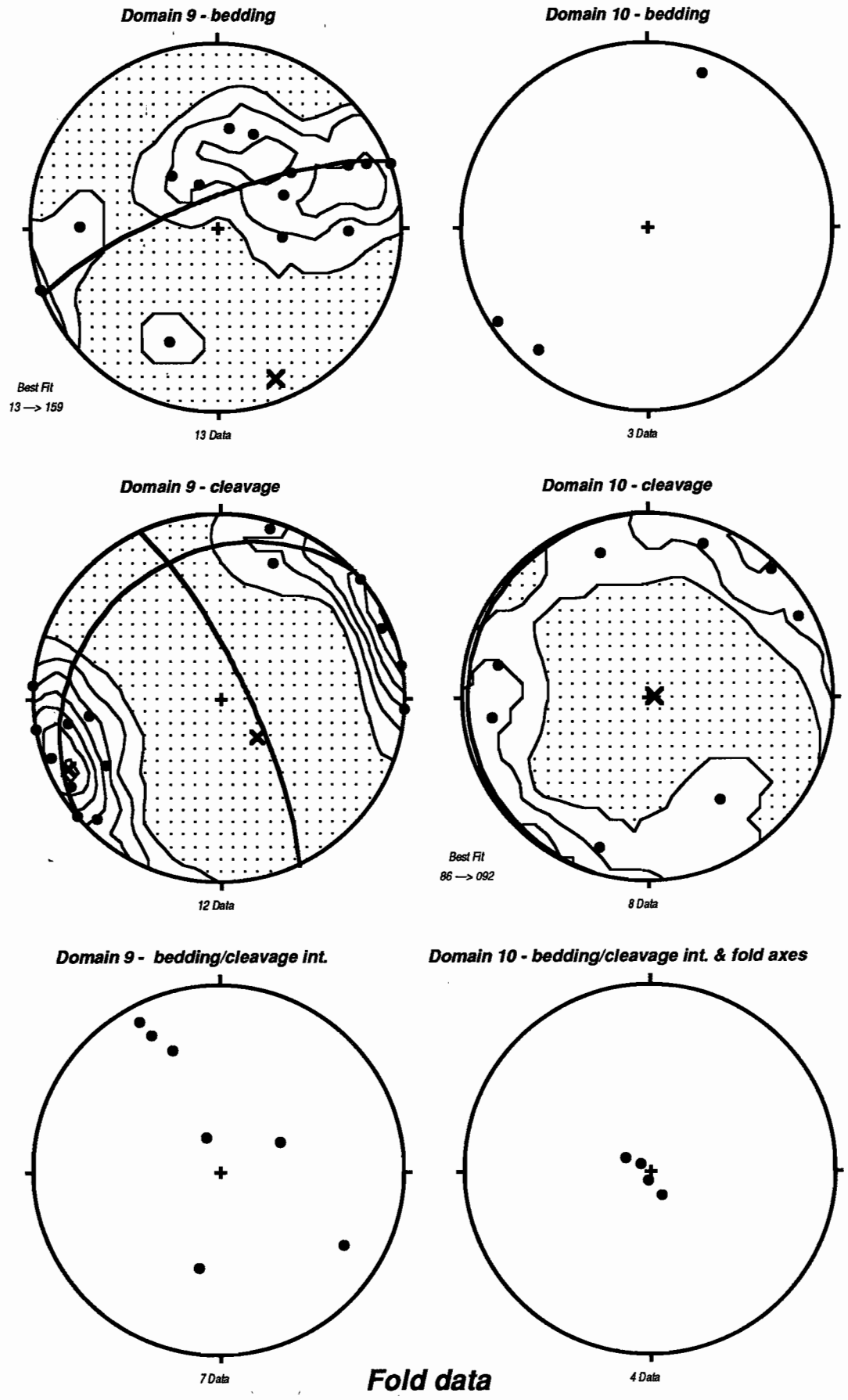

Fig. 7 cont. Stereoplots of domain fold data

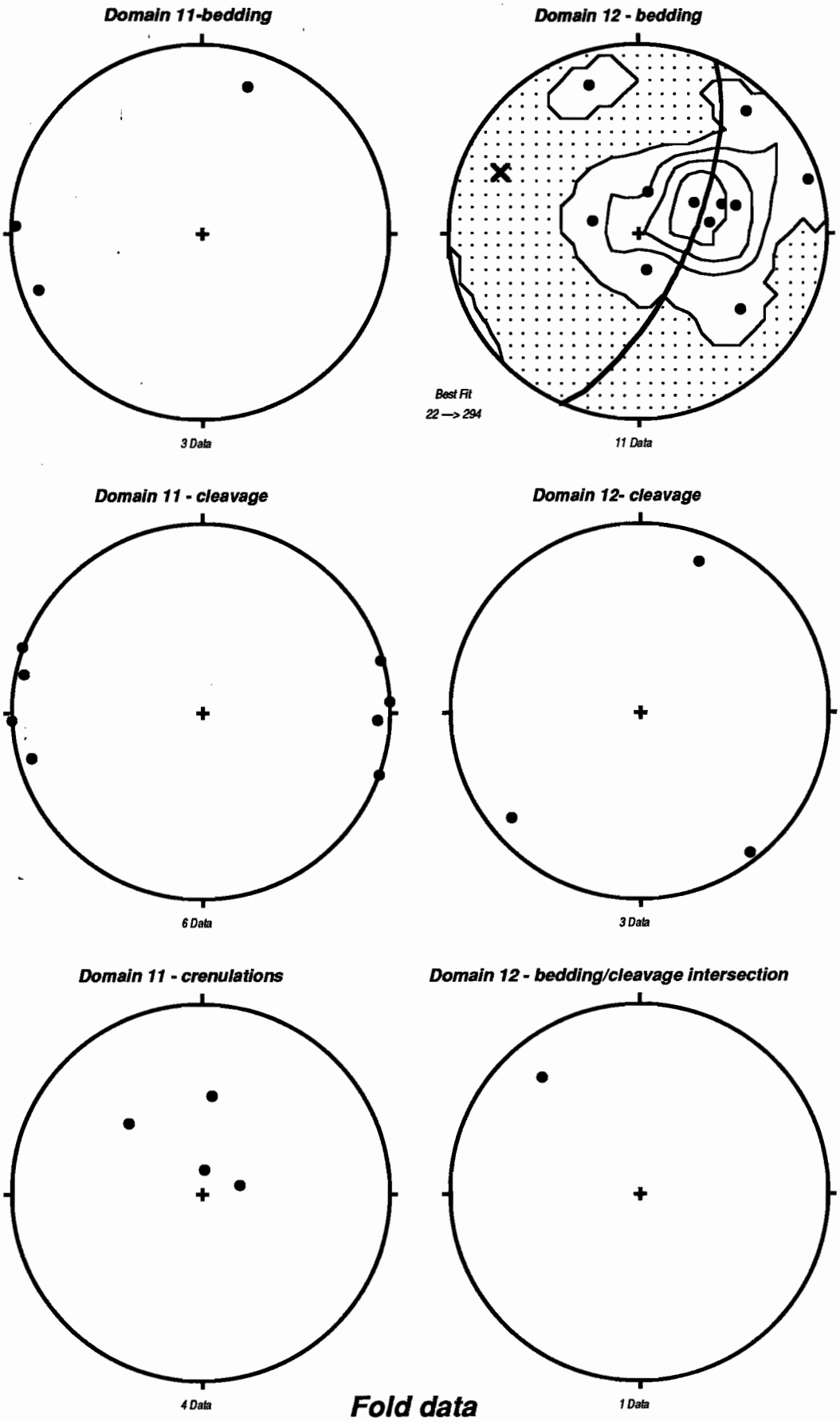

Fig. 7 cont. Stereoplots of domain fold data

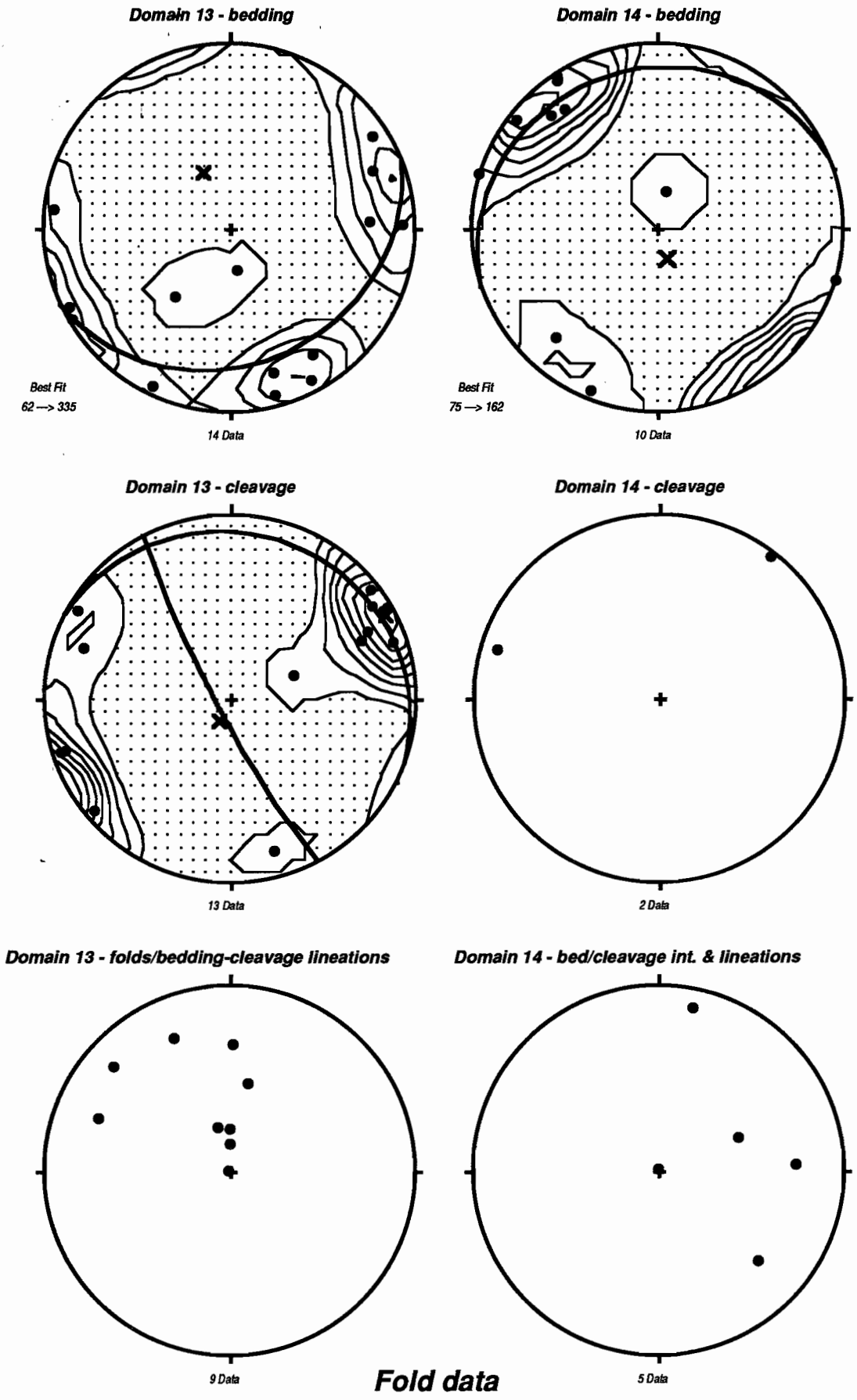

Fig. 7 cont. Stereoplots of domain fold data

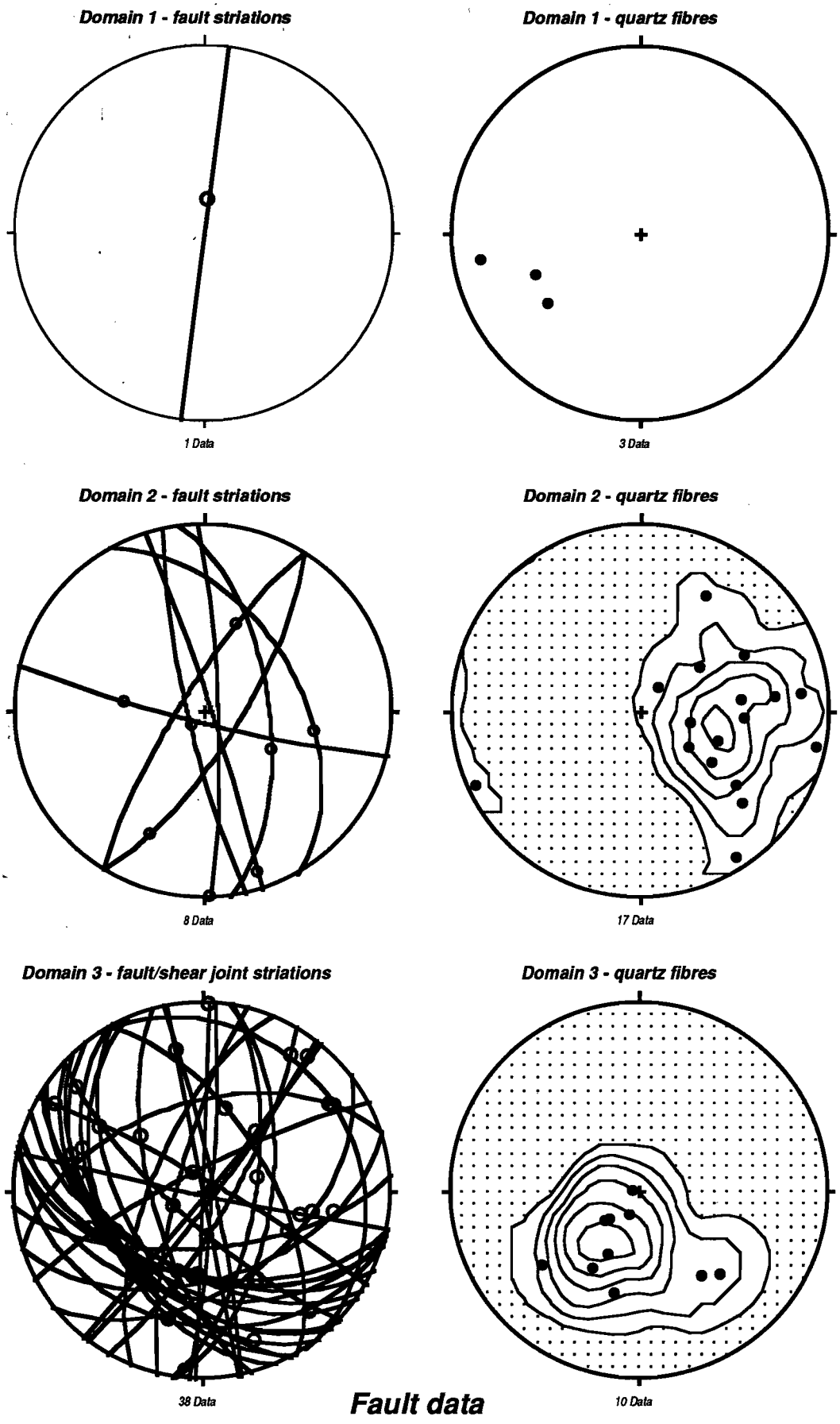

Fig. 8 Steroplots of domain fault data

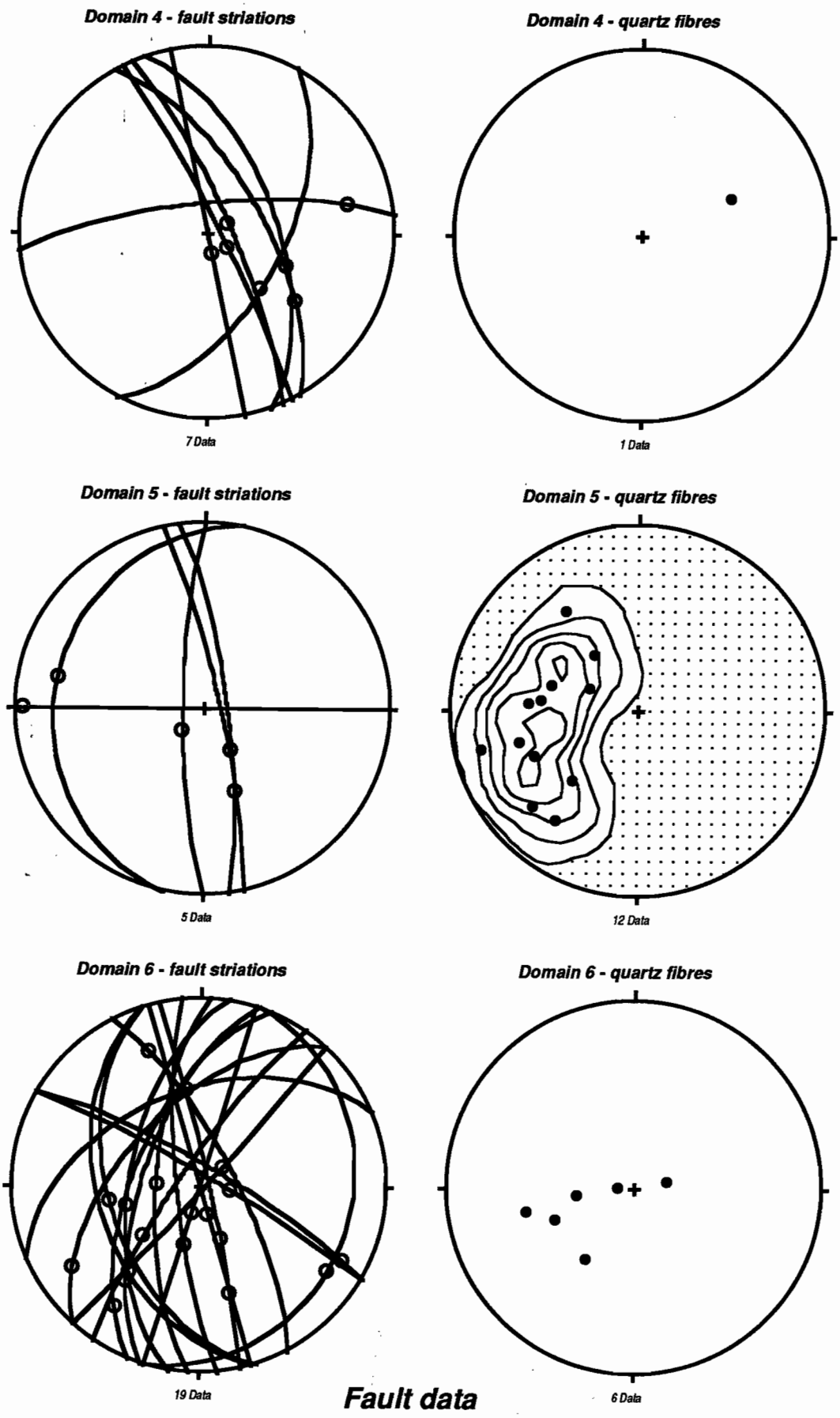

Fig. 8 cont. Stereoplots of domain fault data

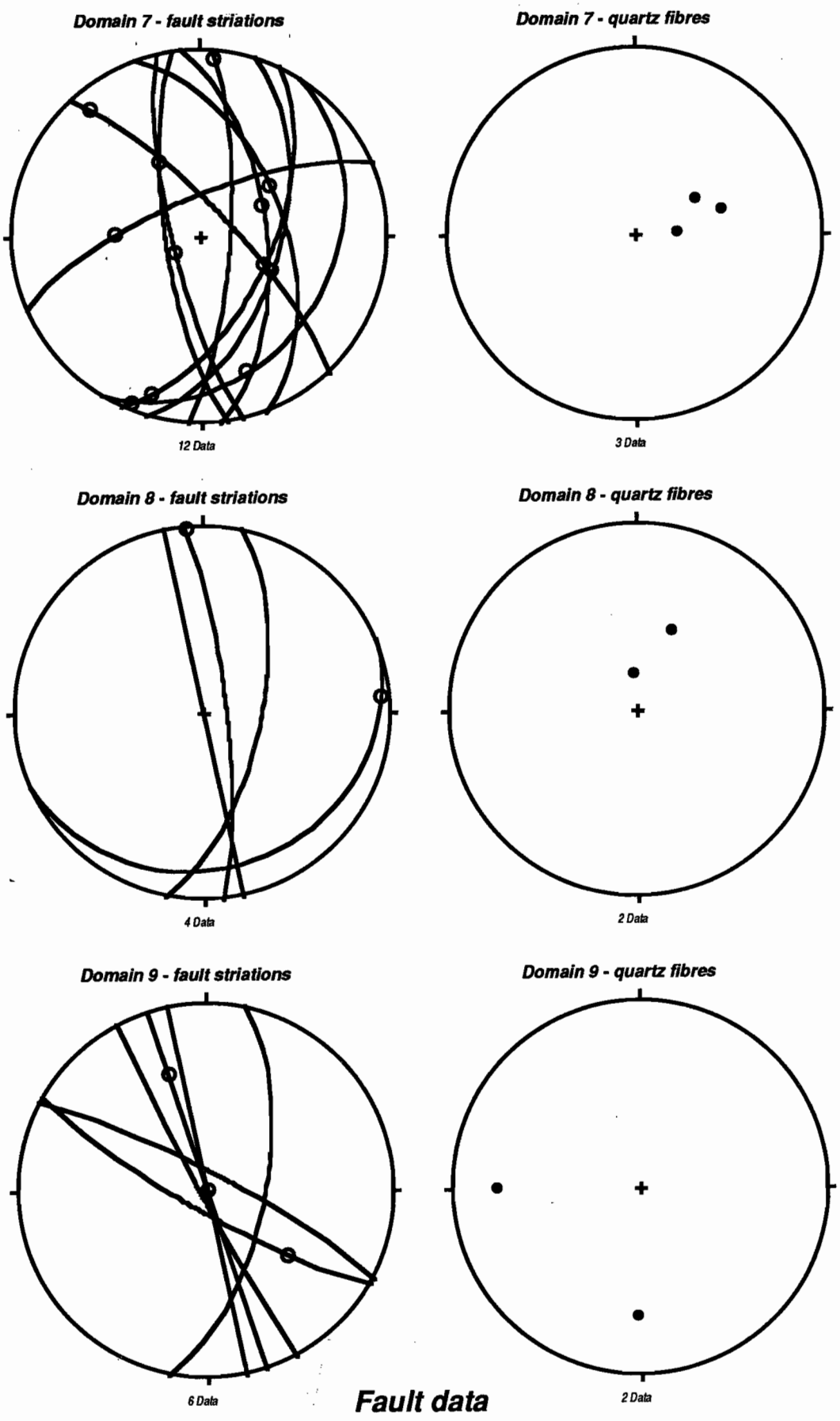

Fig. 8 cont. Stereoplots of domain fault data

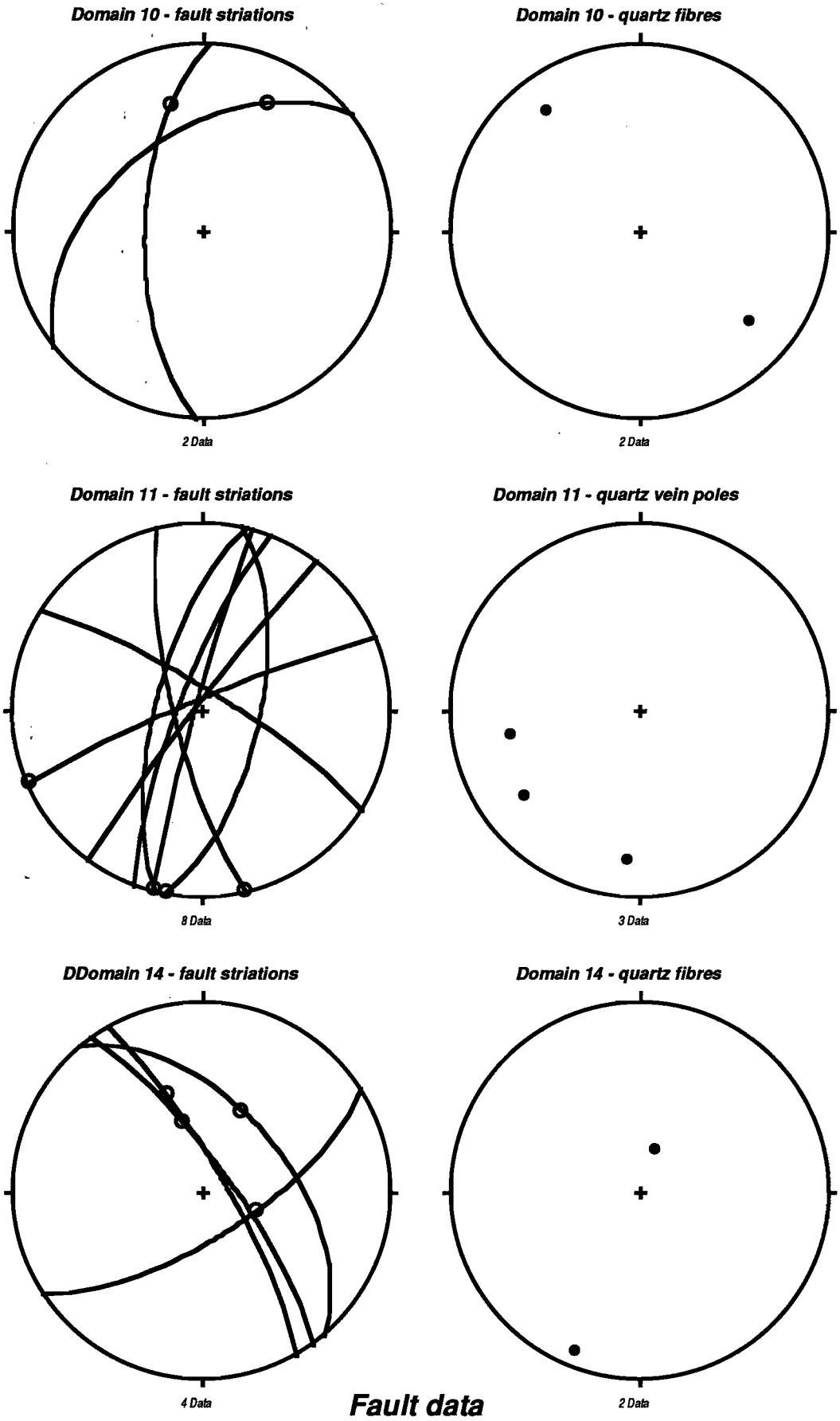

Fig. 8 cont. Stereoplots of domain fault data

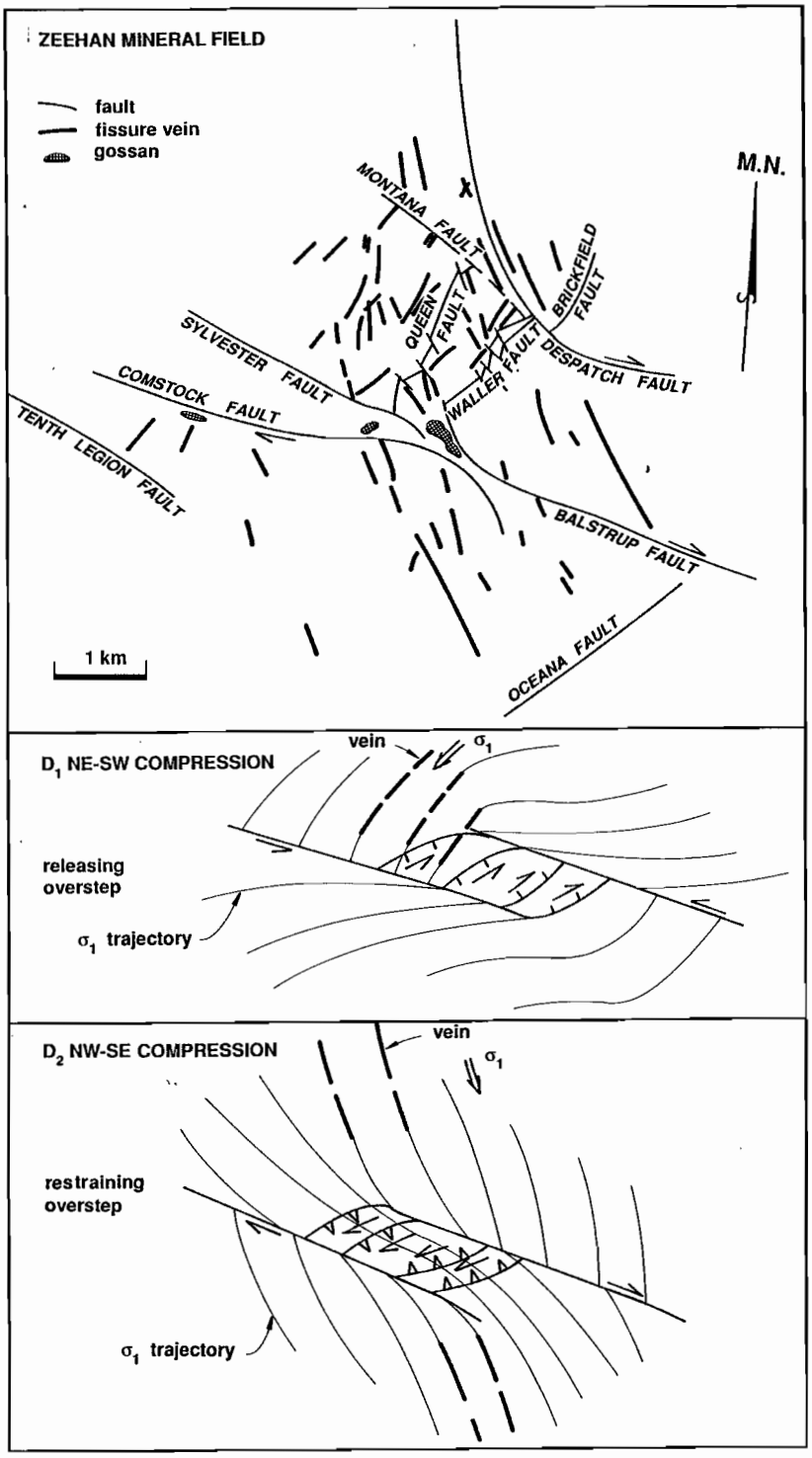

Fig. 9 Simplified plan of the Zeehan Mineral Field showing the major faults and vein systems (adapted from Both and Williams,1968) . The Balstrup, Comstock and Tenth Legion Faults at the south end of the field, and the Despatch Fault at the north end form a left-stepping fault array with releasing characteristics during D_1 and restraining characteristics during D_2. The lower two diagrams show the O1 stress trajectories during the sinistral D_1 and the dextral D_2 events. Note that the two vein orientations are predicted by the model (from Guiraud and Seguret,1985 who adapted models of Rodgers D. A. and Liu Xiaochan).

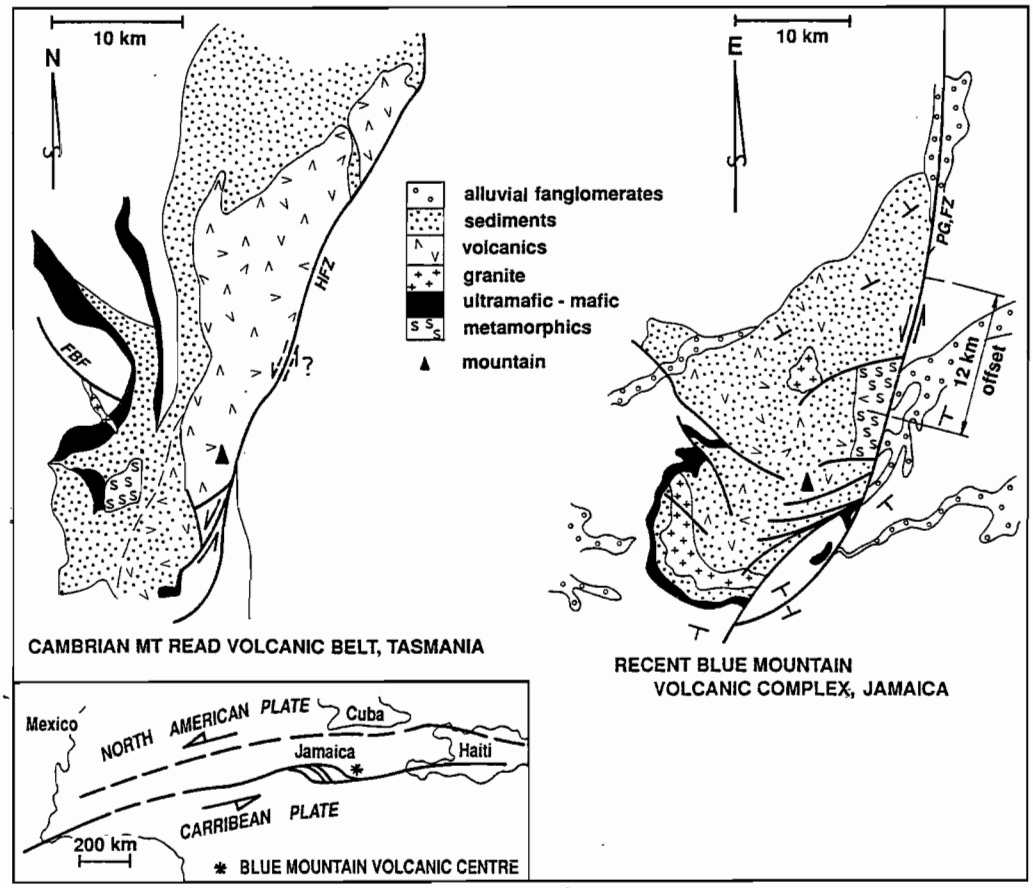

Fig. 10 A comparison between The Mt. Read Volcanics and the Blue Mt. Volcanic complex, Jamaica. The two maps are generalised from Corbett and Lees, (1987) and Mann et. al. (1985) and are shown at approximately the same scale; the right hand map has been rotated through 90 degrees to make a direct comparison between the two areas possible. The Plantain Garden FZ is a right-stepping sinistral fault system which is part of a broad fault zone between the North American and Carribean plates; the volcanic rocks are located at a restraining bend which has involved recent uplift. Note that the rocks are not folded. For further explanation see text.

Appendix 1

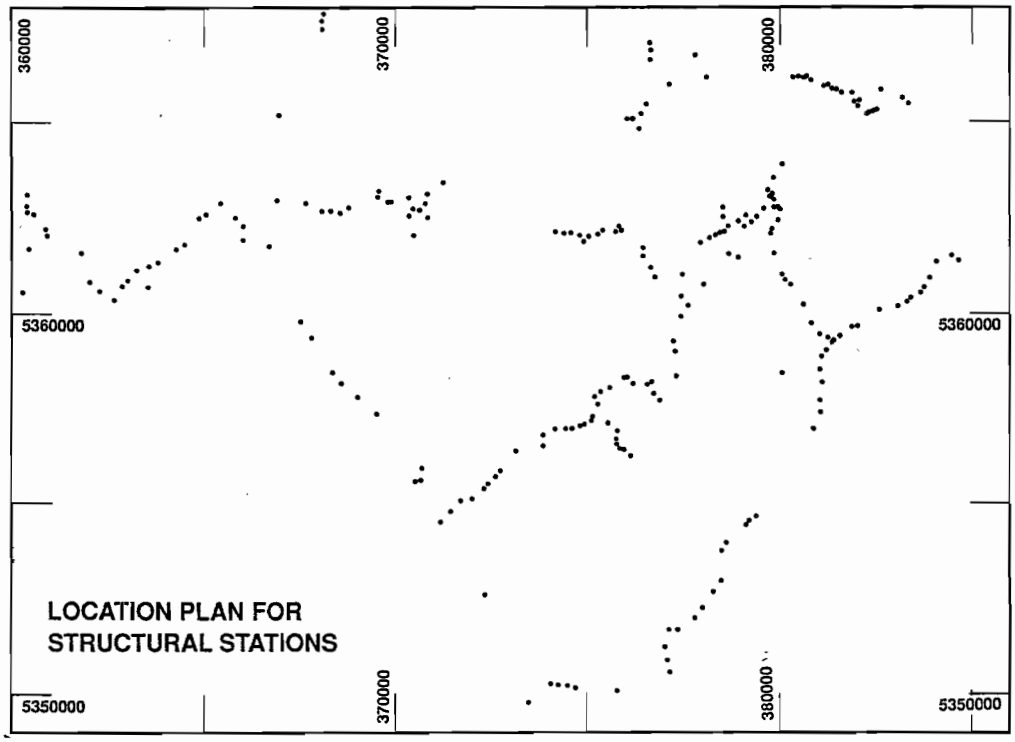
360000
370000
380000
5360000
5360000
LOCATION PLAN FOR
STRUCTURAL STATIONS
5350000
370000
380000
5350000

Appendix 2

AMG coordinates of the stations and the structural readings

	A	B	C	D	E	F	G	H	I	J	K	L	M	N	O	P	Q
1	UNIQUE	ROCK			BEDDING	BEDDING	CLEAVAGE	CLEAVAGE	LINEATION	LINEATION	QTZ VNS	QTZ VNS	QTZ FIB	QTZ FIB	SHEARS	SHEARS	MOVE DIR
2	NUMBER	TYPE	EASTING	NORTHING	DIP	DIP AZ	DIP	DIP AZ	PLU	AZ	DIP	DIP AZ	PLU	AZ	DIP	DIP AZ	PLU
3	1	6	375800	5350100	34	255	73	80	10	148	27	256	38	232	82	276	77
4	2	6	377200	5350600	49	267									83	257	82
5	3	6	377100	5350900	80	252			69	42	13	218	64	50	85	194	55
6	4	6	377050	5351250	78	279	87	257	80	298							
7	5	5	377150	5351700	72	334	90	235	73	330							
8	6	5	377400	5351700	65	314	79	120									
9	7	6	377750	5352000	42	354	72	77	35	350	55	308			51	12	
10	8	5	377950	5352300	43	332	88	237	40	330							
11	9	7	378250	5352700	55	42	90	49	48	332	39	306	65	140	48	60	40
12	10	6	378450	5352970	69	249	76	230									
13	11	7	378450	5353760	90	62					37	292	71	107	75	122	29
14	12	6	378600	5353950	60	62					61	264			84	88	1
15	13	7	379100	5354450	63	82									81	332	81
16	14	1	379350	5354650			90	67									
17	15	2	380850	5356950	48	28											
18	16	7	381050	5357400	65	67	80	50	36	145							
19	17	7	381050	5357720	67	86											
20	18	7	381100	5358150	56	32					25	90	43	194			
21	19	7	381050	5358530	73	62									43	232	29
22	20	8	381100	5358850							27	82					
23	21	7	381220	5359050	77	242					23	36					
24	22	8	381350	5359250	57	144			21	182					51	322	20
25	23	7	381250	5359350	75	257	52	232			9	182			77	235	15
26	24	5	381050	5359450			63	247							60	198	4
27	25	7	380830	5359750	69	252											
28	26	11	380660	5360000			75	97			50	356					
29	27	5	380630	5360240	51	214	84	245	14	134	33	22	87	280	90	79	25
30	28	7	380250	5360750	80	256									68	292	50
31	29	1	380130	5360900							11	237	78	202	90	92	1
32	30	1	380060	5361000											45	247	42
33	31	1	379980	5361200			49	194									
34	32	1	379850	5361550											55	224	52
35	33	1	379760	5362090	80	127	89	90							61	72	52
36	34	1	379800	5362210	65	86	79	71	35	175							
37	35	1	379960	5362420	81	77	73	227	75	255	15	37	72	226	85	78	85
38	36	5	380020	5362700	75	77	87	55	67	142	37	42					
39	37	1	379950	5362770	60	69	90	257	73	177	33	27			68	255	53
40	38	5	379850	5362800	45	252	85	102							87	285	
41	39	1	379730	5363050	62	308	80	69			39	50			61	292	
42	40	3	379840	5363010	76	82	67	70			49	52			80	264	63
43	41	1	379800	5363130			80	70									
44	42	1	379720	5363230	83	102									86	77	40
45	43	1	379850	5363570			85	258									
46	44	3	379970	5363720	90	73	85	218			10	92					
47	45	1	380100	5363900	85	278	80	287	68	252	62	337			81	304	57
48	46	5	380720	5366220					80	8							
49	47	2	380650	5366180			80	70									
50	48	2	380520	5366200			81	82									
51	49	1	380380	5366180			83	261									
52	50	1	380820	5366100			77	245			59	37	67	295			
53	51	1	381170	5365980							65	162					
54	52	1	381280	5366000	50	54	80	62			90	307					
55	53	1	381400	5365900	71	50	83	244									
56	54	1	381490	5365850			88	69	88	175							
57	55	1	381630	5365800	90	87	80	229	79	322							
58	56	1	381900	5365750	83	187	81	64									
59	57	1	381950	5365550			85	249									
60	58	1	382060	5365450			80	257	69	175	75	79	42	274			
61	59	5	382300	5365240			85	67									
62	60	1	382340	5365270	77	240	85	255	69	179							
63	61	1	382420	5365290							40	45	25	227			
64	62	1	382530	5365330			55	284			38	83	51	286			
65	63	3	379550	5362750	87	49	78	57	65	142			65	262	50	252	50
66	64	1	379400	5362550	86	24											
67	65	3	379240	5362400	82	230	83	60	79	35					81	30	15
68	66	1	379060	5362280	89	173					15	320	83	275	48	337	47
69	67	1	379100	5362580													
70	68	1	378900	5362420	68	262	75	254			26	32	52	214			
71	69	1	378660	5362280	54	232	80	265	32	174							
72	70	3	378540	5362150	78	244	73	240	63	192							
73	71	1	378460	5362120											88	132	
74	72	1	378370	5362080			46	82									
75	73	1	378300	5362040			83	87									
76	74	1	378160	5361970											90	107	
77	75	1	377930	5361830													
78	76	5	378520	5362530	90	64											
79	77	5	378525	5362780			85	77					41	257			
80	78	1	378650	5361550							13	332			90	74	
81	79	1	378000	5360740											20	108	16
82	80	7	366950	5362950	61	272	85	70	31	339							
83	81	8	367700	5362875			85	247									
84	82	6	368120	5362680	77	247	85	197									
85	83	5	368350	5362680	20	158	90	80	10	332							
86	84	6	368600	5362650	45	202	90	94	45	192							
87	85	6	368830	5362780	42	234	60	82									
88	86	4	369600	5363050											87	242	
89	87	4	369580	5363200									25	270	90	252	35
90	88	6	370400	5363075	85	67	70	224	12	137					88	250	88
91	89	6	370800	5362900	17	164											
92	90	5	370880	5362500	87	304											
93	91	6	370550	5362050	71	102	90	90							82	152	
94	92	1	382100	5365600	82	2	82	271			62	70	35	254	22	282	22
95	93	1	382650	5365850							68	36	27	216			

	A	B	C	D	E	F	G	H	I	J	K	L	M	N	O	P	Q
96	94	7	383220	5365650	89	256	88	228			59	88					
97	95	8	383380	5365520	35	92											
98	96	4	368200	5367850			50	252					41	320	77	202	
99	97	6	371720	5355090	90	107	55	90	39	17							
100	98	7	372020	5355120	90	110											
101	99	7	372320	5355390	83	90											
102	100	7	372620	5355720	81	97											
103	101	6	371450	5354820	75	82	64	97									
104	102	6	372440	5355510	78	132	90	84									
105	103	6	372750	5355870	60	102	86	77	41	152							
106	104	6	373150	5356380	57	135	64	81									
107	105	5	373850	5356520	81	287	83	92	66	12					18	157	5
108	106	6	373870	5356800	78	120	80	274	82	150	33	197	52	24			
109	107	7	374190	5356970	63	137	79	81	61	142							
110	108	7	374480	5356980	55	90			39	170							
111	109				90	284					30	197	74	353	90	78	
112	110	6	374640	5356980	81	308			79	280							
113	111	6	374840	5357050	89	115	71	105	25	196					80	84	2
114	112	7	374950	5357080	85	114	57	107	10	27							
115	113	5	375120	5357190	84	257	86	274									
116	114	5	375160	5357290	70	112	90	96									
117	115	5	375310	5357620			85	260									
118	116	5	375240	5357800	62	267	75	90	23	343							
119	117	6	375360	5357960	22	14	79	72	25	350							
120	118	1	377670	6361460													
121	119	1	377550	5360990													
122	120	1	377500	5360430													
123	121	1	376830	5360920													
124	122	5	376710	5361200	23	123	80	64	7	147							
125	123	3	376500	5361500			81	67									
126	124	1	376490	5361750			60	253									
127	125	6	375870	5362300	25	229	85	74									
128	126	7	375920	5362200													
129	127	7	375770	5362150			83	82									
130	128	1	375450	5362180			83	58									
131	129	5	375300	5362100	88	267	77	66			35	256					
132	130	6	377560	5360200	70	245	73	77	12	166					55	107	55
133	131	5	377500	5359900	73	254	77	71	8	170					77	94	5
134	132	6	377300	5359250	86	264	72	88	3	88					59	115	13
135	133	5	377320	5359000	30	122	74	85	19	159			71	88	77	47	59
136	134	7	377360	5358340			83	59									
137	135	7	376920	5357700	81	344	85	50	80	342							
138	136	5	376750	5357900													
139	137	7	376590	5358120							43	242	50	74			
140	138	5	376690	5358210	40	247	77	76	3	157							
141	139	1	376220	5358170	80	247	85	50									
142	140	8	376080	5358300			78	68									
143	141	7	375960	5358290			87	50									
144	142	6	375600	5358070	25	332	89	76	22	337							
145	143	5	375550	5357100													
146	144	6	375770	5356910													
147	145	3	374700	5350170							79	312	26	130	47	322	25
148	146	6	374500	5350250	85	57	73	82	85	308							
149	147	3	374260	5350270			81	242									
150	148	6	374060	5350300	78	41	75	18	85	192							
151	149	1	373740	5350020			58	325	3	242							
152	150	6	373460	5349850	77	200	86	224	78	297	31	120					
153	151	1	380000	5358320									59	206	18	45	18
154	152	7	380060	5358410	68	124	85	62	64	137					68	175	10
155	153	5	379180	5354560											88	192	45
156	154	7	366720	5361780	68	245	82	59	20	334	62	12	32	182	81	210	44
157	155	7	366050	5362300	65	267							71	164			
158	156	5	365890	5362500	83	269	71	244					63	226			
159	157	6	365450	5362900	71	327	75	344	70	344							
160	158	7	365070	5362610	71	343	82	251	71	360							
161	159	6	364910	5362500	86	63	82	72							90	30	
162	160	6	364500	5361800			72	109	50	12							
163	161	5	360940	5362050	90	107	87	218	89	13	10	220	70	20	80	60	44
164	162	7	360900	5362240											67	32	
165	163	5	360600	5362620	17	195	80	107	11	12							
166	164	7	360460	5362690	70	42			28	132					78	54	58
167	165	7	360420	5362830					51	67					53	50	
168	166	6	360470	5363100					27	87					28	67	
169	167	5	375100	5362020	83	262											
170	168	7	374940	5361900	75	114	63	95	25	22							
171	169	7	374850	5362060											55	98	45
172	170	6	374600	5362130			70	62									
173	171	6	374410	5362130	79	262											
174	172	6	374200	5362150	65	300	90	270	28	347							
175	173	8	381400	5359290	47	214	75	227	33	148	56	347	38	136	43	194	7
176	174	7	381560	5359390					25	158	31	347	43	144	45	224	43
177	175	8	381860	5359630					33	160							
178	176	5	375800	5356690	62	168	80	277	70	147							
179	177	7	375780	5356570	73	148	87	82	75	107							
180	178	6	375850	5356440	90	136	90	84	88	332	33	254	59	60	72	265	1
181	179	4	375950	5356420	90	284	85	232			75	240			15	347	3
182	180	5	376150	5356250	80	252											
183	181	4	369870	5362920			63	77									
184	182	4	369930	5362910			85	247							40	125	43
185	183	4	370380	5362570			81	77	62	160							
186	184	7	370500	5362740	75	124	35	124	1	64							
187	185	9	370690	5362730	42	240	81	252	25	322							
188	186	5	370900	5363150			59	137									
189	187	5	371300	5363450	42	282	51	337	20	347							
190	188	5	364300	5361690	83	332	84	120	78	2					90	100	

	A	B	C	D	E	F	G	H	I	J	K	L	M	N	O	P	Q
191	189	6	363800	5361350			85	50									
192	190	5	363610	5361250	72	248	85	72	32	2							
193	191	5	363300	5361150	40	37	87	240	23	337							
194	192	5	363050	5360870	20	349	80	237	17	312							
195	193	5	362900	5360710			30	250									
196	194	6	362080	5360820	85	26											
197	195	10	361850	5361600	83	345			89	270							
198	196	7	362680	5360340	55	277											
199	197	7	362300	5360570	88	59	66	246	25	292							
200	198	6	360320	5360530	71	162											
201	199	10	371200	5354540	75	222	75	202									
202	200	1	376659	5367090			84	252	40	12					8	72	7
203	201	1	376720	5366920			36	44							50	12	
204	202	1	376590	5365470	75	92	75	80	55	12					82	292	
205	203	5	376440	5365200					45	334					76	22	
206	204	5	376230	5365100	82	262											
207	205	6	376090	5365100	72	198	83	76	71	142			18	262	80	36	
208	206	7	376410	5364850	70	97	84	80									
209	207	5	376700	5366670	25	58	87	95	20	358							
210	208	6	376350	5367980			72	102							45	86	
211	209	3	378090	5366190			75	282									
212	210	1	377800	5366760	60	92	82	42					38	126			
213	211	5	360500	5361700							30	202			75	230	10
214	212	4	368150	5367680											80	318	72
215	213	4	368160	5367470			33	95							22	327	22
216	214	3	378920	5361450			75	29	67	22					58	292	37
217	215	5	382030	5359670	65	67	85	70			69	14			77	354	24
218	216	5	382610	5360090					10	155					57	118	56
219	217	5	383090	5360180	60	70	78	54					47	68	60	70	42
220	218	5	383320	5360310	49	61	89	82	11	337							
221	219	9	383430	5360400	84	244	51	252	28	328							
222	220	8	383650	5360550	85	63	83	274	15	325					90	246	89
223	221	8	383780	5360670	90	60	74	264									
224	222	8	383910	5360920	85	77	70	259	8	340					90	258	80
225	223	8	384090	5361360	42	254											
226	224	7	384450	5361520	20	110	65	284	2	178							
227	225	7	384680	5361400	50	87	83	94	7	167							
228	226	6	372350	5352630	20	104											
229	227	10	370680	5355610	28	243	85	322									
230	228	7	370540	5355560	32	262	77	50	21	320							
231	229	10	370700	5355920	84	253											
232	230	10	369560	5357350	45	255											
233	231	5	369080	5357780	30	140							62	231			
234	232	6	368610	5358170	62	90	60	59	60	65							
235	233	7	368400	5358450	57	22											
236	234	6	367850	5359350	90	20	83	45	74	340							
237	235	6	367560	5359770			71	80									
238	236	7	366060	5361930	30	280											
239	237	8	367000	5365200	45	188	68	202	22	121					82	28	

page 70 cont.

	R	S	T
1	MOVE DIR	MOVE SENS	
2	AZ		
3	335	WBU	
4	234	?	
5	276	?	
6			
7			
8			
9			
10			
11	101	EBU	
12			
13	203	EBS/DEXT	
14	358	DEXT	
15	332	NWBU	
16			
17			
18			
19			
20			
21	285	WBU	
22			
23			
24	36	WBN/DEX	
25	321	NBW/SIN	
26	284	SBE/SIN	
27			
28			
29	349	SBE/SIN	
30	230	WBU/DEX	
31	2	WBS/SIN	
32	220	WBU	
33			
34	198	SWBU	
35	28	EBU	
36			
37	78	EBU	
38			
39	311	WBU/SIN	
40			
41			
42	206	WBD/SIN	
43			
44	164	EBNU	
45			
46			
47	229	WBU	
48			
49			
50			
51			
52			
53			
54			
55			
56			
57			
58			
59			
60			
61			
62			
63			
64			
65	260	WBU	
66			
67	118	SIN	
68	352	REV	
69			
70			
71			
72			
73		DEXT	
74			
75			
76		DEXT	
77			
78			
79			
80		WBU	
81	125	TBNW	
82			
83			
84			
85			
86			
87			
88		WBU	
89	342	SIN	
90	250	WBU	
91			
92			
93			
94	282	TBW	
95			

page 71 cont.

	R	S	T
96			
97			
98			
99			
100			
101			
102			
103			
104			
105			
106			
107	85	DEXT	
108			
109			
110			
111		WBU	
112			
113	355	DEXT	
114			
115			
116			
117			
118			
119			
120			
121			
122			
123			
124			
125			
126			
127			
128			
129			
130			
131			
132	116	EBU	
133	6	DEXT	
134	196	DEXT	
135	64	REV	
136			
137			
138			
139			
140			
141			
142			
143			
144			
145			
146			
147	37	DEXT	
148			
149			
150			
151			
152			
153	57	TBSW	
154	300	DEXT	
155	103	NBU	
156	129	EBU	
157			
158			
159			
160			
161		DEXT	
162			
163	340	REV	
164			
165			
166	344	NEBD	
167			
168			
169			
170			
171	53	EBU	
172			
173			
174			
175	111	DEXT	
176	238	REV	
177			
178			
179			
180	5	SIN	
181	67	TBSW	
182			
183			
184	95	REV	
185			
186			
187			
188			
189			
190		SIN	

page 72 cont.

	R	S	T
191			
192			
193			
194			
195			
196			
197			
198			
199			
200			
201			
202	49	TBU	
203		TBU	
204		DEXT	
205			
206			
207		SIN	
208			
209			
210			
211			
212			
213	318	SIN	
214	10	REV	
215	327	REV	
216	230	REV	
217	78	SIN	
218	136	REV	
219	113	REV	
220			
221			
222	90	EBU	
223			
224	167	REV	
225			
226			
227			
228			
229			
230			
231			
232			
233			
234			
235			
236			
237			
238			
239			

Structure of the Dundas Mineral Field

David Selley
Centre for Ore Deposit and Exploration Studies

Situated to the east of Zeehan, western Tasmania, the Dundas Mineral Field is host to numerous, small, vein-associated Pb–Zn–Ag ore bodies. It occupies an area of approximately 100 km^2, which flanks the western margin of the Mt Read Volcanic Belt. Lithologies include exotic blocks of Precambrian (?) quartzites, greywackes and phyllites of the Oonah Formation (?) and middle Cambrian serpentinite bodies, some of which occur as rhomb-shaped inliers within late Cambrian "molasse-type" sediments, felsic to intermediate volcaniclastics and mafic lava flows of the Dundas Group.

Much study has been undertaken over the last 30 years in order to evaluate the complex fold and fault relationships in the Zeehan Region (Blissett, 1962; Williams, 1978; Brown, 1986). A summary of this work can be found in Seymour (1980), where he defines four discrete fold generations or trends which are attributable to four respective deformation events. These trends include:

1. D_1 E–W(20°) Loongana/Wilmot trend
2. D_2 ENE–WSW to NNE–SSW Belvoir trend
3. D_3 N–S(10°) West coast range/Valentine trend
4. D_4 NW–SE to NNW–SSE Deloraine/Railton trend

Fold trends with orientations similar to D_{2-4} are encountered in the Dundas Mineral Field. Structural analysis of these trends has been undertaken with an emphasis aimed towards understanding the interrelationships between successive fold generations and their interplay with major block-bounding faults. A model is presented which allows many of these structures to have developed under a single stress field via progressive deformation in domains of localised simple shear.

The field area has been divided into two broad structural domains (north and south domains) on the basis of the orientations, types and relationships of structures, and the stratigraphic level at which they occur. Each domain has responded in its own way to a regional E–W compressive event.

Within the southern domain, a conspicuous N to NW trending structural grain is manifested in numerous compressional structures (000–320), including upright to gently inclined folds, fold related cleavage and extensive, steeply dipping reverse faults. These structures are in turn transected by an array of steeply dipping, WNW trending, ductile shear zones and brittle faults (290–310) which have accommodated dominant sinistral displacements with variable quantities of dip-slip component. A resultant right hand en echelon structural pattern is thus developed. The eastern margin of the Razorback Serpentinite Body is defined by a NE trending dextral fault which is interpreted to have developed late during the structural history of this domain and is not considered to have influenced the structural style extensively.

The compressional structures and the sinistral shear zones and faults are interpreted to have developed synchronously during localised sinistral transpression. Evidence for this is two-fold. Firstly, the geometric relationship between these structures is compatible with that of a simple shear environment where maximum contraction makes an angle of roughly 45° clockwise from the direction of shearing (crustal inhomogeneities, uneven distributions of simple shear, relative magnitudes of the principal stresses and "step-over effects" may result in deviations from this ideal model (Aydin and Page, 1984; Aydin and Nur, 1985)). Thus if sinistral faults were to develop at 300, then compressional structures would be expected to trend 345. Secondly, compressional structures exhibit a progressive anti-clockwise rotation (N to NW) during their development, which is a response of oblique structures to tend towards parallelism with the shear direction as deformation continues.

Within the northern domain, N–NNE trending, W verging asymmetric folds occur within fault bounded blocks of middle Dundas Group. Along the western margin of this domain, major faults exhibit a NE trend and dextral offset. Textures are more brittle than those observed in the southern domain and are considered to have developed under less ductile, near-surface conditions. However, as with the southern domain, compressional structures are interpreted to be largely coeval with the dextral faults. Folds are consistently anticlockwise-transected (NNE by N) by their associated cleavage, a style which is attributed to dextral transpression.

The south and north domains represent zones of localised sinistral and dextral transpression respectively. The acute angle between the sinistral fault system (300) and the dextral faults (050) is roughly 70°, which is consistent with the development of conjugate shear zones under upper crustal conditions. The principal compressive stress for such a system is roughly E–W.

REFERENCES

Aydin, A., Page, B. M. 1984. Diverse Pliocene–Quaternary tectonics in a transform environment, San Francisco Bay region, California. *Geol. Soc. Am. Bull.* 95: 1303–1317.

Aydin, A., Nur, A. 1985. The types and roles of stepovers in strike-slip tectonics. in: Strike-slip deformation, basin formation and sedimentation. *Soc. Econ. Palaeon. Miner. Special pub.* 37.

Blissett,A. H. 1962. One mile geological map series. K/55–5–50. Zeehan. Explan. *Rep. geol. Surv. Tasm.*

Brown, A. V. 1986. Geology of the Dundas–Mt Lindsay–Mt Youngbuck region. *Bull. geol. Surv. Tasm.* 62.

Seymour, D. B. 1980. The Tabberabberan Orogeny in northwest Tasmania. Unpublished PhD Thesis, University of Tasmania.

Williams, E. 1978. The Tasman Fold Belt in Australia. *Tectonophysics* 48: 159–205.

Geochemical zonation within the Owen Conglomerate around the North Lyell deposit

Ian Hart
Centre for Ore Deposit and Exploration Studies

INTRODUCTION

The North Lyell orebody has been one of the richest in the Mt Lyell Copper field, producing 4.5 mt at 5.47% Cu, 34 g/t Ag and 0.4 g/t Au. It was located near the intersection of the Great Lyell Fault and the North Lyell Fault and was one of the more highly altered deposits.

The majority of the deposit occurred within the Central Volcanic Sequence (unit D of Cox, 1981), however some alteration has been found within the adjacent Owen Conglomerate. It would appear that the Owen has experienced hydrothermal fluids related to those in the volcanics, yet has only been mineralised in small areas related to the most intense alteration. The reasons for the localisation of this mineralisation (within the Owen), and its timing have not yet been established

AIMS AND METHODS

The basic aims of the study are:

1. To determine the age of mineralisation using textural evidence in the hematite–barite alteration, and direct isotopic dating of any suitable material within the mineralisation.
2. Investigate the zonation of alteration within the Owen Conglomerate to determine the nature of fluids and the interactions responsible for the mineralisation.

Methods used in the study to date include measurement of the whole rock, trace element, mineral and isotopic zonation within the Owen Conglomerate both across and along strike near the North Lyell deposit. Statistical evaluation of the data is used to ascertain the relationship between the various minerals and trace elements. A study of the provenance of the Owen on a section from Cape Horn to Mt Lyell will also be done, to compare with the provenance of altered samples from the North Lyell area to see if there is a host rock control on alteration.

SAMPLING AND RESULTS

A total of 38 rock chip samples have been taken from the hematite/barite body at North Lyell, Lyell Tharsis, Batchelors Quarry and the adjacent waterfall area. Whole rock XRF and XRD analysis and petrological examination of the specimens has been undertaken, along with electron microprobe analysis of chlorites and white micas (as well as some sulphides and phosphates).

The results of the XRF analyses have been subjected to Spearman Rank Correlation and Principal Component Analysis (after log adjustment), to ascertain the positive and negative associations of the various components. Using these methods it is hoped to gain an understanding of the geochemistry of the fluids within the Owen Conglomerate to compare with the mineralising fluids within the volcanics and the hydrothermal fluids(?) within the Pioneer sandstone (above the unconformable and conformable contacts with the Owen).

The data obtained from the microprobe analyses have been compiled in graph form to recognise any regional or local trends which may be apparent in the rocks. The Fe ratio of chlorites and fluorine content of the micas were of particular interest due to the association of these elements with alteration fluids. Ionic composition of unknown minerals was also determined from the microprobe data.

The Spearman Rank Correlation between selected elements is provided in Fig. 1 and shows the association of all major elements. There is a good positive

correlation between the elements within each individual element group, which represent different styles of mineralisation. The majority of elements within group 1 show a negative correlation with those in group 2, and the third group of elements (Ba + Sr) have a very strong positive affiliation with each other but negligible correlation with the other groups.

The major associations appear to be:

1. Group 1 — Al_2O_3 + K_2O + Cr + Rb (sericite)
2. Group 2 — Fe_2O_3 + P_2O_5 + La + Sb (hematite/apatite)
3. Group 3 — Ba + Sr (barite)

The elements occurring within each particular group are shown with the suspected alteration styles associated with the element correlations.

Previous authors such as Hills (1990), have suggested that the Haulage Unconformity acted as a structural and geochemical barrier to the alteration fluids circulating during the Devonian(?) deformation. However, geochemical evidence suggests that some beds within the Pioneer Sandstone have undergone alteration by fluids similar to those circulating within the Owen Conglomerate. It is also possible that these fluids penetrated the overlying Gordon Limestone.

If this is the case, the question of selective mechanisms for alteration and mineralisation are raised (i.e. are there structural, lithological or geochemical controls?), and the number of alteration phases (i.e. was there more than period of fluid activity?).

FURTHER STUDY

Areas of further research include:

- Further fieldwork to study provenance of the Owen for comparison with altered and unaltered samples from the North Lyell area to check for host rock control on alteration
- Compilation of geochemical data to ascertain alteration fluid composition and compare with various lithology compositions, and use a computer based modelling program to ascertain possible reactions of invading fluids within various lithologies.
- Microprobe analysis of zircon grains for REE to determine the likelihood of whether or not the grains are detrital or have some secondary hydrothermal influence affecting them.
- Investigation of Gordon Limestone for evidence of the nature of the alteration from the North Lyell fluids.
- Examine drill core from North Lyell area.

REFERENCES

Cox, S.F., 1981. The statigraphic and structural setting of the Mt Lyell volcanic hosted sulphide deposits. Econ. Geol. 76: 231–245

Hills, P.B., 1990. Mt Lyell copper–gold–silver deposits. *In* F.E. Hughes (ed.) Geology of the mineral deposits of Australia and Papua New Guinea. AusIMM Melbourne: 1257–1266,

Spearman Rank Correlation

	SIO2	TIO2	AL2O3	FE2O3	K2O	P2O5	CR	SB	NB	ZR	SR	RB	LA	BA
SIO2	1.000													
TIO2	0.143	1.000												
AL2O3	-0.187	-0.351	1.000											
FE2O3	-0.642	-0.147	0.205	1.000										
K2O	0.017	-0.064	0.456	-0.309	1.000									
P2O5	-0.501	-0.231	0.007	0.707	-0.492	1.000								
CR	0.212	-0.104	0.314	-0.473	0.482	-0.494	1.000							
SB	-0.260	0.039	-0.272	0.551	-0.628	0.595	-0.727	1.000						
NB	0.326	0.870	-0.456	-0.240	-0.091	-0.270	-0.234	0.212	1.000					
ZR	0.333	0.645	-0.142	-0.309	0.343	-0.377	0.121	-0.143	0.654	1.000				
SR	-0.239	0.479	-0.589	0.387	-0.637	0.487	-0.702	0.616	0.481	-0.013	1.000			
RB	0.080	-0.387	0.627	-0.209	0.505	-0.275	0.595	-0.567	-0.389	0.103	-0.781	1.000		
LA	-0.306	-0.383	0.242	0.416	-0.238	0.626	-0.106	0.256	-0.391	-0.232	0.063	0.242	1.000	
BA	-0.330	0.552	-0.516	0.276	-0.442	0.278	-0.570	0.442	0.528	0.076	0.894	-0.635	-0.091	1.000

Fig. 1 Spearman rank correlation between log normalised selected elements.

Regional geophysical assessment of Huskisson–Hellyer section

R.F. Berry
Centre for Ore Deposit and Exploration Studies

Dr D.E. Leaman was asked to assess the first regional section produced for the AMIRA project (Rattenbury, 1990). The model sections are attached. The two major findings were:

1. That regional magnetics indicates substantial shallow magnetic sources between the Rosebery and Charter Faults which are incompatible with the large thickness of Dundas Group show on the section (Fig 1).
2. That gravity is relatively low across this area and does not support a large thickness of Dundas Group if the normal density assumptions are made (Fig. 2).

These results suggest three options that need to be considered:

1. Firstly assumptions about the stratigraphy of the area need to be checked and especially exposures of high magnetic material. In producing the magnetic model Leaman used Crimson Creek basalts, serpentinite and some basaltic units in Dundas Group rocks to obtain the the spiky profile. Some of these should be exposed in the area. Especially the presence and significance of basaltic rocks near the Rosebery Fault needs investigation. The gravity model suggested by Leaman (Fig. 2a) makes some assumptions outside the control of the section. By varying structure at depth it is possible to make the gravity data more compatible with the surface structural data. For example Fig. 2b was a modification which maintains the original Dundas Group interpretation but thins the CVC rapidly and extends the Merideth Granite further under the area.
2. Secondly the density of Dundas Group is very dependent on the mix of sandstone to siltstone (and ?basalt). This may vary across the area.
3. Finally, the structural evidence for a thick section of Dundas Group depends on projection along the fold axis. The thick section may be the result of cross structures repeating parts of the section along the fold hinge.

All these suggestions require some additional checking. Mr D Selley will carry out a field work program in this area this summer, as part of his PhD study of the Dundas Group, to see if the discrepancy can be overcome. A copy of the original report is available on request.

ACKNOWLEDGEMENTS

Mr M. Roach provided detailed assistance in producing the colour sections here and in fiddling to check model sensitivity.

REFERENCES

Leaman D.E. 1991. Assessment of "…. balanced cross section … by M.S. Rattenbury" for CODES–AMIRA Project P291 using regional geophysical data. Unpublished report: 10pp.

Rattenbury M.S. 1990. Palaeozoic fault kinematics and a balanced cross section through the Huskisson–Que–Hellyer–Mackintosh region, West Coast, Tasmania. CODES–AMIRA Project P291 Report 1: 1–16.

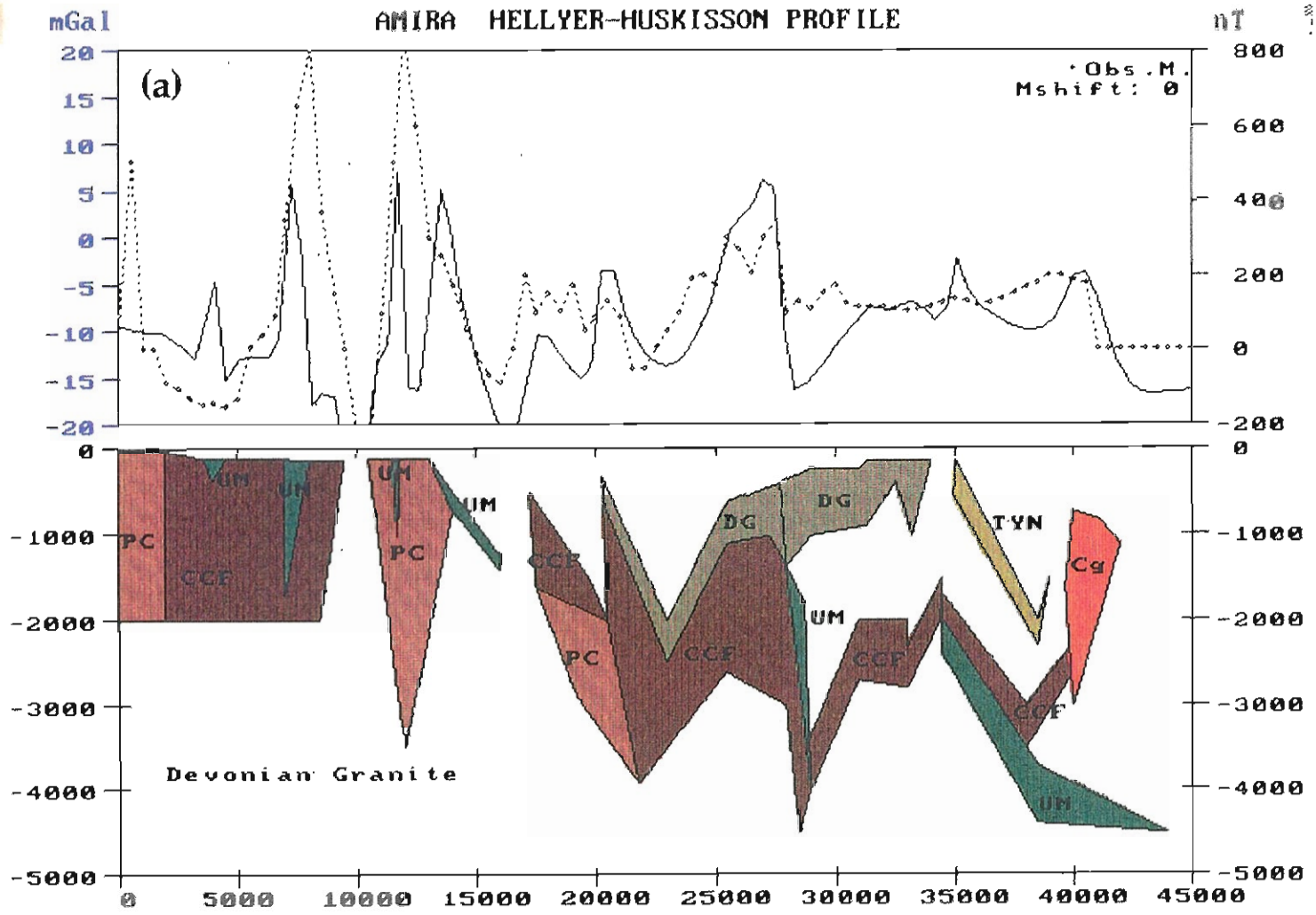

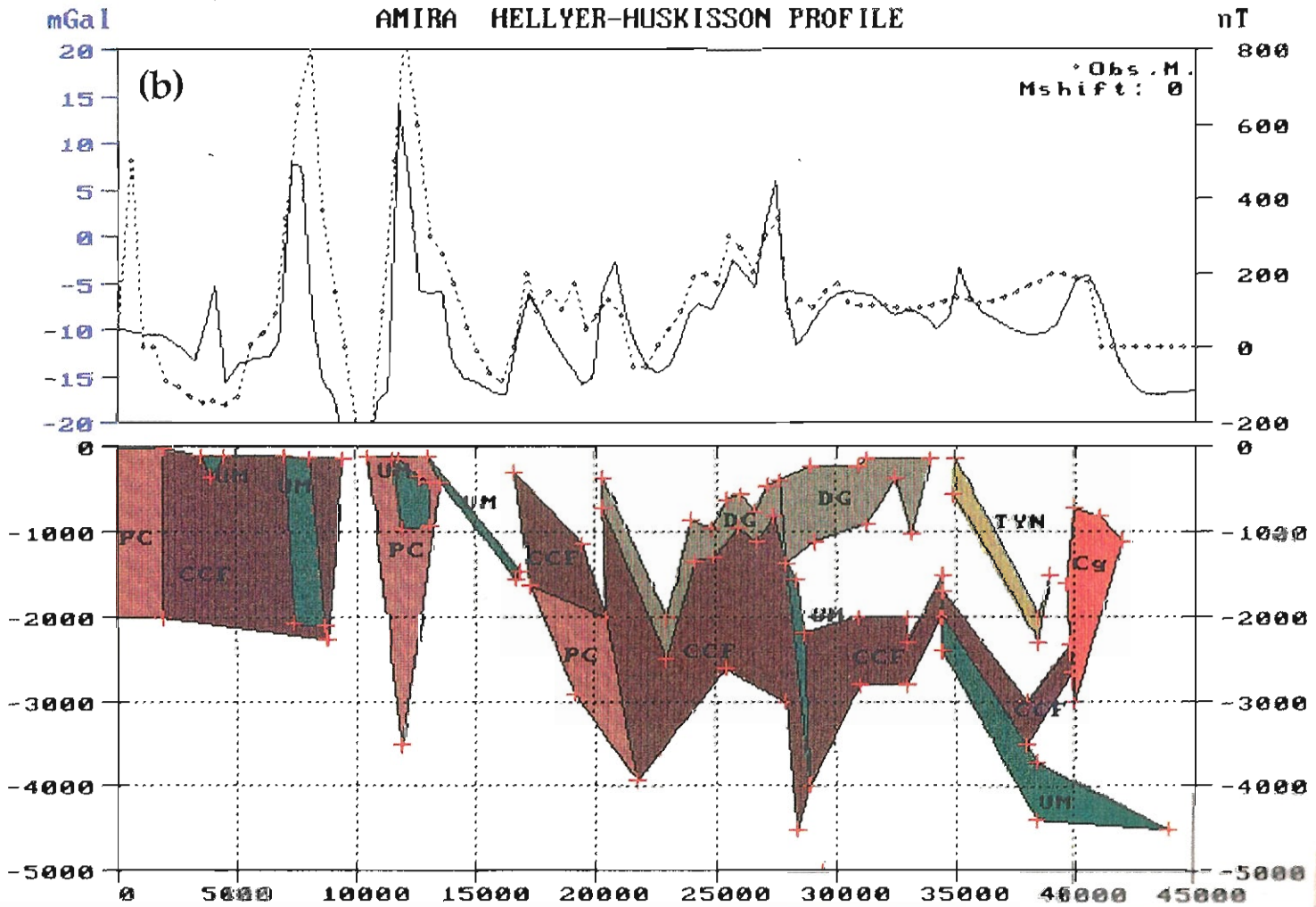

Fig. 1 Magnetic model along Husskison–Hellyer section. This model shows the requirement for highly magnetic material at reasonably shallow depth across the section as implied by the spiky profile. The original section does not suggest the presence of such magnetic components at 2 to 4 km. (b) minor modifications of Leaman model to match some spikes better.

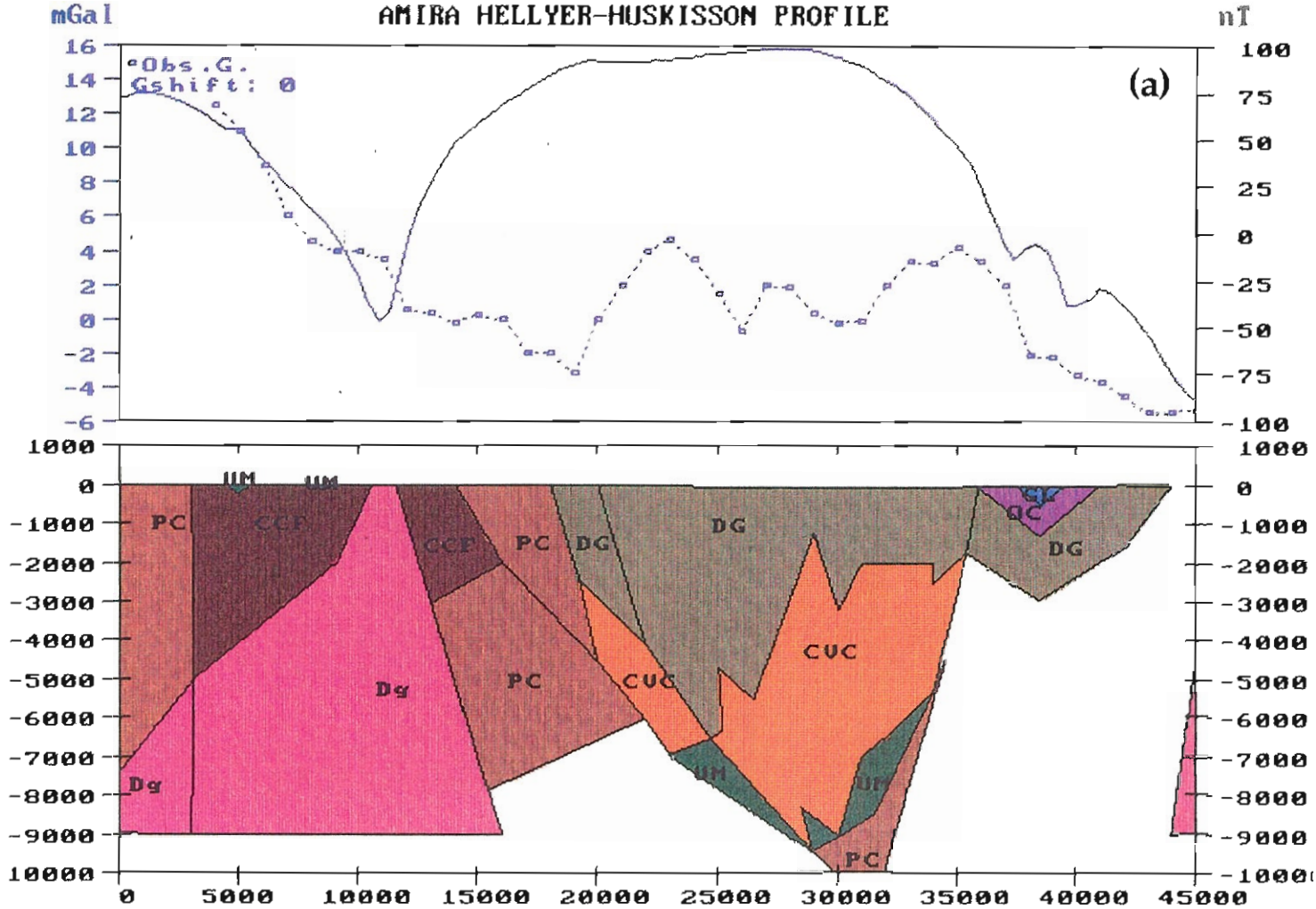

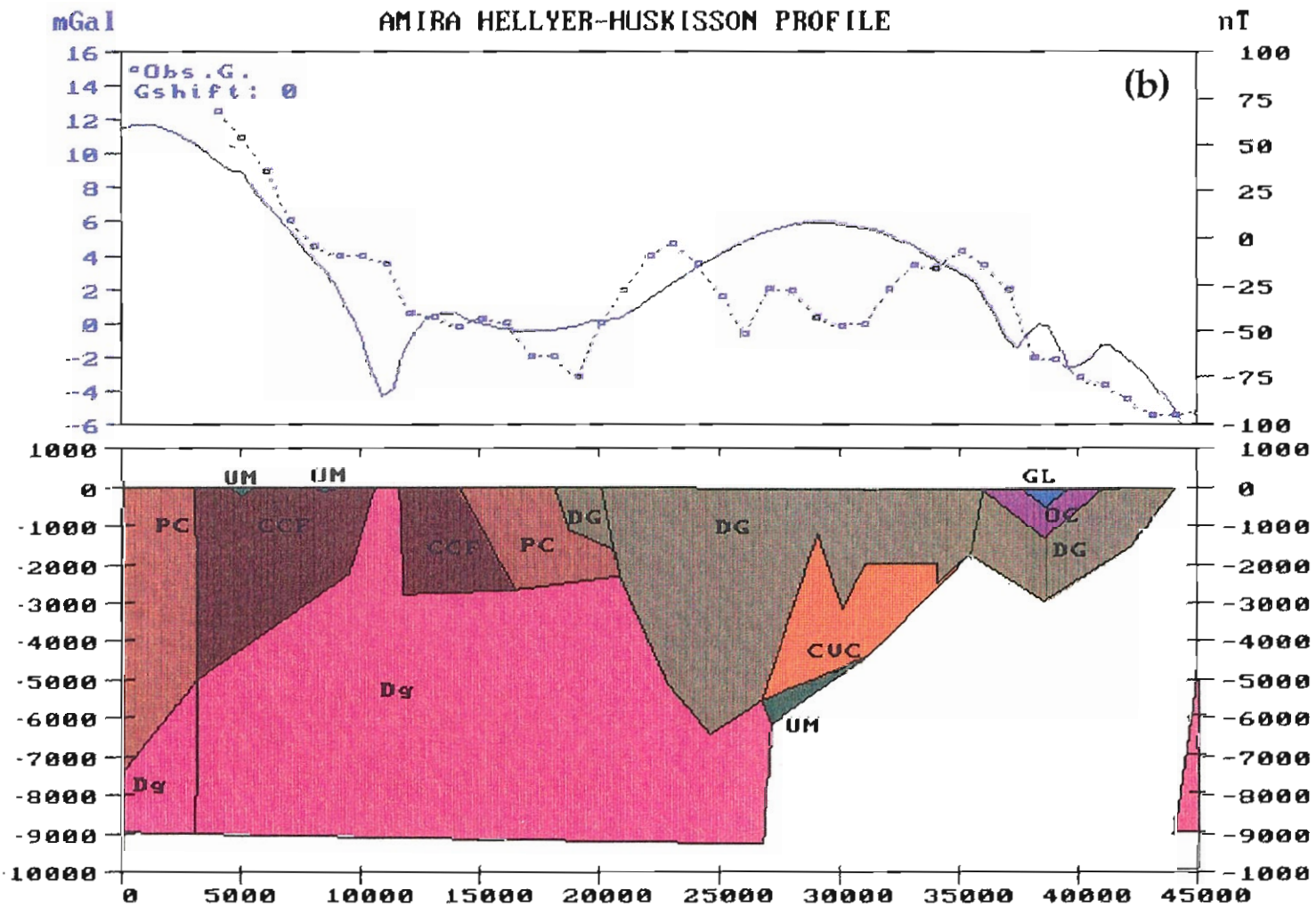

Fig. 2 Gravity model along Husskison–Hellyer section. (a) Gravity model along section versus observed using section of Rattenbury (1990) and density model provided by Leaman. (b) Modified version of section bringing the calculated gravity more into line with observed field and yet maintaining the essential features of the original section. Density contrasts as in (a).